Synthesis of Novel Inhibitors of IdeS, a Bacterial Cysteine Protease

Including Studies of Stereoselective Reductive Aminations

KRISTINA BERGGREN

UNIVERSITY OF GOTHENBURG

DOCTORAL THESIS

Submitted for partial fulfillment of the requirements for the degree of
Doctor of Philosophy in Chemistry

Synthesis of Novel Inhibitors of IdeS, a Bacterial Cysteine Protease
Including Studies of Stereoselective Reductive Aminations

KRISTINA BERGGREN

ISBN 978-91-628-8347-8

Department of Chemistry
University of Gothenburg
SE-412 96 Gothenburg
Sweden

Printed by Ineko AB
Kållered, 2011

[här skrivs något klokt eller roligt som sammanfattar de senaste åren, helst på latin]

Quidquid latine dictum sit, altum videtur.

ABSTRACT

The cysteine protease IdeS is an IgG degrading enzyme secreted by the bacterium *Streptococcus pyogenes* to evade the human immune system. In this thesis several inhibitors of IdeS have been synthesized and evaluated. Such inhibitors should be highly useful when elucidating the detailed mechanism of IdeS action. They might also have a potential as treatment of acute and severe infections caused by the bacteria. Further, IdeS has a therapeutic application of its own due to the proteolytic ability and an IdeS inhibitor might contribute during the development.

Only irreversible, unselective inhibitors of IdeS were known five years ago. In this thesis, three strategies with the aim to synthesize and identify more inhibitors have been undertaken. Focus was first set on compounds with a substructure resembling the known inhibitors but with reversible warheads, i.e. nitrile, azide and aldehyde functions. The aldehyde derivatives were found to provide the first reversible inhibitors of IdeS.

Then, to avoid covalent interactions and obtain more selective inhibitors, a substrate based strategy was undertaken. A 3-aminopiperidine fragment was used as replacement of either of the two residues adjacent to the scissile bond in IgG. Such fragments can be synthesized from *N*-protected 3-aminopiperidone and amino acid esters in reductive aminations in which a stereogenic center is formed. A series of di-, tri- and tetrapeptide analogues, together with eight peptides covering the cleavage site of IgG, were screened for their capacity to inhibit the cysteine proteases IdeS, SpeB and papain. Several analogues showed inhibition capacity, two compounds showed also high selectivity for IdeS. In contrast, none of the tested peptides showed any inhibition. Computational docking studies indicate that the identified IdeS peptide analogues and the non-active peptides do not share the same binding site in IdeS. Probably, the piperidine moiety hinders the inhibitor to enter the catalytic site.

A more detailed study of the stereoselectivity in the reductive aminations affording the 3-aminopiperidine fragment showed that a large protecting group (trityl) together with a large reducing agent (NaBH(O-2-ethylhexanoyl)$_3$) gave the highest diastereomeric ratio. The highest ratio obtained was 21:79 when L-proline methyl ester was used. The newly formed stereogenic center had the *R*-configuration, determined by chemical correlation. Computer based conformational analysis combined with Boltzmann distribution calculations implies an axial attack by the reducing reagent on the intermediary imine.

To improve the potency of the two identified di- and tripeptide analogues synthetic routes to conformationally restricted *N*-containing bicyclic derivatives was undertaken in a third strategy. Five compounds with different bicyclic scaffolds were screened for their inhibition capacity towards IdeS and papain. One of the compounds was able to inhibit the first step of proteolytic cleavage of IgG by IdeS, a process usually completed in seconds.

Keywords:
Cysteine protease inhibition, IdeS, SpeB, Papain, Conformational restriction, Peptidomimetics, Stereoselective reductive amination

LIST OF PUBLICATIONS

This thesis is based on the following papers, which are referred to in the text by their Roman numerals:

I **Synthesis and biological evaluation of reversible inhibitors of IdeS, a bacterial cysteine protease and virulence determinant**
Kristina Berggren, Björn Johansson, Tomas Fex, Jan Kihlberg, Lars Björck, Kristina Luthman *Bioorganic & Medicinal Chemistry*, **2009**, 17, 3463-3470.

II **Stereoselective reductive amination with 3-piperidone and amino acid esters for the synthesis of Gly-Xaa mimetics**
Kristina Berggren, Claes Bergström, Lars Kristian Hansen, Tomas Fex, Jan Kihlberg, Kristina Luthman. Submitted to *Journal of Organic Chemistry*

III **3-Aminopiperidine Based Peptide Analogues as Selective Noncovalent Inhibitors of the Bacterial Cysteine Protease IdeS**
Kristina Berggren, Reine Vindebro, Claes Bergström, Christian Spoerry, Helena Persson, Tomas Fex, Jan Kihlberg, Ulrich von Pawel-Rammingen, Kristina Luthman. Submitted to *Journal of Medicinal Chemistry*

IV **Nitrogen-containing bicyclic derivatives as potential inhibitors of IdeS**
Kristina Berggren, Devaraj Subramanian, Reine Vindebro, Christian Spoerry, Helena Persson, Tomas Fex, Jan Kihlberg, Ulrich von Pawel-Rammingen, Kristina Luthman.
In manuscript

ABBREVIATIONS

Ac	acetyl
AD	amylase tris(3,5-dimethyl-phenylcarbamate)
alloc	allyloxycarbonyl
aq.	aqueous
ax	axial
Boc	*tert*-butyloxycarbonyl
Cbz	benzyloxycarbonyl
config.	configuration
dba	dibenzylidene acetone
DCC	*N*,*N*′-dicyclohexyl carbodiimide
DCM	dichloromethane
DEAD	diethyl azodicarboxylate
DIAD	diisopropyl azodicarboxylate
DIBAL	diisobutylaluminum
DIPEA	diisopropylethylamine
DMAP	4-dimethylaminopyridine
DMF	*N,N*-dimethylformamide
DMSO	dimethylsulfoxide
dr	diastereomeric ratio
EDC	*N*-(3-dimethylaminopropyl)-*N*′-ethylcarbodiimide
Eq.	equation
equiv	equivalents
er	enantiomeric ratio
Et	ethyl
Fab	Fragment antigen binding
Fmoc	9-fluorenylmethoxycarbonyl
GAS	Group A Streptococcus
h	hours
HF	Hartree-Fock
Bt	benzotriazole
HTIB	[hydroxy(tosyloxy)iodo]-benzene
HPLC	high pressure liquid chromatography
IdeS	Immunoglobulin G-degrading enzyme of *S. pyogenes*
IgG	Immunoglobulin G
Da	Dalton
LC/MS	liquid chromatography/mass spectrometry
Me	methyl
min	minutes
MW	microwave
NIS	*N*-iodosuccinimide
NMP	*N*-methyl-2-pyrrolidone
NMR	Nuclear Magnetic Resonance
on	over night
OPLS	Optimized Potentials for Liquid Simulations
PDB ID	Protein Data Base identity
pip	piperidine, in this thesis
ppm	part per million
PRCG	Polak-Ribiere Conjugate Gradient
pyBOP	(benzotriazol-1-yl-oxy)-tripyrrolidinophosphonium hexafluorophosphate
quant.	quantitative
rac	racemic
rt	room temperature
RU	response units
SDS-PAGE	sodium dodecyl sulfate polyacrylamide gel electrophoresis
SpeB	Streptococcal pyogenic exotoxin B
SPR	Surface Plasmon Resonance
STSS	streptococcal toxic shock syndrome
t	time
TBAF	tetrabutylammonium fluoride
TBDMS	*tert*-butyldimethylsilyl

*t*Bu	*tert*-butyl
TFA	trifluoroacetic acid
THF	tetrahydrofuran
TLCK	tosyl lysyl chloromethyl ketone
TPCK	tosyl phenylalanyl chloromethyl ketone
Tr	trityl = trifenylmethyl
TS	transition state
Ts	toluene-4-sulfonyl
Z-LVG-DAM	benzyloxycarbonyl -LysValGly- diazomethylketone

ABBREVIATIONS OF AMINO ACIDS

A	Ala	Alanine
C	Cys	Cysteine
D	Asp	Aspartic acid
E	Glu	Glutamic acid
F	Phe	Phenylalanine
G	Gly	Glycine
H	His	Histidine
I	Ile	Isoleucine
K	Lys	Lysine
L	Leu	Leucine
M	Met	Metionine
N	Asn	Aspargine
P	Pro	Proline
Q	Gln	Glutamine
R	Arg	Arginine
S	Ser	Serine
T	Thr	Threonine
V	Val	Valine
W	Trp	Tryptophan
Y	Tyr	Tyrosine

Table of Contents

The bacterium Streptococcus pyogenes *evades the human immune system and cause mild diseases but also life-threatening conditions. It escapes the human immune system by cleavage of the antibody IgG from its surface, mediated by a cysteine protease. To prevent such cleavage access to an inhibitor of the protease might be advantageous. The development of such an inhibitor for therapeutic applications starts with studies aimed to increase the knowledge about the enzyme and its mechanism of action.*

1. BACKGROUND

1.2 CYSTEINE PROTEASES

A cysteine protease is an enzyme that catalyzes hydrolysis of peptide bonds, i.e. peptide chains are cleaved, mediated by a nucleophilic thiol group present in the active site.

Cysteine proteases are present in most living organisms, from protozoa, viruses and bacteria to plants, mammals and humans. In the MEROPS database all known proteases are classified and ranked based on their structural resemblance.[1] Today (June 2011) there are about 700 cysteine proteases grouped into 89 families (C1-C89) which are further grouped into eight clans (denoted C followed by another letter, A-F). During the last ten years, an average of seven families has been registered annually. Of the eight clans the CA clan is the largest with 27 families. In this thesis, three enzymes from the CA clan have been investigated; IdeS (IgG degrading enzyme from *Streptcococcus pyogenes*) (C66) and SpeB (Streptococcal pyogenic exotoxin B) (C10), both from the same bacterium, and also the plant cysteine protease papain (C1) (FIGURE 1).

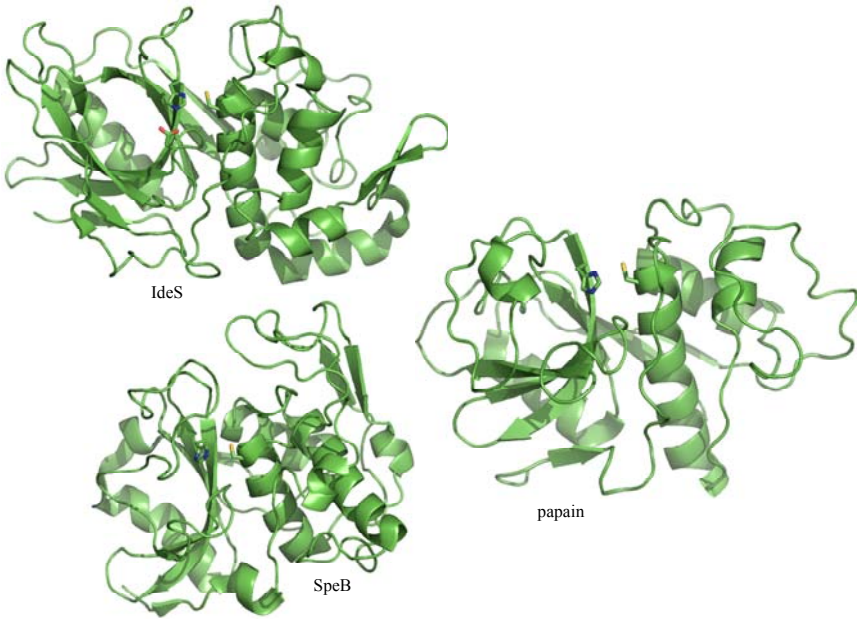

FIGURE 1. IdeS[2], SpeB[3] and papain[4] adopt a so-called papain-like fold with the catalytic site located between the two domains shown as Richardson diagrams.[5-6]

As mentioned above, proteases catalyze the hydrolysis of peptides. In order to be able to hydrolyze a certain substrate, the enzyme depends on the active site to interact with the amino acid residues of that substrate and on the catalytic site to perform the hydrolysis. Most often a specific amide bond in the substrate is cleaved, that bond is called the scissile bond. The nomenclature used for the specific interactions between a substrate and the enzyme was suggested by Schechter and Berger (FIGURE 2).[7-8]

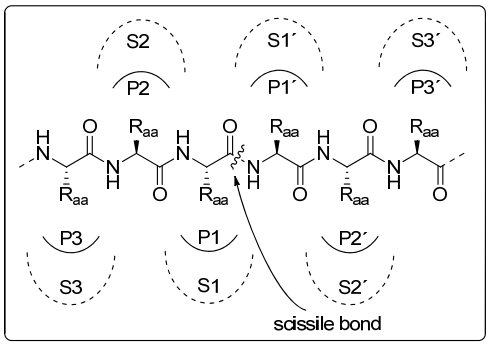

FIGURE 2. Schematic representation of the interactions between the substrate (P = peptide) and the enzyme (S = subsite) in the active site. Picture modified from reference.[8]

P denotes the substrate (P for peptide) and S denotes the subsites of the enzyme. The numbering of the peptide residues starts on both sides of the scissile bond and increases both towards the *C*-terminal (P1´, P2´, P3´ and so on to the right) and towards the *N*-terminal (P1, P2, P3 and so on to the left). All numbers for the *C*-terminal side are primed. The subsites of the enzyme match the substrate, meaning that the region of the S1´-subsite interacts complementary with the P1´-side chain, the S2´-region with P2´-side chain and so on. If the substrate and the enzyme complement each other, the cysteine residue in the S1-subsite eventually attacks the carbonyl group of the P1 residue. The attack by the S1-cysteine is the first step in the catalytic process which eventually leads to cleavage of a peptide chain.

The general mechanism for such cysteine protease mediated cleavage is outlined in FIGURE 3.[9] For clarity only the cysteine residue of the enzyme is shown, here denoted as enz-S. In all cysteine proteases the thiol group of the cysteine residue is deprotonated by an adjacent histidine residue and these two residues operate together as an ion pair in a catalytic dyad. However, in several other cysteine proteases yet a third residue (either Glu, Asp or Asn) is important for the catalytic activity. The third residue interacts via hydrogen bonding to the His residue to position the imidazole ring or by further increasing the nucleophilicity of the thiolate anion.

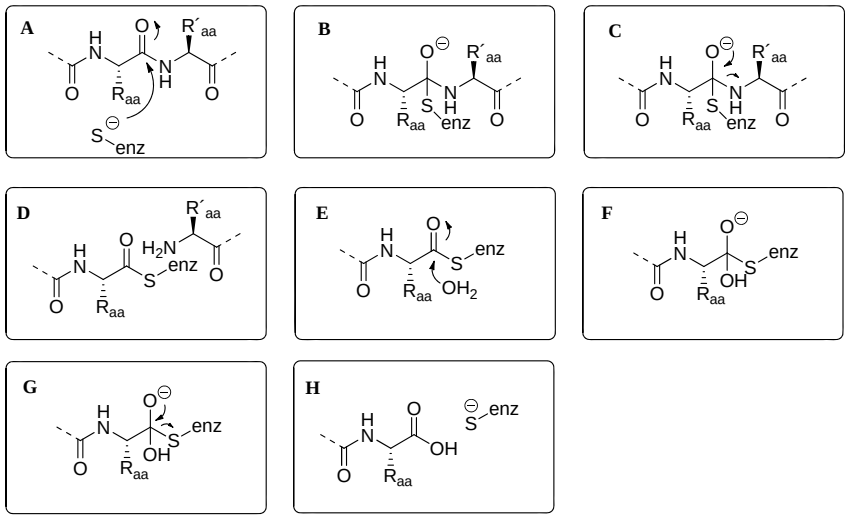

FIGURE 3. Schematic mechanism of the hydrolysis and thus cleavage of a peptide chain mediated by a cysteine protease, here depicted as enz-S.

For example, the Cys-His-Asp residues can operate in a catalytic triad. The imidazole ring of the His-residue mediates the protonation of the amine leaving (FIGURE 3D) and the subsequent

deprotonation of the water molecule (FIGURE 3E). The two tetrahedral intermediates (FIGURES 3B and F) are believed to be stabilized by an oxyanion hole via interactions between the negatively charged oxygen and one or more amino acid residues in the enzyme. This said, a general mechanism as described here should only be considered to be "general" as the catalytic mechanism for cysteine proteases is not yet fully understood in detail and may vary between different proteases.[9-10]

In humans, as much as 26% of all proteases are cysteine proteases.[11] Many physiological processes depend on cysteine proteases.[12] For example, cathepsin B is involved in the metabolic degradation of peptides.[13] Traditionally, cysteine proteases have been attributed to lysosomal activities, but as the knowledge about their physiological functions increases they are also considered as targets for drug development.[14] For example, calpains (C2) are found in brain tissue where they hydrolyze peptides when activated by Ca^{2+} signaling.[15] The physiological function of calpains is poorly understood but proteolytic activities causing tissue degradation in disorders such as stroke, cardiac ischemia and cataract have been proposed.[16] Cathepsin K (C1) is involved in the skeleton renewing process by hydrolytic degradation of old collagen (type I).[12] Imbalance in the degradation and reformation of the bone matrix can lead to osteoporosis, a disease with increased risk of bone fracture. Cathepsin K has been identified as a target for drug development for osteoporosis. Cathepsins are also involved in rheumatoid arthritis, a disease characterized by joint disorders due to inflammation and destruction of bone and cartilage. Another example of bioactive cysteine proteases is the caspases (C14) which are responsible for cell death programming (apoptosis).[10]

Parasitic infections may also be treated by using cysteine proteases as targets for drug development.[12] For example, falcipains have been considered a new potential target for treatment of malaria as they are involved in hemoglobin degradation. Hemoglobin hydrolysis provide amino acids used in the development of the parasite responsible for malaria.[17] Cruzain is involved throughout the life cycle of the parasite responsible for Chagas disease where the host´s heart and nervous system are affected.

One way of regulating an enzyme´s activity is to inhibit the same.

1.2 CYSTEINE PROTEASE INHIBITORS

An enzyme inhibitor is a substance that decreases the rate of an enzyme catalyzed reaction.

As mentioned in the previous chapter, the thiolate anion of a cysteine protease attacks the scissile bond in peptides which eventually leads to a cleavage of the peptide chain.[15] In order to hinder such cleavage an inhibitor can be used. The inhibitor binds to the enzyme and decreases its activity, the classification of inhibitors is based on where and how such binding occurs as well as the type of binding (FIGURE 4).[15, 18] Inhibitors bind either into the active site as active-site directed inhibitors or at another site as allosteric inhibitors. An active site-directed inhibitor can either bind covalently or non-covalently. Covalent inhibitors are electrophiles that are attacked by the nucleophilic cysteine residue in the active site to form a covalent bond which prevents further enzymatic reactions. Non-covalent inhibitors must depend on other interactions in order to remain in the binding site. Electrostatic interactions such as hydrogen bonds, salt bridges, and pi-pi interactions between aryl groups are the most important for protein recognition and binding with high specificity.[18-19]

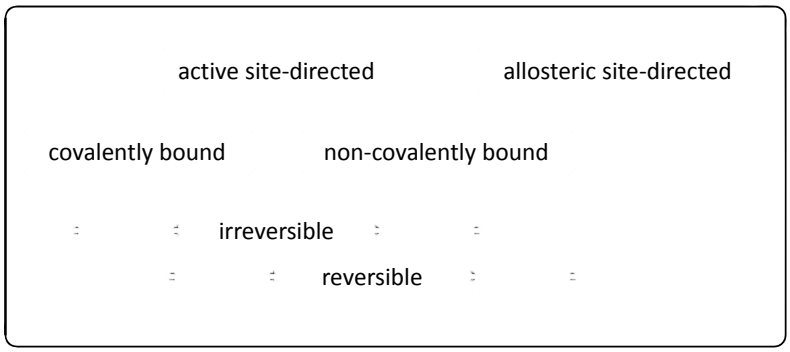

FIGURE 4. The classification of inhibitors is based on how and where they bind to the enzyme. The borders are sometimes difficult to draw, as the mechanism and hence the type of binding is not always known.

Non-covalently bound inhibitors are reversible and the enzyme can be reactivated. Covalently bound inhibitors are either irreversible or reversible. An irreversible inhibitor reacts with the thiol group of the cysteine residue and blocks further modifications. For example, an alkylating agent may act as an irreversible inhibitor as the new bond is stable under biological conditions (FIGURE 5). Yet, other agents may act as reversible inhibitors when the formed adduct is rather labile, for example the equilibrium process between an aldehyde and the enzyme can be reversed to eventually release the free enzyme (FIGURE 5). Alternatively, for an acylated enzyme, the enzyme can be reactivated upon hydrolysis (cf. FIGURE 3D). Such acylating inhibitors are sometimes called tight-binding inhibitors.

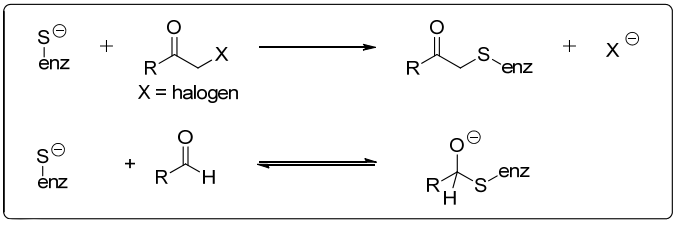

FIGURE 5. Schematic examples of irreversible and reversible inhibitors, both halomethyl ketones and aldehydes form a covalent bond to the enzyme, denoted enz-S.

The residence time is the ultimate limit for the classification of an inhibitor as either reversible or irreversible. If the enzyme-inhibitor adduct is stable enough to withstand hydrolysis, dilution, gel filtration or dialysis the inhibitor is classified as an irreversible inhibitor.[15] Inhibitors can further be classified according to how they bind to the active site compared to the substrate.[18] For example, the classical reversible, competitive inhibitor is competing with the substrate for the active site and must have higher affinity than that of the substrate in order to win. Yet another classification is based on the catalytic mechanism, i.e. mechanism-based inhibitors are analogues either of the substrate, the transition state (i.e. the tetrahedral intermediate) or the product. Another class worth mentioning also acting as irreversible inhibitors is the affinity labeling compounds. An affinity label is an electrophilic agent reacting with the active site residue and was historically used for the ultimate classification of the protease type. The chloromethyl ketones TPCK (tosyl phenylalanyl chloromethyl ketone)[20] and TLCK (tosyl lysyl chloromethyl ketone)[21] have been used as affinity labels (FIGURE 6).

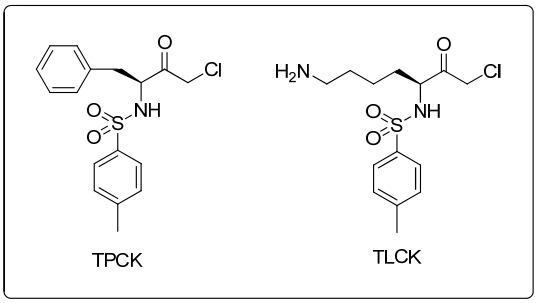

FIGURE 6. TPCK and TLCK are covalent, irreversible inhibitors.

Development of inhibitors targeting cysteine proteases has for long been based on converting the substrate into an inhibitor by replacing the P1-residue with an electrophilic moiety.[22] Often, two to four residues of the substrate is used.[13] The electrophilic functionality in such inhibitor structures is sometimes called the warhead.[22] In 1997 and 2002, two extensive review articles were published listing such warheads used in cysteine protease inhibitors.[15, 22] Warheads such as halomethyl ketones, epoxides and diazomethylketones (sometimes called diazomethane inhibitors and hence abbreviated DAM) connected to short peptides inhibit cysteine proteases irreversibly. Iodoacetate, E-64[23] and Z-LVG-DAM[24] are a few examples of irreversible inhibitors (FIGURE 7).

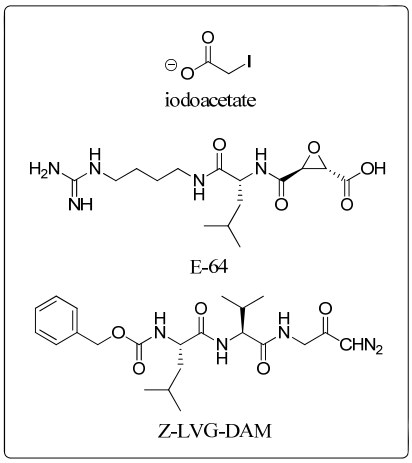

FIGURE 7. Covalent irreversible inhibitors containing different electrophilic warheads.

Iodoacetate is used for quenching enzyme reactions while testing potential inhibitors. The irreversible process is inevitable when the halogen atom is expelled via a nucleophilic attack by the thiolate anion. Depending on the enzyme the interaction between E-64 (or analogues) and the active site orients the inhibitor differently.[22] Either C2 or C3 is attacked when the epoxide is ring-opened via the nucleophilic attack. The detailed mechanism for Z-LVG-DAM is not yet fully understood.[25] Events discussed are for example nucleophilic attack on the carbonyl group, protonation of the CH group by histidine and formation of a three-membered ring in the transition state before N_2 is eventually released. Covalent reversible inhibitors depend on warheads such as aldehydes, nitriles or acylating agents, the intermediates formed differ in geometry dependent on the electrophile (FIGURE 8).[15]

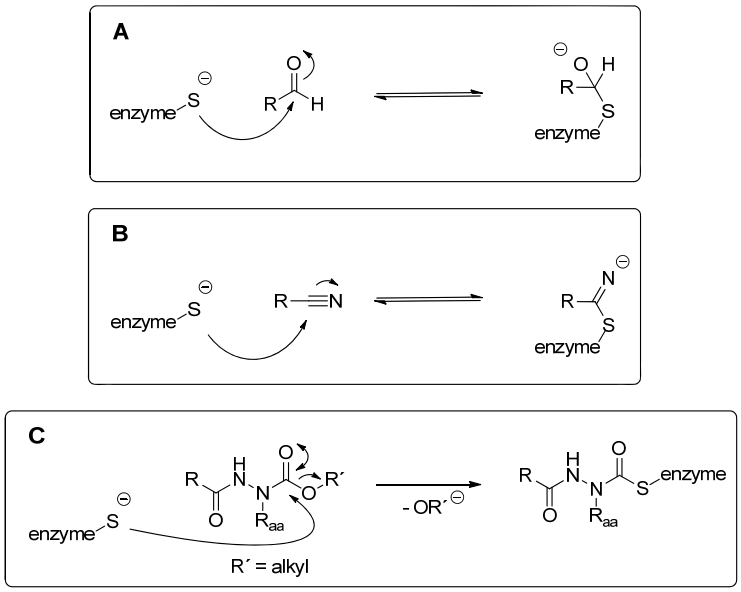

FIGURE 8. Covalent reversible inhibitors forming enzyme adducts with different geometry.

The enzyme and the aldehyde form an adduct which may be stabilized by the oxyanion hole in a similar fashion as the enzyme-substrate complex. The nitriles are said to be weaker inhibitors compared to aldehydes, the stabilization of the different adducts may be the explanation. A general example of an acylating inhibitor is the aza-peptide shown in FIGURE 8. In an aza-peptide one or more α-carbons have been replaced by nitrogen and most often this nitrogen is substituted, i.e. aza-peptides consist of aza-amino acids. The substituted nitrogen alters the 3D structure of the inhibitor and decreases the electronegativity of the scissile bond´s carbonyl group. Sometimes these changes make the adduct more difficult to hydrolyze compared to normal acyl-adducts.[26]

By mining the literature, the latest trends in the development of cysteine protease inhibitors can be seen. In the last five years, about 52 articles within the topic "Cysteine Protease Inhibitors" have been published in Journal of Medicinal Chemistry and Bioorganic & Medicinal Chemistry. More than half of the articles (35) report newly synthesized inhibitors targeting different cysteine proteases such as falcipain (9 hits), cathepsin (7 hits), cruzain (5 hits) and caspase (4 hits). Most of the inhibitors are short peptides or peptidomimetics, only a few consist of non-peptidic structures and most often their inhibitory activity depends on an electrophilic warhead. Despite this, there are a few examples of the contrary. Non-covalent inhibitors which lack the reactive moiety depend instead on specific interactions which tend to be more selective. High selectivity means that other similar targets are not affected and such inhibitors tend to cause less toxicological events. For comparison, the first non-covalent inhibitors based on arylaminoethyl amides were reported in 2002 (cathepsin K) (FIGURE 9A). Then, non-peptidic cathepsin S inhibitors containing a fused piperidine/pyrazole bicyclic system were reported in 2004 (FIGURE 9B). Also, non-peptidic 2-cyanopyrimidines have been reported to inhibit cathepsin K (FIGURE 9C). In 2010 a caspase-1 inhibitor with a secondary amine instead of an aldehyde showed inhibitory activity (FIGURE 9D).

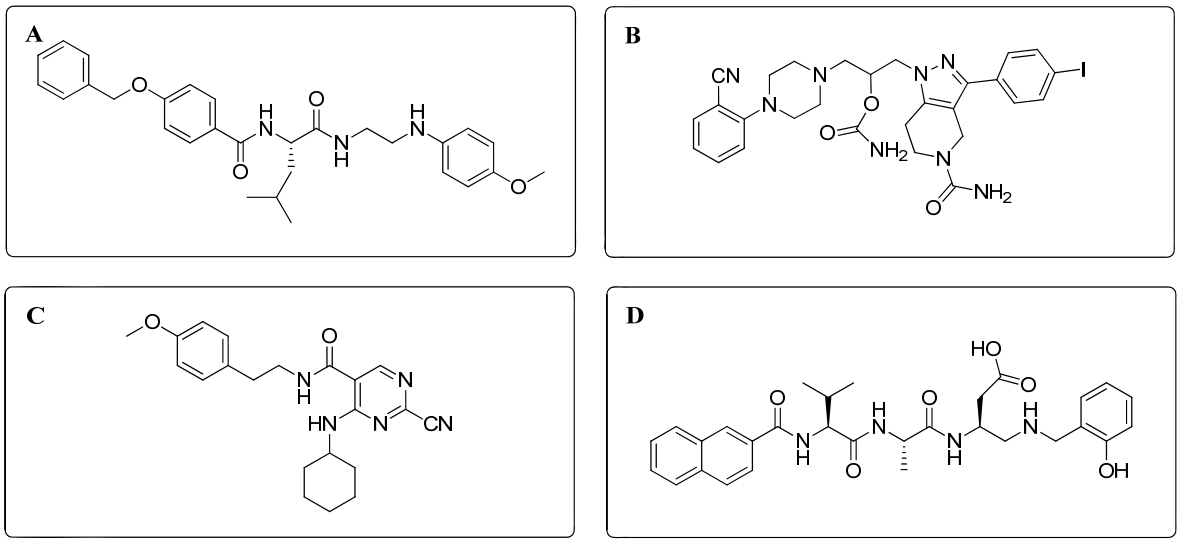

FIGURE 9A-D. Recently published non-covalent and nonpeptide-like cysteine protease inhibitors.

1.3 THREE MEMBERS OF THE CA CLAN

Papain, SpeB and IdeS are cysteine proteases catalyzing the hydrolysis of the same substrate, the human antibody immunoglobulin G (IgG). In this thesis the main focus is set on IdeS, whereas SpeB and papain have been used for selectivity studies.

1.3.1 Papain is a plant cysteine protease found in papaya latex (*Carcia papaya*) in the 1870s.[27] The enzyme is used in manufacture and cooking industry.[28] Papain prevents wool to shrink and is a known meat tenderizer as it hydrolyzes collagen. It also prevents cold haze in beer. Papain is the by far most studied cysteine protease and the 3D X-ray structure of the C_α backbone was solved already in 1968.[29] Many refined structures have been deposited at the protein data bank since then, e.g. PDB ID: 9PAP.[4] The active form of papain consists of 212 amino acids.[9] Residues Cys47 and His159 constitute the dyad responsible for the proteolytic activity, the enzyme is active in a pH range of 4-8. Studies of the catalytic process using one-site mutations of papain where Asn175 was replaced with either glutamine or alanine (i.e. N175Q and N175A) showed that Asn175 enhances the catalytic rate, but is not essential for the activity.[30] Asn175 has been suggested to position His195 into orientations facilitating the catalysis during the different steps of the enzymatic reaction. Further, as the two catalytic residues are located on different domains additional amino acid residues are needed to hold the active site residues in place for the catalytic action. The oxyanion hole in papain consists of Gln19 and the *NH*-group of Cys25. Papain cleaves peptide chains preferentially between Arg or Phe (P1) and Gln (P1´) residues, most often a Leu residue is present at the P2-position but also Phe is tolerated. In fact, papain is able to hydrolyze a wide range of substrates and has a broad specificity.[1, 31] Papain cleaves the human antibody IgG at position 224, between His224 and Thr225. Papain is irreversibly inhibited by iodoacetate, Z-LVG-DAM and E-64, the latter by attack of the epoxide at C2.[22] Also TPCK and TLCK are inhibiting papain, but to different extent.[32] In fact, the difference is as high as 20 times favoring TLCK. Drenth *et al*. report that the Lys residue in TLCK is pointing towards Asp160 present close to the catalytic site.[29]

1.3.2 SpeB (Streptococcal pyogenic exotoxin B, also called streptopain or SCP, Streptococcal cysteine protease) was discovered in 1945 as the first isolated cysteine protease of a prokaryotic

organism.[33] The enzyme is secreted as a zymogen by the bacterium *S. pyogenes* and auto-catalyzes cleavage into the mature SpeB, consisting of 253 residues.[34-35] SpeB is involved in host-patogen interactions and increases the invasive action of *S. pyogenes* by hydrolysis of human fibronectin and vitronectin.[36] It also prevents normal functions of the human immune system by cleavage of M proteins and C5a peptidases. SpeB cleaves the human antibody IgG between residues Gly236 and Gly237 and also other antibodies, such as IgA, IgD, IgE, and IgM.[37] SpeB shows little specificity and is able to hydrolyze peptides with Lys, Asn, Ala and Gly in the P1-position.[1, 31] In P2 most often hydrophobic residues are positioned, while the P2´-residue is most often Val or Phe. SpeB is irreversibly inhibited by iodoacetate, Z-LVG and E-64.

Three 3D structures of SpeB have been deposited at the protein data bank.[38] In 2000, the structure of the inactive zymogen (PDB ID: 1DKI) was published.[34] Two years ago, two structures of the mature enzyme were released. The mature enzyme was either C47S-mutated (PDB ID: 2JTC)[3] or inhibited by E-64 (PDB ID: 2UZJ).[39] The first structure was determined by NMR spectroscopy the latter by X-ray diffraction. The inhibited enzyme mSpeB-E64 crystallizes as a dimer with an interacting area of 1270 $Å^2$ between the two enzyme monomers. The authors speculate that SpeB is activated by forming such a dimer, as His195 is found in the correct position for catalytic activity only in the dimer albeit inhibited form. Indeed, the way the imidazole ring is assigned in the 2JTC-structure there is no hydrogen bond between Cys47Ser and His195. Possibly, by interconversion of the non-assignable nitrogen and carbon atoms in the imidazole ring, a hydrogen bond might exist.[19] The two structures are shown in FIGURE 10. However, to establish whether the dimer hypothesis for SpeB activation is correct or just an artifact from the crystallization needs to be studied in more detail and is beyond the scope of the present study.

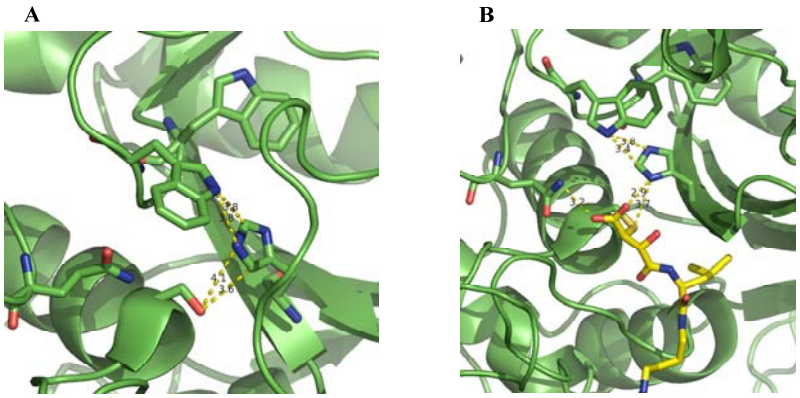

FIGURE 10. 3D structures of SpeB[6] **A)** the C47S-mutated structure (PDB ID: 2JTC); **B)** the E-64 inhibited structure (PDB ID: 2UZJ).

1.3.3 IdeS (Immunoglobulin G-degrading enzyme of *S. pyogenes*, also called **Mac-1**) was discovered by two independent research teams in 2001 and 2002.[40-42] As the name indicates the cysteine protease catalyzes the hydrolysis of the human antibody IgG.[43] IdeS is secreted by *S. pyogenes* as a mature enzyme of 339 residues and is used by the bacterium as a defense mechanism, further discussed in the next chapter.[44]

Already today IdeS has potential medical applications due to its proteolytic activity, it has been shown to block arthritis development induced by IgG.[45] Studies in rabbits also show that IdeS may be used to prevent rejection after renal transplantations by its highly selective degradation of IgG.[46] In addition, autoimmune conditions where IgG labels endogenous compounds as pathogenic may be treated by IdeS injected into the circulatory system.

Studies of the catalytic action of IdeS have been performed using one-site mutations which showed that four residues are involved in the catalytic process, i.e. Cys94, His262, Asp284 and Asp286.[47] When the X-ray structure was solved, the distances between hydrogen bond donor and acceptor groups in C94S - His262 and His262 - Asp284 were measured to 3.5 and 2.7 Å, respectively, indicating that IdeS works via a catalytic triad.[44] It was also seen that the oxyanion hole consists of Lys84 and the backbone of Cys94. The fourth residue Asp286 is also involved in stabilizing the oxyanion hole by interacting with the side chain of Lys84.

Even if mature IdeS is present it does not hydrolyze peptides randomly. IdeS is strictly specific for its substrate and cleaves the peptide chain of IgG between Gly236 and Gly237 (further discussed in the next chapter).[43] A wide range of potential substrates have been tested without detecting any cleavage products. IdeS does not even cleave short peptides resembling the IgG sequence. IdeS becomes irreversible inhibited by iodoacetate, Z-LVG-DAM, TPCK and TLCK but does not react with E-64.

Three crystal structures of IdeS have been deposited at the protein data bank.[38] Two of the structures are mutated forms in which the active site cysteine is replaced by either a serine residue, i.e. C94S (PDB ID: 1Y0A)[44] or an alanine residue, i.e. C94A (PDB ID: 2AVW).[2] The latter structure and the wild-type structure (PDB ID: 2AU1)[2] were refined iteratively.

To summarize, the three cysteine proteases (papain, SpeB and IdeS) show a similar 3D fold. IdeS and papain activities depend on catalytic triads, while SpeB contains a catalytic dyad. SpeB and papain cleave a broad spectrum of substrates while the only identified substrate of IdeS is the IgG antibody. IdeS and SpeB attack IgG at Gly236 while papain cleaves IgG at His224. They are all inhibited by the same compounds (iodoacetate, Z-LVG-DAM, TPCK and TLCK) but IdeS is not affected by E-64. A major feature of IdeS is the presence of the Arg259 residue in the vicinity of the catalytic site, this residue has to move before substrate binding. Such a residue is neither present in SpeB nor papain.

1.4 THE BACTERIA/HOST-SYSTEM – *putting it all together*

The Gram-positive bacterium *Streptococcus pyogenes* colonizes humans and is commonly present in the throat and on the skin.[48] *S. pyogenes* is the causative agent for relatively mild human diseases such as pharyngitis (sore throat) and scarlatania (scarlet fever) as well as of the acute life-threatening conditions sepsis (presence of toxins in blood or tissue), streptococcal toxic shock syndrome (STSS) (hypertension and multiple organ failure) and necrotizing fasciitis (severe muscle breakdown). Moreover, initially mild infections can cause severe complications such as acute rheumatic fever which untreated can lead to serious heart infections. *S. pyogenes* is sensitive towards penicillin and shows no significant resistance. However, in the 1980s sudden unexplainable infections caused by *S. pyogenes* arose worldwide. The only treatment of the more severe and acute state of STSS consists of intravenous injections of the antibody immunoglobulin G (IgG) in high doses.[49] The global burden of Group A Streptococcus (GAS) diseases is difficult to estimate. Population-based data has been used to calculate over 500.000 deaths annually and about 600.000 cases of pharyngitis due to the invasive bacteria.[50]

The antibody IgG is an important part of the human immune system which signals and triggers phagocytosis, i.e. the removal of invading bacteria out of the body. IgG consists of four peptide chains folded into 12 distinct domains (FIGURE 11).[51] The chains are held together by disulfide-bridges (marked as black dots) and several sugar moieties. The two identical heavy chains resemble the shape of the capital letter Y. At the crotch the identical light chains are attached to each heavy chain. This part of IgG is called the F_{ab} region (Fragment antigen binding). Most of

the domains are constant but the two at the top are variable domains. The hinge region is highly flexible and the residues Gly236-Gly237 and His224-Thr225 constitute the scissile bonds for IdeS/SpeB and papain, respectively. In one IgG molecule there is one hinge region consisting of two individual peptide chains. Thus, there exist two scissile bonds for each IgG antibody molecule.

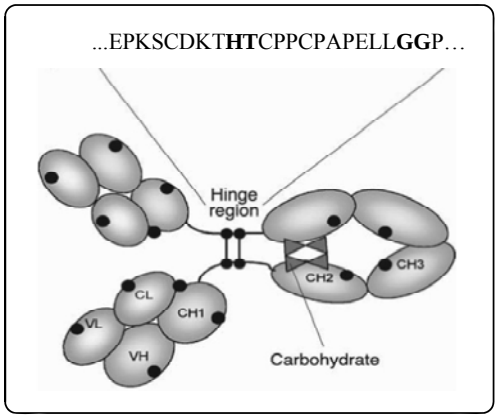

FIGURE 11. Schematic picture of IgG with the residues in the hinge region written out.[43]

The bacterium *S. pyogenes* protects itself by various defense systems to escape from the human immune system, one of these defense mechanisms is outlined in FIGURE 12.[37, 52]

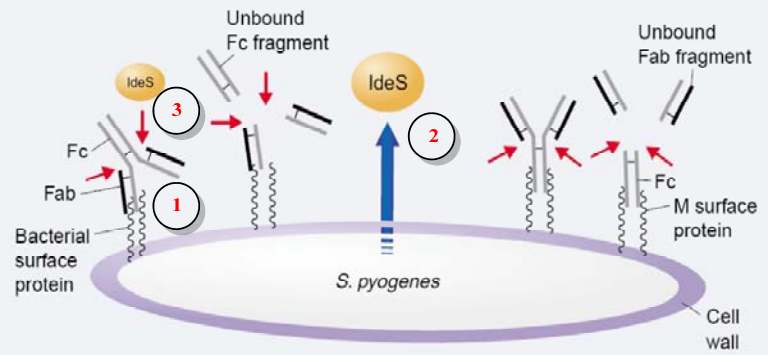

FIGURE 12. Schematic picture of the action of IdeS, modified from reference.[37] On the cell wall of the bacteria the Y-shaped IgG binds to bacterial surface proteins (**1**), this signals to the immune system to remove the invading microorganisms. However, the bacteria secrete IdeS (indicated by a blue arrow) (**2**) which cleave IgG in the hinge region (indicated by red arrows) (**3**). When IgG is cleaved the signaling to macrophages to remove the bacteria out of the body is no longer working. Thus, the bacteria escape the human immune system.

In FIGURE 13, the X-ray structures of IdeS and IgG are shown, in comparison IgG is a large protein. The magenta region of IgG indicates the flexible hinge region where IgG is cleaved by the cysteine proteases.

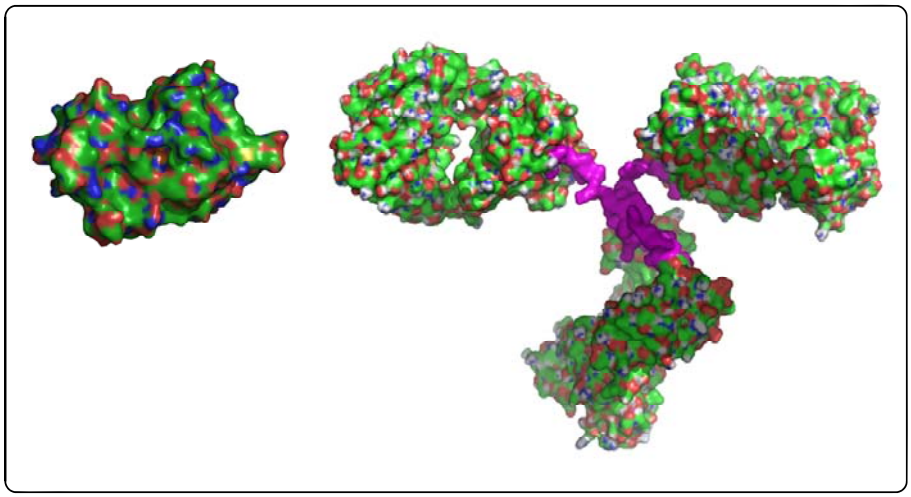

FIGURE 13. X-ray crystal structures of IdeS (left) (PDB ID: 1Y0A) and IgG (PDB ID: 1IGT)[53] (right), both at the same scale.[6]

As mention above, the mechanism of action of IdeS is not yet fully understood. Kinetic studies involving Hill plot analysis show that there are two cooperative binding sites present in IdeS.[43] This can be due to a dimerization of the enzyme. Cooperative binding may be explained by one IdeS-IgG binding event promotes another enzyme to bind to that IgG molecule. In fact, a dimeric structure of IdeS has been revealed by X-ray crystallography (PDB ID: 2AU1) and also detected when using size exclusion chromatography (FIGURE 14).[2]

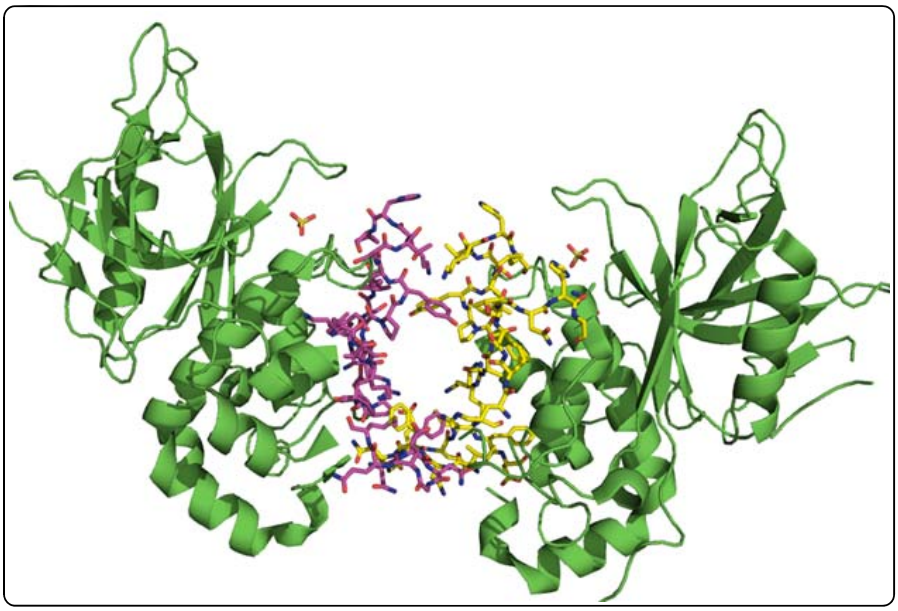

FIGURE 14. Two monomers of IdeS team up as a dimer in the crystal structure (PDB: 2AVW monomer E and F).[6] The residues from each monomer of the interface are colored in either magenta or yellow. A tunnel is seen at the center of the interface.

The surface area buried when two IdeS monomers come together is reported to be as large as 1800 $Å^2$ for each dimer, i.e. 900 $Å^2$ for each monomer interfacing the other monomer. However, the IdeS dimer hypothesis is rejected by Olsen *et al.* saying that the interface is too small for a dimer only being 830 $Å^2$ or even 660 $Å^2$.[39] To aid the analysis of interfaces in true dimers versus interactions due to crystal packing, Janin *et al.* have used 70 examples to identify the

characteristic features of dimers and crystal packing complexes.[54] For a dimer, features such as an interface of 3900 Å^2, 100 residues and as much as 19 hydrogen bonds are usually seen. Weak dimers have, on average interfaces of 1620 Å^2 (but yet smaller interaction areas have been reported) made up of 50 residues but only seven hydrogen bonds, whereas crystal packing interactions are much smaller; 570 Å^2, still consisting of 48 residues and yet only five hydrogen bonds. Thus, if a small interface is seen together with only a few hydrogen bonds, the dimerization is most likely due to crystal packing and is therefore not considered biologically relevant. The interface of the IdeS dimer consists of maximum 19 residues, if counting also the residues being part of a tunnel present perpendicular through the interface. Four residues from one monomer are interacting with the other monomer via hydrogen bonds. In light of the features defined by Janin *et al*., the dimer hypothesis is not likely to be biologically important for IdeS. Further evidences lead to the same conclusion. According to Janin *et al.,* the composition of residues involved in the interface can also aid the analysis. Interfaces are enriched in Met, Tyr and Trp, but highly polar residues such as Lys, Glu or Asp are rarely seen. Also, residues making contact with the same residue from the other monomer are common (as the dimer is made up of two identical monomers). In such pairs, Leu residues are highly represented (known as Leu zippers) followed by Phe, Val and Arg. However, both Arg and Glu are even more likely to match up in a crystal packing interface. Studying the dimer of IdeS, the upper part of the interface is made up by a pair of Tyr residues not interacting (FIGURE 14). Neither do the four present Leu residues (FIGURE 15A).

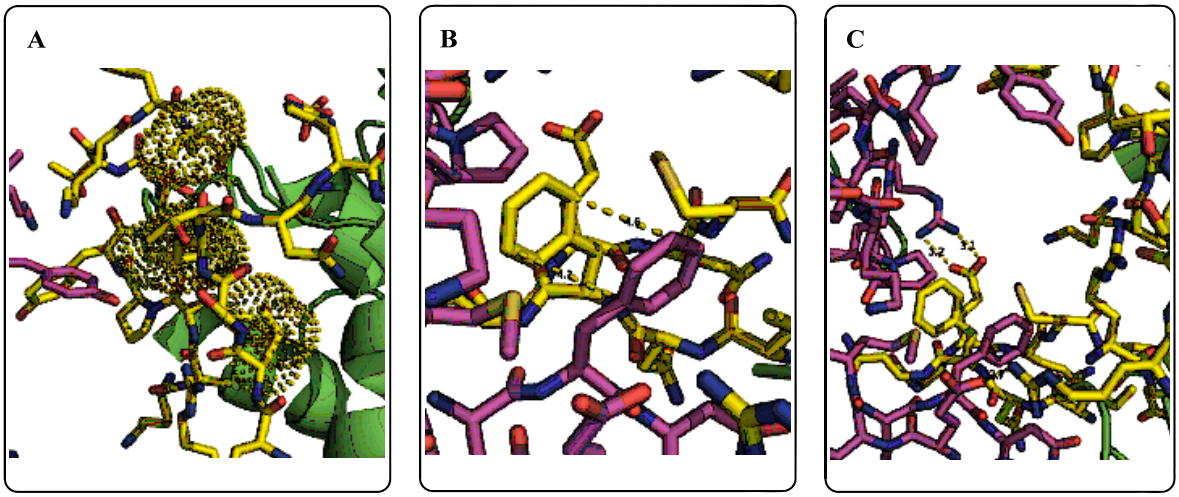

FIGURE 15. Zoomed residues from FIGURE 14, **A)** Leu residues, represented by dots, are not interacting with the other monomer; **B)** The two Phe_{129} from each monomer are interacting; **C)** Salt-bridges are formed across the monomers.

In the lower part of the interface, pairs of both Phe and Met residues are seen. The two aromatic side chains of Phe129 match up in a pi-pi system with a distance of 4.2 Å (FIGURE 15B). However, salt bridges are seen as the polar side chains of Glu132 and Arg185 interact which disfavors the dimer hypothesis (FIGURE 15C). Moreover, according to Janin *et al*. crystals packed as dimers are artifacts only seen when studying structures using X-ray crystallography using highly concentrated solutions. On the contrary, in dilute solutions the monomers are in equilibrium with weak dimers, meaning not all monomers form dimers. Thus, the border between weak dimers and true dimers actually being biologically relevant becomes unclear. The dimerization is speculated to be an activation process for IdeS, as the enzyme is secreted in a mature form and not as a zymogen.[2]

Further, studies with mutated enzymes were used for the dimer elucidation. Results from an IdeS F129I mutant showed less binding between the enzyme and the substrate and also a 200-fold lower catalytic activity than that of the wild-type.[2] This indicates that the Phe129 residue is important both for enzyme-substrate contact and for the catalytic process. But does it really indicate that the dimerization is needed for activity? Most often, proper folding of the enzyme is crucial for activity. Upon mutation the overall structure could be altered and thus weakly inactivating the enzyme anyway. However, the outcome of the Hill plot analysis could also be explained by the presence of an exosite in IdeS.[43] An exosite means that the enzyme and IgG interact also at a remote site different from the catalytic site. In fact, experiments have shown that the product formed after papain cleavage of IgG, with the G_{236}-G_{237} residues still present, is further hydrolyzed by IdeS. This and also the high degree of specificity observed for IdeS add arguments for the presence of an exosite. Finally, also the presence and function of the Arg259 residue has to be explained as it must move in order to reveal the catalytic site for IgG before the proteolytic process can begin.

Taken together, both the dimer and exosite hypotheses need to be further investigated in order to understand the detailed mechanism of IdeS proteolytic ability.

2. AIM

The aim of this thesis was to synthesize and identify compounds with the capability to selectively inhibit IdeS, a bacterial cysteine protease. Such compounds could be useful in further investigations aiming to elucidate the mechanism of IdeS. A compound structurally similar to the substrate could be useful for X-ray structure determination of active IdeS. Further, a selective inhibitor of IdeS might aid the development of therapeutic IdeS treatments.

In order to develop selective inhibitors of IdeS, the focus was first set to reversible inhibitors. Then, the overall strive was to avoid the covalent bond-dependency. Non-covalently bound inhibitors were aimed for in a substrate-based approach wherein peptide analogues were synthesized and evaluated. To increase the potency of the inhibitors the strategy to decrease their conformational flexibility was undertaken and bicyclic derivatives came into focus.

In this thesis the following actions were undertaken:

- Development of synthetic routes and synthesis of *p*-tosyl amino derivatives with reversible functions as warheads and to screen their IdeS inhibition capability (PAPER I)
- Development of synthetic routes using the 3-aminopiperidine fragments in a substrate-based approach, and to screen such peptide analogues for their IdeS inhibition capacities (PAPER III)
- Improvement of the potencies of identified 3-aminopiperidine-based inhibitors by reducing the conformational flexibility by developing synthetic routes towards bicyclic compounds and screen those (PAPER IV)
- Evaluation of the selectivity profile of the identified IdeS inhibitors towards the related cysteine proteases papain and SpeB (PAPER III, IV)
- Investigation of the stereoselectivity in reductive aminations with 3-aminopiperidone and different amino acids esters used in the synthetic route to 3-aminopiperidine based peptide analogues (PAPER II)
- Attempted usage of computational studies to try to understand the different inhibition profiles of peptides and peptide analogues (included in the work of PAPER III)

3. INTRODUCTION

3.1 INTRODUCTION TO THE TPCK/TLCK ANALOGUES (PAPER I)

The development of inhibitors against IdeS started with the aim to avoid the need of an irreversible covalently bound warhead. In order to find selective inhibitors, which have more specific interactions with the enzyme, the focus was first set to reversible inhibitors. The inhibition potency of TPCK and TLCK against IdeS have been reported but without detailed data.[55], papain is affected differently by the two inhibitors.[32] This fact arouses questions like: Is the warhead alone responsible for all inhibitory effect of IdeS? and Does the R-group substituent contribute to the binding to IdeS? The design of potential reversible inhibitors of IdeS was based on the structures of TPCK and TLCK and by decreasing the reactivity of the warhead it was anticipated that the contribution of the side chain would show. The *p*-tosylamido function was kept whereas both the side chain R-groups and warheads were varied (FIGURE 16). To challenge the need of the amino group in TLCK norleucine, also called *n*-butylglycine was used. The azide function had recently been shown to inhibit caspase-1 (cysteine proteases with a strict need for an Asp residue in P1-position) and was therefore included.[56] The alcohol was included to challenge the overall need of a warhead.

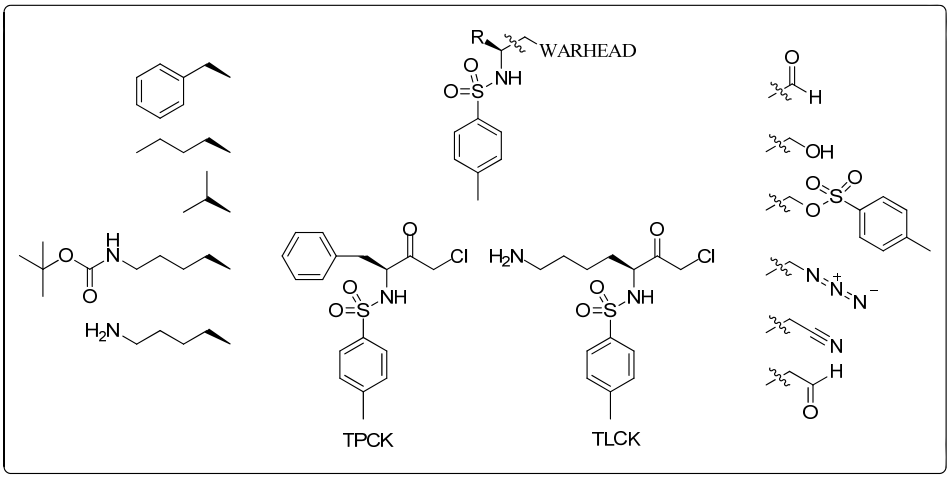

FIGURE 16. R-substituents and warheads used in the TPCK/TLCK analogues. All combinations were aimed for.

3.2 INTRODUCTION TO PIPERIDINE-BASED ANALOGUES (PAPER III)

IdeS catalyzes the hydrolysis of the peptide bond between G_{236} and G_{237} in the hinge region of IgG, but it cannot cleave short peptides containing the same amino acid sequence covering the GG sequence in IgG.[44] If short peptides are not hydrolyzed, can they still interact with IdeS, prevent IgG to bind and thus inhibit IdeS? To answer this question a series of di-, tri- and tetrapeptide analogues based on either the LLGG or the LGGP sequences were synthesized and tested for potential inhibitory activity. In the analogues one of the two glycine residues was replaced by a piperidine moiety thus forming either pip_{236}G- or Gpip_{237}-fragments (FIGURE 17). The 3-aminopiperidine fragment has not been used in a peptidomimetic strategy before. As a new stereogenic center was introduced in the peptide analogues (marked with an asterisk in FIGURE 17) the resulting enantiomers or diastereomers were aimed to be tested separately. Also, eight peptides of different length covering P_4-P'_4 of the IgG sequence were purchased and tested for their ability to inhibit IdeS.

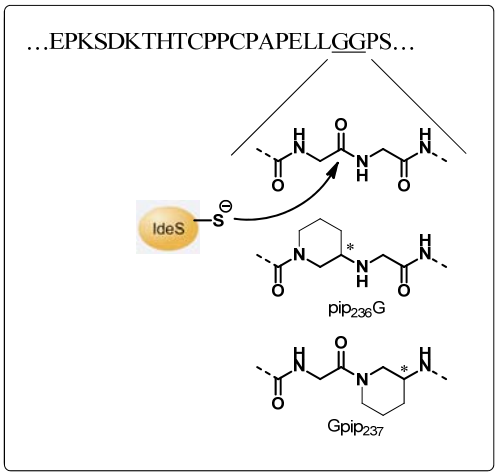

FIGURE 17. In the synthesized di-, tri- or tetrapeptide analogues of the hinge sequence of IgG a piperidine moiety replaces either the Gly_{236}- or Gly_{237}-residue of the scissile bond. The new stereogenic center present in the peptide analogues is marked with an asterisk.

3.3 INTRODUCTION TO BICYCLIC DERIVATIVES (PAPER IV)

The results from the inhibition assay performed with the piperidine analogues showed that $Lpip_{236}G$ and $pip_{236}G$ acted as IdeS inhibitors. Therefore, in order to increase the potency a project was started aiming for potential inhibitors with a more rigid structure. The strategy was to fuse another ring onto the piperidine moiety (FIGURE 18).

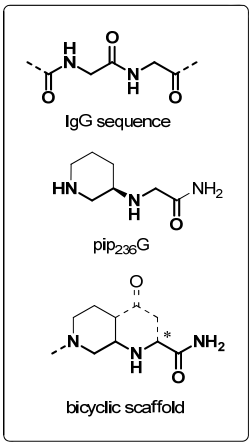

FIGURE 18. The substructure of $pip_{236}G$ was kept in the bicyclic scaffold. Another ring fused onto piperidine would increase the rigidity and possibly the potency of the potential bicyclic inhibitors.

Features such as control of the stereogenic center, opportunity for elongation both *C*- and *N*-terminally and avoidance of peptide bonds were desired. In fact, somewhat related compounds have been synthesized as dimers and also pentamers, so called @-tides (FIGURE 19).[57-58] NMR spectroscopic studies of the @-tides indicate that they have hydrogen bonding capacity in a linear fashion, thus resembling β-strands.[58] In fact, proteases have been reported to interact with peptides adopting extended conformations in their active site.[59]

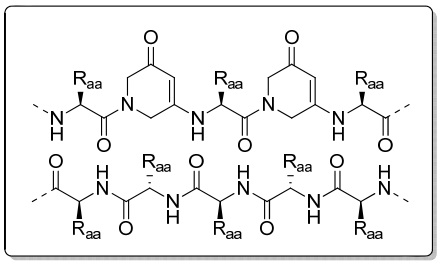

FIGURE 19. A penta-@-tide is constituted by three amino acid residues held together by two piperidone-based fragments abbreviated as @. As shown, the penta-@-tide may form six hydrogen bonds to a schematic peptide.

The two bicyclic systems shown in FIGURE 20 may have capacity to interact with a protein structure (such as IdeS) and thus act as inhibitors of IdeS.

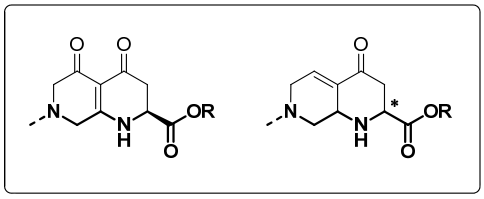

FIGURE 20. Starting points for the synthesis of bicyclic scaffolds.

4. SYNTHESIS

4.1 SYNTHESIS OF TPCK/TLCK ANALOGUES (PAPER I)

The chemistry shown in the following chapter is based on functional group transformations. For example, starting from an α-amino acid alcohol both the corresponding aldehyde and its higher homolog might be synthesized via several synthetic steps. The key step is the nitrile formation which introduces an additional carbon atom.

The synthetic route to the TPCK analogues in which R represents either benzyl, *n*-butyl or *i*-propyl is shown in SCHEME 1. Along the presentation of the reaction pathways examples from the literature covering similar reactions will be added and discussed.

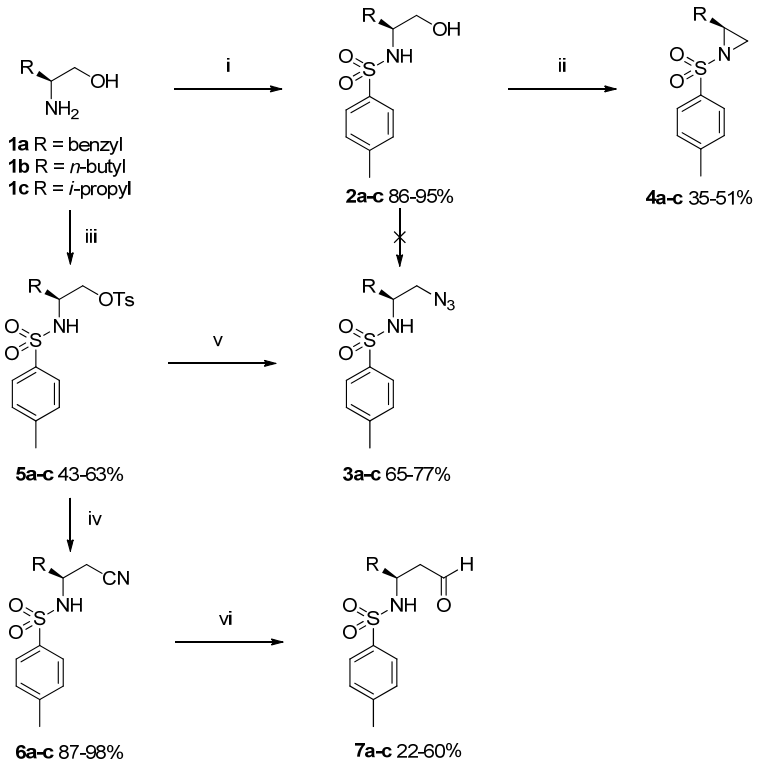

SCHEME 1. Synthetic route to TPCK analogues. *Reagents and conditions:* (i) TsCl (1 equiv.), Et_3N, DMAP, DCM, 0 °C => rt, on; (ii) PPh_3, DIAD, DCM; (iii) TsCl (2 equiv.), pyridine, DCM, 0 °C => rt, 6 h; (iv) NaCN (2 equiv.), DMSO, 35 °C, 6 h or on; (v) NaN_3 (2 equiv.), DMSO, 35 °C, 6 h or on; (vi) DIBAL-H in toluene, -65 °C, 50 to 90 min.

Initially, the free amino group in L-phenylalaninol, L-norleucinol and L-valinol (**1a-c**) was reacted with tosyl chloride mediated by triethylamine and DMAP to form *N*-tosylated alcohols (**2a-c**) (86-95%).[60] Interestingly, in the literature other amino alcohol derivatives were both *N*- and *O*-tosylated using the same conditions. In order to afford the desired mono-tosylated product, it was reported that the alcohol moiety in the example shown in SCHEME 2 had to be protected prior to the *N*-tosylation and consequently deprotected afterwards.[61]

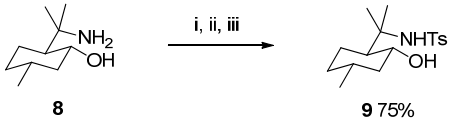

SCHEME 2. Literature example of *N*-tosylation via TBDMS-protection. *Reagents and conditions:* (i) 1) *n*-BuLi, diethyl ether, -78 ºC; 2) TBDMSCl, diethyl ether, -78 ºC; (ii) TsCl, Et_3N, DCM; (iii) TBAF x $3H_2O$, THF.

An example of a chemoselective reaction is showed in SCHEME 3 where *N*-tosylation is favoured over *O*-tosylation affording **11a**.[62] As the nitrogen is more nucleophilic the *N*-tosylation is much faster than the corresponding reaction with the alcohol and protecting group chemistry is in most cases not needed. However, the selectivity is highly dependent on the substrate. The phenylglycine derivative needed *O*-protection of the two alcohol functions to afford the desired product **11b**.

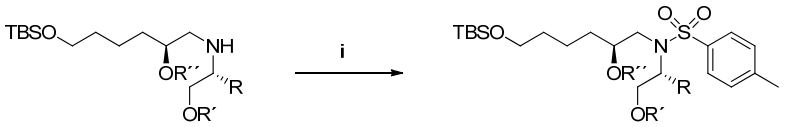

10a R = Me, R´ = R´´ = H
10b R = Ph, R´ = R´´ = TMS

11a R = Me, R´ = R´´ = H 75%
11b R = Ph, R´ = R´´ = TMS 99%

SCHEME 3. Literature example of *N*-tosylation without and with the need of *O*-bisprotection.[62] *Reagents and conditions:* **11a:** (i) TsCl (1.1 equiv.), Et_3N (2 equiv.), DCM, 0 ºC; **11b** (i) TsCl (4 equiv.), pyridine and Et_3N (2 equiv.), DCM, 15 h.

The route to the TPCK analogues continued with attempts to convert the alcohols (**2a-c**) to the corresponding azides (**3a-c**) (SCHEME 1). In the literature, Mitsunobu conditions and Fmoc-protected L-amino alcohols afforded azides (80-87%) (SCHEME 4).[63]

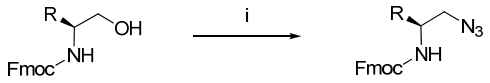

12a R = *i*-propyl-
12b R = $PhCH_2$-
12c R = $BocNH(CH_2)_4$-

13a-c 80-87%

SCHEME 4. Example of azide formation.[63] *Reagents and conditions:* (i) PPh_3, DEAD, HN_3.

Surprisingly, in the reactions in SCHEME 1 between **2a-c** and NaN_3 mediated by PPh_3 and DIAD, aziridines **4a-c** were instead formed (SCHEME 1). This was confirmed by ^1H NMR spectra that showed no peak for the sulfonamide N*H*-proton. In contrast to the Fmoc-protected precursors, aziridine formation has been observed for several Boc-protected L-amino acids also using Mitsunobu conditions with yields in the 73-86% range.[64] So, aziridine formation occurs with β-amino alcohol derivatives when a sufficiently strong base promotes a nucleophilic attack by the nitrogen onto the β-carbon carrying a good leaving group in the right position to be expelled in an S_N2-fashion (SCHEME 5A).[65] The choice of protecting group seems to contribute to the different reaction outcomes.

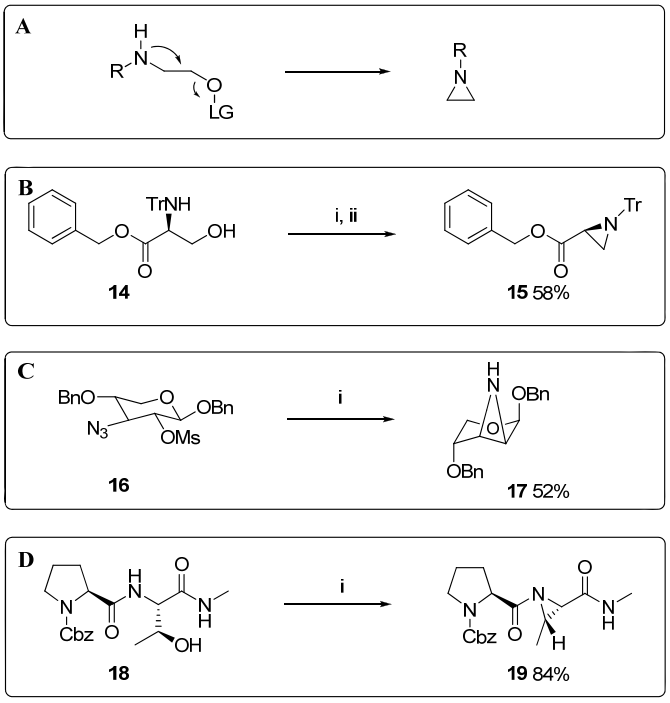

SCHEME 5. A) General reaction mechanism for aziridine formation. Literature examples of aziridine formation **B**) (i) TsCl, pyridine 0 ºC, 24 h, (ii) Et_3N, THF, reflux, 24 h; **C**) (i) $LiAlH_4$; **D**) (i) PPh_3, DIAD, THF.

A good leaving group may be mesylate, sometimes tosylate and as experienced here, a phosphine oxide. Some literature examples of aziridine formation are given; *N*-trityl protected L-serinol benzyl ester **14** was converted to the mesylate derivative and under basic conditions (Et_3N) in refluxing THF the aziridine **15** was formed (SCHEME 5B).[66] A 4-azido pentos derivative (**16**) was reduced to the primary amine, after ring inversion the amine could expel the mesylate and the aziridine **17** was formed (SCHEME 5C).[67] In a prolyl-threonine derivate, the amide-nitrogen expelled the phosphine oxide to form the aziridine **19** (SCHEME 5D).[68]

With the confirmed aziridine formation in hand, attempts to compete with the intra-molecular ring closure reaction were made. Starting from the alcohol (**2b**, **2c**) the reaction was performed with an excess of NaN_3 (3 and 10 equiv.) using Mitsunobu conditions (SCHEME 1). However, the aziridine (**4b, 4c)** was still obtained as the only product. Probably, the azide ion worked as a base and facilitated the ring closure.

Since both cyanide and azide ions are nucleophiles the tosyl-substituted aziridine may eventually be ring opened, however occasionally without satisfying regioselectivity.[69] Most often, the unsubstituted methylene is attacked (SCHEME 6, route A) but also the substituted sterically hindered carbon can be attacked (route B) and then mixtures of regioisomers are formed. Of course, if both aziridine carbons are substituted the regioselectivity issue is even more pronounced.

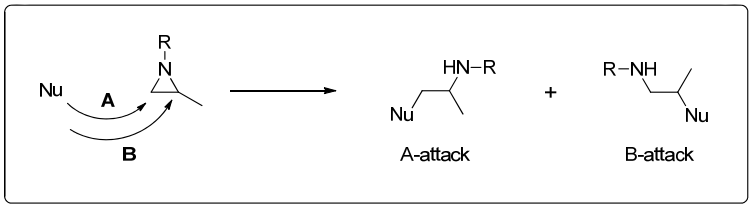

SCHEME 6. General mechanism for aziridine ring opening. Nucleophilic attack via either route **A**) or **B**) affords different regioisomers. Mixtures of the two regioisomers may be formed.

When TMSCN or $TMSN_3$ are used together with TBAF to initialize the aziridine ring-opening reactions, high yields and high regioselectivities have been reported.[70] However, nosyl-activated aziridines can be ring-opened directly with NaCN.[71]

However, in order to avoid mixtures of regioisomers, the route in SCHEME 1 had to change directions. The L-amino alcohols (**1a-c**) were instead ditosylated to afford **5** (43-63%) by using two equivalents of TsCl (SCHEME 1).[72] Pyridine was used as base in order to minimize the risk of aziridine formation. Now, no such products were obtained.

Displacement of the OTs group in (**5b**) by KCN or NaCN in DMF did not result in any nitrile formation despite the fact that high yields of nitriles were reported in the literature.[72] This could be due to the very low solubility of KCN in DMF. The solubility issue has also been recognized by others who instead used Bu_4NCN in ethyl acetate to displace a mesylate.[73] In our hands this did not give satisfying results. Likewise, the usage of Bu_4NBr and NaCN to form Bu_4NCN *in situ* was tested together with tosylester **5,** but did not show promising results.[73] Fortunately, NaCN dissolves readily in DMSO. Sobolewki *et al.* reported 65% yield when using NaCN in DMSO for the S_N2 reaction to afford Boc-PheCH_2CN.[74] For the ditosylated starting material **5a-c** full conversion was obtained when using NaCN in DMSO with gentle heating (35 ºC) which afforded the nitriles **6a-c** (87-98%) (SCHEME 1). The obtained yield was higher than previously reported and no further purification was needed.

The same conditions were used for the azide formation (**3a-c**) using NaN_3 in DMSO (65-77%) (SCHEME 1). The nitriles (**6a-c**) were further converted to the corresponding aldehydes (**7a-c**) (SCHEME 1). Not only has the reaction to be carefully handled as such, also the work-up procedure needs some consideration. DIBAL-H is sold as a solution in a variety of solvents (DCM, THF, or toluene). Often, methanol is used to quench the excess of reagents after the reaction. Methanol also breaks the gelatinous Al-based complexes often formed before the acidic hydrolysis to the product takes place. In order to isolate the product the extraction process has to be optimized. However, quenching the reaction with either methanol/water, citric acid or tartaric acid did not provide any satisfying results.[75-76] With help from the author of the paper reporting a DIBAL reduction of the very same substrate in 85% yield, the work-up procedure was sorted out.[77] Finally, cold acetone was used for quenching the reagent and breaking the Al-complexes. Subsequent hydrolysis with diluted HCl gave the desired aldehydes (**7a-c**), although in low to moderate yield (22-60%) after flash chromatography.

Since ε-protected L-lysinol is not commercially available the beginning of the route described in SCHEME 1 had to be modified in order to obtain the corresponding TLCK analogues. Initially, attempts were made to reduce the carboxylic acid moiety of ε-Cbz protected L-lysine (**20**) by $LiAlH_4$ followed by tosylation aiming to get **22** (SCHEME 7). Instead, a by-product (**23**) was formed (SCHEME 7). Apparently, the Cbz-group had also been reduced to a methyl group due to the harsh conditions during the $LiAlH_4$-reduction. Both the newly formed secondary amine and the primary amine became tosylated. *N*-Methylation from Cbz-protected precursors has been reported earlier.

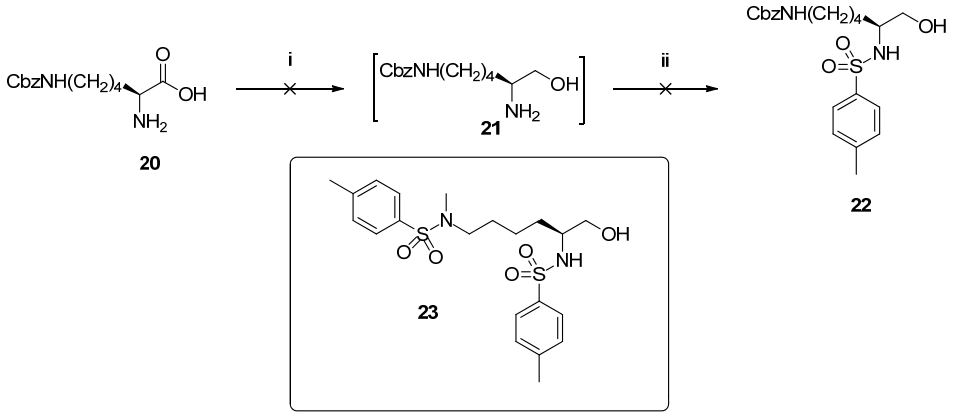

SCHEME 7. The expected product **22** was not formed, instead **23** was isolated. *Reagents and conditions:* (i) $LiAlH_4$, THF; reflux; (ii) TsCl (1 equiv.), Et_3N, DMAP, DCM, rt, on.

When lowering the temperature the reaction did not go to completion. Reduction by $LiAlH_4$ at 0 ºC and direct ditosylation gave too low yield. The strategy was abandoned and the focus was set to other alternatives.

Textbooks in organic chemistry claim that an ester functionality needs a powerful reducing agent such as $LiAlH_4$ in order to react. It is also claimed that esters are reduced by $NaBH_4$, although so slowly that the reaction is not practical to use. However, several exceptions have been reported[78] and discussions of $NaBH_4$-reductions of esters have been on-going for long.[79] Accordingly, $NaBH_4$ reduction of sulfonamide protected phenylalanine methyl ester was reported to give the corresponding alcohol in 91% yield.[80]

As experienced, Cbz-groups are being labile at reducing conditions but as the Boc-group is known to be more stable the choice of protecting group was reconsidered. Also, the *N*-tosylation reaction was put first in the synthetic route to the TLCK analogues. The free amine in ε-Boc-lysine methyl ester (**24**) was converted into sulfonamide **25** (95%) (SCHEME 8).

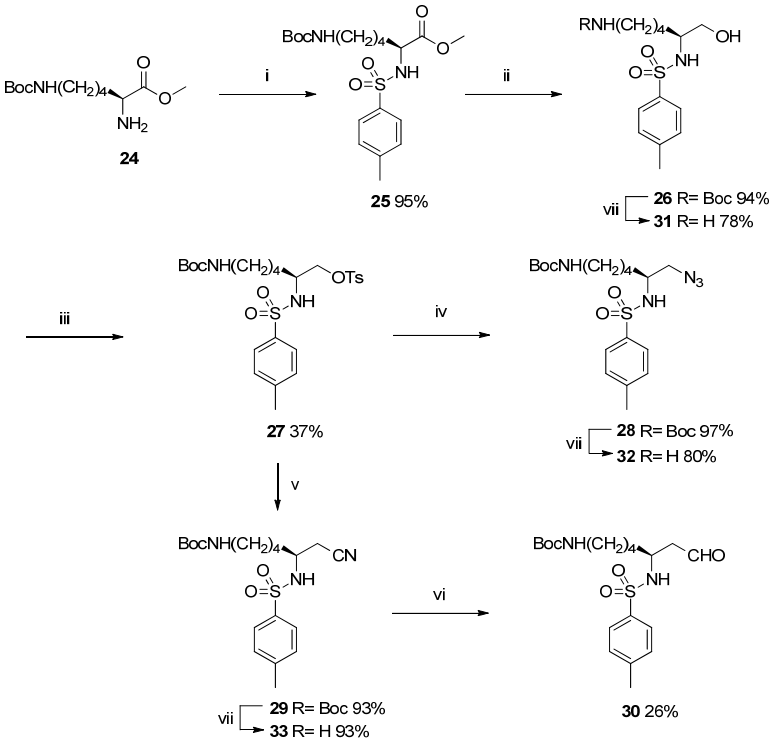

SCHEME 8. Synthetic route to TLCK analogues. (i) TsCl, Et_3N, DCM, 0 °C => rt, on; (ii) $NaBH_4$, THF:ethanol, 0 °C => rt, on; (iii) TsCl, pyridine, DMAP, DCM, 0 °C => rt, on; (iv) NaN_3 (2 equiv.), DMSO, rt, on; (v) NaCN (2 equiv.), DMSO, 35 °C, on; (vi) 1) DIBAL-H in toluene, THF, -65 °C, 45 min., 2) dilute aq. HCl; (vii) TFA/DCM, rt, 60-90 min.

Then the methyl ester was reduced by $NaBH_4$ to afford alcohol **26** (94%). Subsequent *O*-tosylation of **26** afforded the ditosylated derivative **27** (37%). Again, pyridine was needed as the base in order to avoid aziridine formation. The ditosylated derivative (**27**) could now be used in the same manner as described for the synthesis of the TPCK analogues, i.e. the *O*Ts-group was expelled by either NaN_3 or NaCN to give azide **28** or nitrile **29**, respectively. The nitrile (**29**) was further converted via DIBAL-H reduction and acidic hydrolysis to aldehyde **30**. The Boc-protecting group of **26**, **28**, and **29** was removed by TFA/DCM to afford **31**, **32** and **33**, respectively.

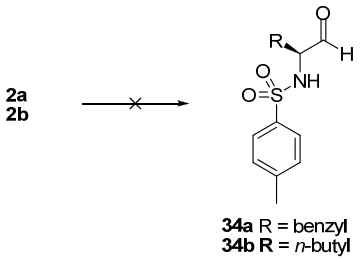

SCHEME 9. Unfortunately, attempts to reach aldehydes **34a** and **34b** were not successful.

Additionally, some attempts were also made to synthesize the L-amino aldehydes (**34a**, **34b**) (SCHEME 9). However, gentle oxidation of *N*-Ts protected L-amino alcohol by either Dess-Martin periodinane, or Swern oxidation did not show satisfying results. Although such aldehydes are known in the literature either as starting materials or intermediates, they are not used as final products. Moreover, the nucleophilic properties of the sulfonamide have been shown to cause unexpected reactions and formation of dimers.[81] The Dess-Martin protocol showed conversion of

the starting material but the product could not be isolated in the high purity requested for compounds used in biological assays. Due to the acidic properties of the sulfonamide the intermediate did not react as expected and by-products were obtained.

In these highly convergent synthetic routes several TPCK/TLCK analogues were synthesized, which were tested for inhibition capacity, further discussed in the evaluation chapter.

4.2 SYNTHESIS OF PIPERIDINE ANALOGUES (PAPER II and III)

This chapter is divided into five sections, starting with formation of the new stereogenic centre by reductive amination, via a study of stereoselectivity in such reductive aminations followed by calculations of conformational distributions, and finally the synthesis of the piperidine-based analogues.

4.2.1 Reductive amination-formation of new stereogenic centre

Peptide synthesis is inevitably a sequence of repetitive processes, so is also the synthesis of the di-, tri- and tetrapeptide analogues of LLGG and LGGP in this thesis (FIGURE 21). The sequence starts with connecting the piperidine moiety to the amino acid that follows Gly_{236} or Gly_{237} in the IgG sequence (either glycine or proline), and thereby a new stereogenic centre is formed. Thereafter, the $pip_{236}G$ moiety is coupled to L-proline *C*-terminally. Finally, the *N*-terminal L-amino acids are coupled.

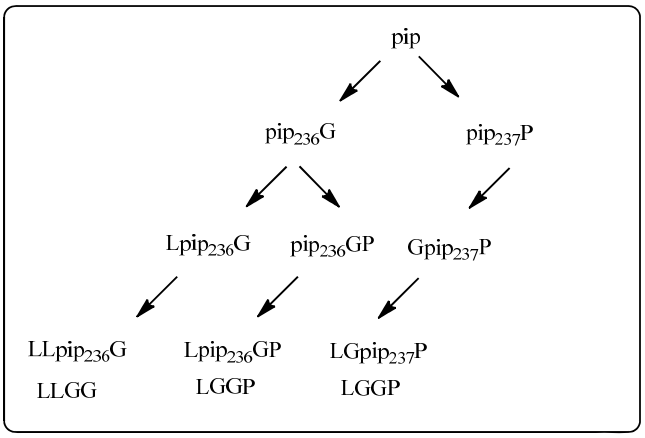

FIGURE 21. The schematic route for synthesis of peptide analogues. By forming the stereogenic center in the first reaction, the absolute configurations in all the following compounds will be known, provided that no racemization occurs.

Reductive amination between Boc-protected 3-piperidone **35** and ethyl glycinate **36** was used to synthesize the pip_{236}Gly-fragment of the peptide analogues. The unsymmetrical ketone is prochiral and upon imine formation and subsequent reduction a stereogenic centre is formed and the racemic product (*rac*)-**37** was collected (76%) (SCHEME 10).

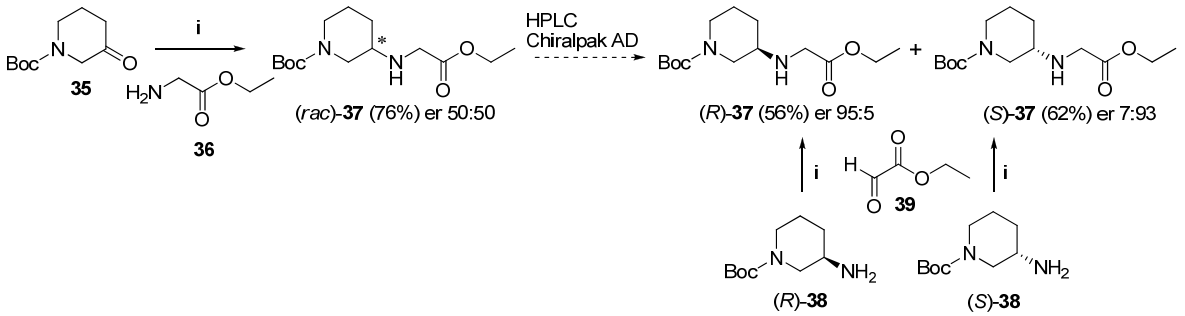

SCHEME 10. Synthesis of $pip_{236}G$. *Reagents and conditions:* (i) $NABH(OAc)_3$, AcOH, DCM, rt, on.

The pip_{236}Gly-fragment can also be synthesized by reductive amination using interchanged functionalities of the starting materials. The stereogenic centre is unchanged while amine (*R*)-**38** reacts with ethyl glyoxylate (**39**) to form (*R*)-**37** with an enantiomeric ratio (er) of 95:5 (SCHEME 10). The enantiomer (*S*)-**37** was also synthesized, with a somewhat lower er 7:93 (SCHEME 10). The reason for not obtaining enantiomerically pure products in these reactions might be due to not strictly enantiopure starting materials. The ratio was considered to be too low to be useful for synthesis of the piperidine-based inhibitors. However, the two enantiomers synthesized from the 3-piperidone (**35**) could be identified by the samples from the reactions starting from the 3-aminopiperidine ((*R*)- and (*S*)-**38**) and comparison of the retention times from HPLC (chiralpak AD) analysis, so called chemical correlation.

Reductive amination is the reaction between either ammonia, a primary or a secondary amine and a ketone or an aldehyde to form primary, secondary or tertiary amines via an imine intermediate which is seldom isolated.[82] The reaction is a two-step process in which the nitrogen of the amine attacks the carbonyl carbon and water is expelled to form an imine (either aldimine or ketimine) which is subsequently reduced to afford the product.

Also for the $Gpip_{237}$ analogues the formation of the new stereogenic center is the first step in the route. The reductive amination between **35** and L-proline amide **40** affords **41** with a diastereomeric ratio (dr) of 59:41 (68%) (SCHEME 11). When a secondary amine reacts with a ketone and water is expelled the formed intermediate is a tertiary iminium salt. The iminium salt may eventually be deprotonated to form the more stable enamine. However, enamines are not reduced by the hydrides used for reductive aminations, as the following example shows.

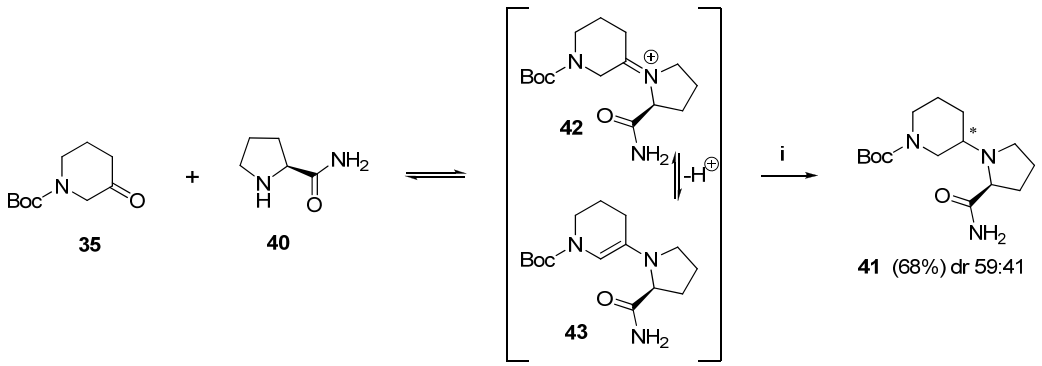

SCHEME 11. Synthesis of $pip_{237}P$ leading to $Gpip_{237}$ analogues. *Reagents and conditions:* (i) $NaBH(OAc)_3$, AcOH, DCM, rt, on.

The double bond electrons in enamine **44** is prevented to migrate to the nitrogen as the nitrogen is already fully substituted (SCHEME 12). The enamine was not reduced to the corresponding

saturated cyclohexyl derivative by a traditional hydride reagent, L-selectride (LiBH(*sec*-butyl)$_3$).[83] Enamine formation is usually suppressed in an acidic environment.

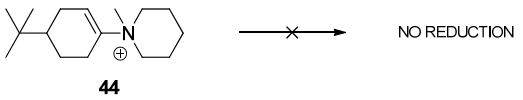

SCHEME 12. Literature example showing evidence for non-reducible enamines. The enamine is unable to rearrange into the corresponding iminium ion needed for the reduction. LiBH(*sec*-butyl)$_3$ was used as the reducing agent.[83]

4.2.2 Study of stereoselective reductive aminations (PAPER II)

Stereoselectivity is applicable for reactions when two stereoisomers are formed and one of the two is favoured. An iminium salt (**45**) structurally similar to the intermediate **42** shown in SCHEME 11, but now derived from asymmetric 3-methylcyclohexanone and symmetric pyrrolidine is attacked by $NaBH_3CN$ to form **46**:**47** in a ratio of 74:26, favouring equatorial attack and hence the axial amine (86%) SCHEME 13.[83] For comparison of structures and ratios, some more examples are shown.

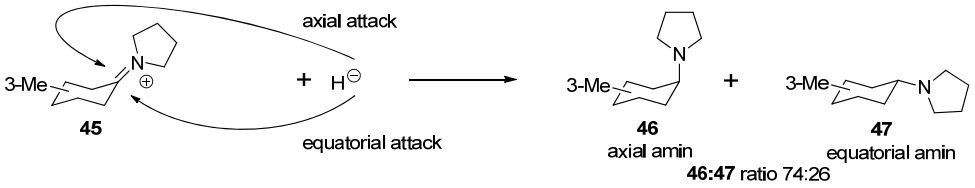

SCHEME 13. Literature example of diastereomers formed in a reductive amination using $NaBH_3CN$ as reducing agent.[83]A hydride attack from the equatorial direction forms the axial amine, whereas when the hydride attack comes from the axial direction the equatorial amine is formed.

Reports of asymmetric synthesis to afford both natural and new amino acids are extensive in the literature, but the use of amino acid esters as starting materials in a reductive amination is sparse. However, an example of reductive amination using an oxo-proline derivative (**48**) which directs the hydride attack ($NaBH_3CN$) of the intermediate imine to the opposite side of the *t*-butyl ester moiety, the reaction results in a dr of 87:13 of (*SS*)-**50**:(*RS*)-**50** (SCHEME 14).[84]

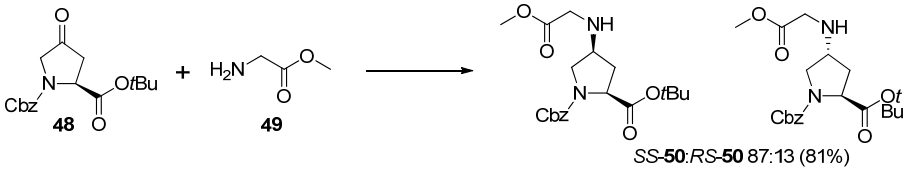

SCHEME 14. Literature examples of reductive amination with $NaBH_3CN$ starting from amino acid esters.[84]

The two examples shown are similar to ours, yet different. The ratios shown are higher, how can we improve the ratio? The reaction shown in SCHEME 11 needs some more detailed consideration and can be redrawn (CHART 1). When both starting materials are asymmetric the stereoselectivity issue becomes more complex. The intermediates form either *Z*- or *E*-isomers of the iminium salt.[85] The impact of the stereogenic centre in the amino acid is different for the two isomers. When such a substituent is large enough it might constitute a steric hindrance for the approaching reducing agent. Both *Z*- and *E*-isomers can afford the *RS*- and *SS*-diastereomers when the new stereogenic centre is formed. The stereogenic centre of the L-amino acid ester moiety is unaffected and keeps the *S*-configuration.

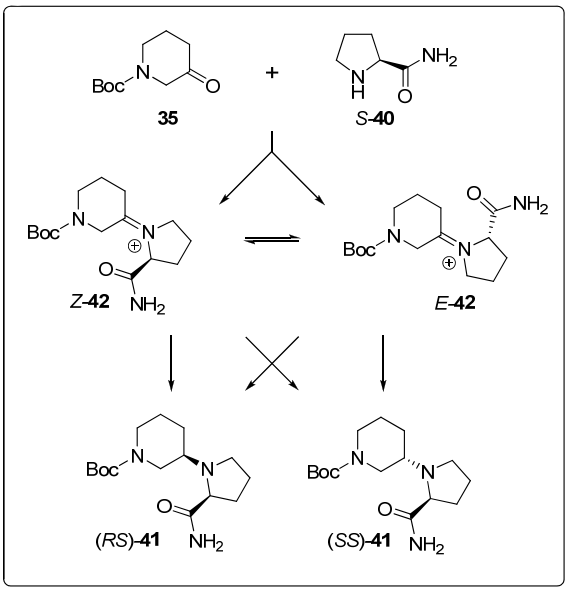

CHART 1. *Z*- and *E*-isomer **42** as intermediates in reductive amination towards **41**.

What can we do to drive the equilibrium in any direction? For a cyclohexane-based system one methyl group can in fact alter the position of the equilibrium. There are two possible chair conformations of methylcyclohexane (**51**) with the substituent either in an axial or equatorial position (FIGURE 22A). The energy difference between the two conformers is 7.2 kJ/mol, which corresponds to a ratio of 95:5, favoring the conformation with an equatorial methyl substituent.

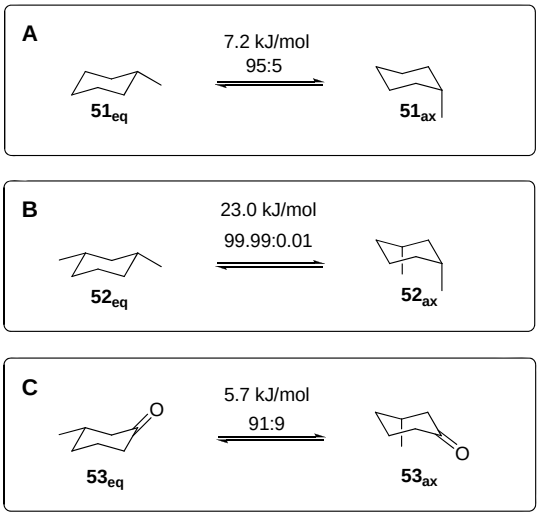

FIGURE 22A-C. Cyclohexane-based conformations with energy differences and isomeric ratios. In all examples the equatorially substituted conformer is favored (shown to the left).

The two methyl groups in *cis*-1,3-dimethylcyclohexane force the ring to adopt the conformation with both groups equatorially positioned (FIGURE 22B). In 3-methylcyclohexanone (**53**), the energy difference is much smaller, and close to that for the equilibrium of $\mathbf{51_{eq}}$:$\mathbf{51_{ax}}$, the ratio is 91:9 still in favor of the conformation with an equatorially positioned substituent (FIGURE 22C). The 1,3-diaxial interaction is less pronounced in $\mathbf{53_{ax}}$ compared to the disubstituted cyclohexane ($\mathbf{52_{ax}}$) as the carbonyl group is directed outwards from the ring.

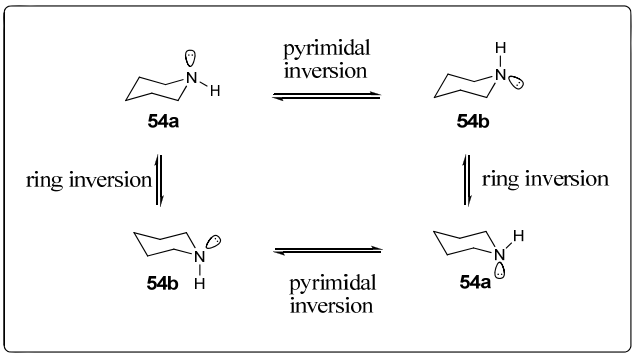

FIGURE 23. Pyramidal and ring inversion of piperidine.[86]

As cyclohexane, piperidine also adopts the characteristic chair conformation and ring inversion occurs. The bond angles are similar in both rings but the C-N bond is somewhat shorter and the chair conformations of piperidine are somewhat more puckered than for cyclohexane. In contrast to cyclohexane, piperidine has two distinct chair conformations as pyramidal inversion of the nitrogen occurs (FIGURE 23). However, the pyramidal inversion is very fast. For separate detection of the two isomers (= invertomers) NMR studies have been performed at temperatures as low as -174 ºC.[86] However, the ring inversion is slower and detectable already at -100 ºC.

Although not being a reductive amination, **35** and enantiopure phenylethanamine **55** reacted with trialkyl phosphite ($P(OEt)_3$) affording a dr of 40:60 (SCHEME 15).[87] In fact, the intermediate is similar to the iminium ions seen earlier but the hydride is exchanged for a nucleophilic phosphite reagent.

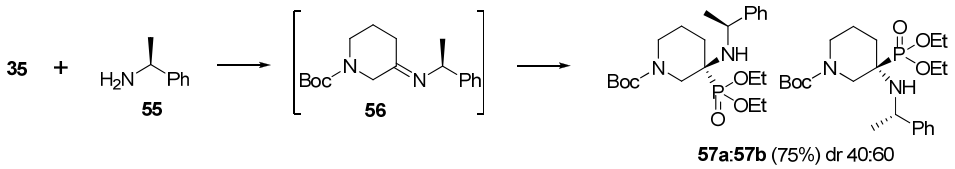

SCHEME 15. Literature example of a reaction with similar intermediate as obtained in the reductive aminations used in this thesis. *Reagents and conditions:* $P(OEt)_3$, AcOH, EtOH, 50 ºC.[87]

What is the origin of the observed stereoselectivity? Could the presence of a stereogenic centre in the intermediate affect the stereochemical outcome of the reaction? Could the stereoselectivity be improved? To answer such questions a study of the stereoselective outcome in the piperidone-amino acids system was undertaken.

In order to evaluate the possibilities to control the stereoselectivity using unsubstituted *N*-protected 3-piperidone and L-amino acid esters a study of the stereoselectivity in reductive aminations was undertaken. The following four parameters were varied; the *N*-protecting group, the amino acid, its ester moiety and the reducing reagent (FIGURE 24).

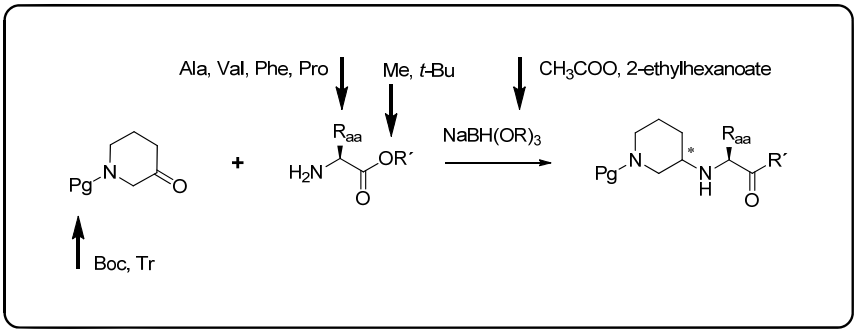

FIGURE 24. In the schematic reductive amination four parameters were evaluated regarding to their influence on the dr of the products.

The *N*-protecting group used was either Boc or trityl (Tr) which are different in features such as flexibility, size, compactness and hybridization. The amino acids alanine, valine, phenylalanine and proline were chosen to represent differences in size and rigidness. Methyl and *t*-butyl esters were used as they have different bulkiness. Six different borohydride reagents, derived from $NaBH_4$ and increasingly bulky carboxylic acids, were first evaluated as reducing agents, two of them were then used for further evaluations. Thus, the chosen parameters are not affecting the structure of the final unprotected product, except for the specific amino acid used. As the diastereomers did not separate on silica gel, they were analyzed by HPLC equipped with a column containing a chiral stationary phase (Chiralpak AD). In this thesis, the diastereomeric ratio (dr) is always reported in the order as the peaks eluted. The dr obtained is a measurement of the stereoselectivity, 50:50 means no favoured diastereomer.

The six different borohydride-based reducing agents were evaluated in the reductive amination of Boc-protected 3-piperidone (**35**) and valine methyl ester (**58**) (TABLE 1). The reagents in TABLE 1, Entries 3-6, were prepared *in situ* from $NaBH_4$ and the listed carboxylic acids and were used according to the general protocol for direct reductive aminations. All reducing agents but $NaBH_3CN$ gave yields above 70%. In addition, all reducing agents derived from acyclic carboxylic acids, showed low or no stereoselectivity. For further reactions, $NaBH(OAc)_3$ and $NaBH(O\text{-}2\text{-ethylhexanoyl})_3$ were chosen.

TABLE 1. Influence of reducing reagent on yield and dr[a]

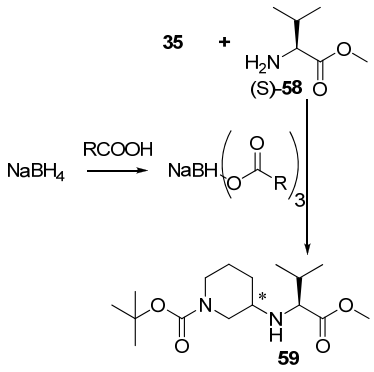

Entry	*reagent or R*	*yield*[b]	*dr*[c]
1	$NaBH(OAc)_3$	85	48 : 52
2	$NaBH_3CN$+AcOH	43	39 : 61
3	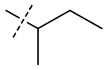	78	50 : 50
4	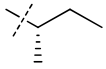	72	50 : 50
5	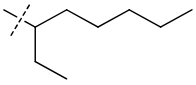	71	56 : 44
6	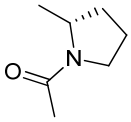	72	59 : 41

[a]Reactions were carried out with N-Boc-3-piperidone (1.0 equiv.), L-valine methyl ester (1.0 equiv.), mol. sieves and the listed reducing reagents (1.0 equiv.) in DCM at rt overnight. The reducing reagents were either used as such or formed in situ from $NaBH_4$ (1 equiv.) and the listed carboxylic acids (3.5 equiv.) in DCM at rt overnight; [b]Isolated yields (%); [c]The ratio reflects the elution order of the diastereomers from HPLC (Chiralpak AD) analysis.

Results such as yields and dr from reductive aminations performed using small and large reducing reagents when exploring the effects of different protecting groups on piperidone and of side chains and ester groups of different amino acids are shown in TABLE 2. Also the absolute configuration of the product is reported when known (for determination of absolute stereochemistry, see Appendix 1). The dr is reflecting the elution order from the HPLC (Chiralpak AD), and care must be taken when comparing different data. For example, the diastereomers of methyl and *t*-butyl esters of the same amino acid are not necessarily eluting in the same order. When the absolute stereochemistry is known, the reported ratio is still reflecting the elution order from the HPLC (Chiralpak AD). Also for the proline derivatives the elution order was reversed when the *N*-protecting group changed from Boc to trityl.

TABLE 2. Influence of protecting groups, L-amino acid esters and reducing reagents on yield and dr[a]

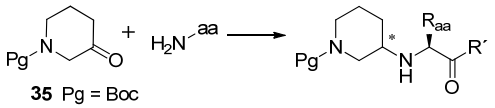

35 Pg = Boc
60 Pg = Tr

61 Pg = Boc, R_{aa} = Ala, R´ = OMe
62 Pg = Boc, R_{aa} = Ala, R´ = O*t*Bu
59 Pg = Boc, R_{aa} = Val, R´ = OMe
63 Pg = Boc, R_{aa} = L-Pro residue R´ = OMe
41 Pg = Boc, R_{aa} = L-Pro residue R´ = NH_2
64 Pg = Tr, R_{aa} = Ala, R´ = O*t*Bu
65 Pg = Tr, R_{aa} = Val, R´ = OMe
66 Pg = Tr, R_{aa} = Val, R´ = O*t*Bu
67 Pg = Tr, R_{aa} = Phe R´ = OMe
68 Pg = Tr, R_{aa} = L-Pro residue R´ = OMe

			Pg = Boc	*Pg = Tr*
Entry	*L-aa ester*	*reagent[b]*	*yield / dr[c] / config [d]*	*yield / dr[c] / config [d]*
1	AlaOMe	A	62/44:56/ -	-
2	AlaOMe	B	38/49:51/ -	-
3	AlaO*t*Bu	A	30/56:44/*SS:RS*	
4	AlaO*t*Bu	B	78/52:48/*SS:RS*	
5	AlaO*t*Bu	A		61/50:50/ -
6	AlaO*t*Bu	B		45/56:44/ -
7	ValOMe	A	85/48:52/ -	
8	ValOMe	B	71/56:44/ -	
9	ValOMe	A		67/55:45/ -
10	ValOMe	B		69/39:61/ -
11	ValO*t*Bu	A		49/53:47[e]/ -
12	ValO*t*Bu	B		44/36:64[e]/ -
13	PheOMe	A		62/61:39/ -
14	PheOMe	B		53/41:59/ -
15	ProOMe	A	74/59:41/*RS:SS*	
16	ProOMe	B	74/62:38/*RS:SS*	
17	ProOMe	A		47/38:62/*SS:RS*
18	ProOMe	B		55/21:79[f]/*SS:RS*
19	ProOMe	C		52/50:50/*SS:RS*
20	ProOMe	D		15/20:80/*SS:RS*
21	$ProNH_2$	A	68/59:41/*RS:SS*	

[a]Reactions were carried out with N-protected 3-piperidone (1.0 equiv.), the listed L-amino acid esters (1.0 equiv.), molecular sieves and reducing reagents (1.0 equiv.) in DCM at rt overnight. The reducing reagents were either used as such or formed in situ from $NaBH_4$ (1.0 equiv.) and 2-ethyl hexanoic acid (3.5 equiv.) in DCM at rt overnight; [b]Reagent A = $(NaBH(OAc)_3$, Reagent B = $NaBH(O\text{-}2\text{-}ethylhexanoyl)_3$, Reagent C = $NaCNBH_3$ + AcOH, Reagent D = $NaBH(O\text{-}N\text{-}acetyl\text{-}prolinoyl)_3$; [c]Isolated yields (%) with dr based on the elution order from HPLC (Chiralpak AD); [d]Absolute configuration as determined by X-ray crystallography (Ala) or chemical correlation (Pro); [e]dr is calculated from the two peaks representing each OtBu-group of the diastereomers in the ^1H NMR spectrum of the product mixture; [f]The reaction has been carried out in triplicate (dr = 19:81, 20:80, 24:76).

Six reactions using alanine methyl or *t*-butyl esters showed a large variation in yields (30-78%) and virtually no stereoselectivity (TABLE 2, Entries 1-6). Neither the bulk of the larger ester moiety (*t*-butyl), the bulk of the larger reducing reagent (B) nor the bulk of the larger *N*-protecting group (Tr) could affect the stereoselectivity compared to the smaller substituents used. The results for the valine-based reactions showed also a fairly large variation in the yields (44-85%) (TABLE 2, Entries 7-12). The reactions performed with Boc-protected 3-piperidone showed no stereoselectivity (TABLE 2, Entries 7-8). However, by using trityl and the larger reducing agent (B) the stereoselectivity increased for both the methyl and *t*-butyl esters to 39:61 and 36:64, respectively (TABLE 2, Entries 9-12). As the ratio was close to 50:50 when using the smaller reducing reagent, the increased stereoselectivity is mainly a consequence of the size of the reducing reagent. The yields in the reactions with Tr-3-piperidone and phenylalanine esters are 53-62% (TABLE 2, Entries 13 and 14). Interestingly, the diastereomeric ratio (~60:40) is inverted when the reducing reagent is changed. When using proline esters, the results become more interesting (TABLE 2, Entries 15-21). Firstly, the *RS*-diastereomer is nearly always formed in excess (*N.B.* the elution order from the HPLC (Chiralpak AD) changes with the protecting group). Using either the proline ester or amide did not affect the stereoselectivity as the ratios were the same (59:41), both favoring the *RS*-diastereomer (TABLE 2, Entries 15 and 21). Neither did the size of the reducing reagent affect the ratio (TABLE 2, Entries 15 and 16). However, when the largest protecting group is used together with the large reducing reagent (B) the ratio increases to 21:79, still favoring the *RS*-diastereomer. Interestingly, when using an even larger reducing reagent (D), the ratio does not increase, instead the yield drops to 15% (TABLE 2, Entry 20). This can indicate that the ratio cannot be improved further and this is the highest dr possible to obtain in the 3-piperidone-amino acid system.

To conclude, in the reductive aminations performed with *N*-protected 3-piperidone and alanine esters none stereoselectivity could be observed. Most probably, the side chain of alanine is too small to affect the stereoselectivity, even a large *N*-trityl protecting group, the *t*-butyl ester or a large reducing reagent ((±)-2-ethylhexanoyl) cannot compensate for the small methyl side chain of alanine. When the side chain is increased, as for valine, and the large reducing reagent is used the stereoselectivity can be affected to some extent giving a dr of about 40:60. For the even larger but more flexible side chain of phenylalanine such combinations are not needed, the ratio is in the 60:40 range also when using a smaller reducing agent ($NaBH(OAc)_3$). This implies that an increased ratio would be possible to obtain when using a larger *N*-protecting group. However, for the most bulky amino acid, proline, the stereoselectivity is not further increased (from 60:40) until both the larger protecting group and the larger reducing reagent are combined, providing the highest ratio (21:79) obtained in this study.

4.2.3 Calculation of conformational distributions

Conformations matter. For example, often an enzyme inhibitor has to change its spatial arrangement from the most stable conformation (the global minimum) in order to bind with optimal complementarity to the active site of an enzyme. If the change of conformation means a large deviation in energy from the global minimum it is unlikely that the binding will be strong. The limit of such deviation has been suggested to be 12 kJ/mol in order to secure a strong affinity between the inhibitor and the enzyme.[88] In fact, if the energy of two conformations differ by12 kJ/mol, the higher energy level is populated by less than 1% of the molecules, the rest adopt the global minimum conformation. A theoretical example of Boltzmann distributions of seven conformations is seen in TABLE 3. Seven energy levels N_i, each increased +2 kJ/mol from the previous more stable level, were used to calculate the Boltzmann distribution (%) of the conformers occupying those energy levels (Eq. 1 and 2). Of course, the global minimum is always

the most populated level and as seen, the populations decrease as the energy increases for the higher levels.

$$N_{i+1}/N_i = e^{-\Delta E/RT} \qquad \text{Eq. 1}$$

$$\Sigma_i N_i = N \qquad \text{Eq. 2}$$

TABLE 3. Example of Boltzmann distribution in per cent for a pre-chosen set of seven energy levels, increased by + 2kJ/mol intervals.[a]

N_i	*ΔE (kJ/mol)*	*distribution (%)*
N_0	0	55.6
N_1	2	24.8
N_2	4	11.1
N_3	6	4.9
N_4	8	2.2
N_5	10	1.0
N_6	12	0.4
		Σ 100%

[a]Equation 1 was calculated with R = 8.314 J/mol/K and T = 298 K.

Since most of the reductive aminations performed with N-protected 3-piperidone in this thesis show diastereomeric ratios of either 40:60 or 60:40, we wanted to investigate the preferred conformations of the intermediates in more detail to try to understand the origin of the stereoselectivity and also possibly predict the direction of attack by the reducing reagent.

Conformational searches were performed individually on the *Z*- and *E*-imine intermediates formed in the synthesis of **68**, **63** and **62** (**68i**, **63i**, and **62i**, respectively) using the MacroModel program and the OPLS2005 force field.[49] Only 11 conformers were found for each isomer of **68i** when trityl was used as the protecting group, compared to the Boc-protected isomers which gave up to 30 conformers each. All conformers, within 12 kJ/mol from the global minimum, were visually inspected and divided into the *Z1*, *Z2*, *E3* or *E4* chair conformations as depicted in FIGURE 25.

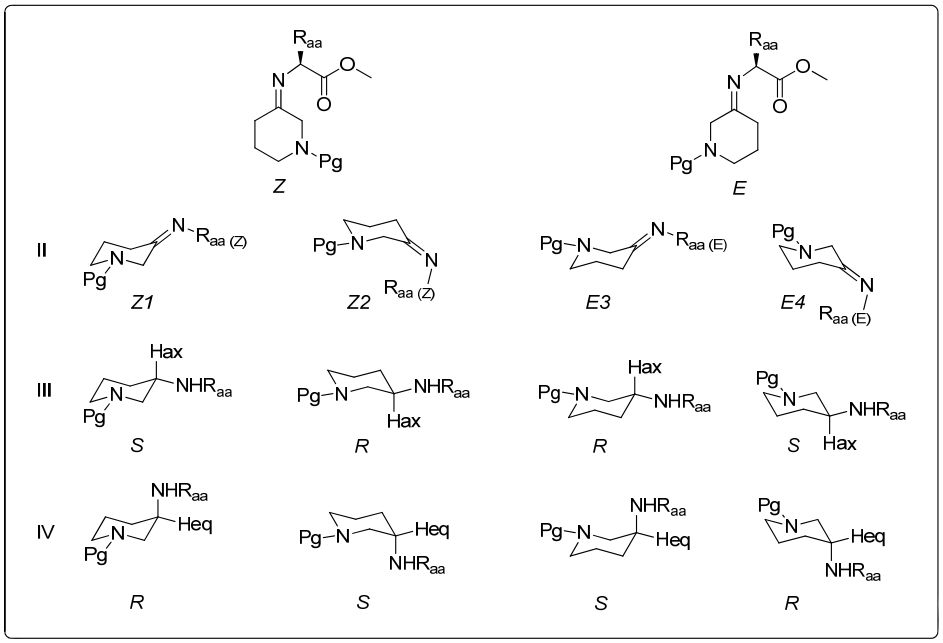

FIGURE 25. Chair conformations of *Z*- and *E*-imines (row II) as intermediates. The intermediates can be attacked axially (H_{ax}, row III) or equatorially (H_{eq}, row IV) to afford the *R*- and *S*-configuration at the new stereogenic center.

For both *Z*- and *E*-isomers two chair conformations are possible (row II) and those can either be attacked from the axial direction (products shown in row III, H_{ax}) or from the equatorial direction (products shown in row IV as H_{eq}). The stereoselective outcome is a delicate issue of equilibria. For instance, hydride attack from the axial direction on *Z1*- and *E3*-isomers affords products with *S*- and *R*-configuration, respectively. Thus, the position of the equilibrium of the *Z*- and *E*-isomers becomes important in order to get a high stereoselectivity. Moreover, an axial attack on the *Z1*- and *Z2*-isomers also affords products with *S*- and *R*-configurations, respectively. Therefore the position of the equilibrium of *Z1* and *Z2* also becomes important for a high stereoselectivity. Stabilization of one of all possible chair conformations (or destabilization of the others) may enhance the stereoselectivity towards one of the diastereomers.

From now on, the pre-existing stereogenic centre will be omitted for clarity. The reduction of the *Z*- and *E*-imines must be governed by the possibility of a ring inversion in piperidine and by the fact that the hydride reagents can approach from either the axial or equatorial direction, or both.

From the conformational search, the structures of the most stable chair conformation of the *Z1*-, *Z2*-, *E3*- and *E4*-isomers of **68i** were obtained (FIGURE 26). The *Z2*-**68i** isomer is the most stable, but the relative energies between the isomers are very close.

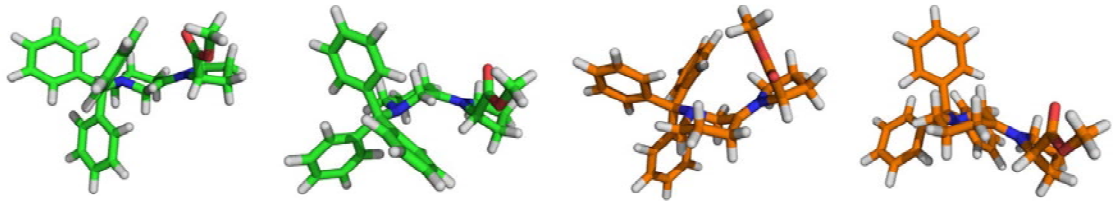

	*Z*1-**6**	*Z*2-**6**	*E*3-**6**	*E*4-**6**
ΔE (kJ/mol)	2.3	0	1.5	3.1
Distribution (%)	18	45	25	12

FIGURE 26. The most stable chair conformation of the *Z*1-, *Z*2-, *E*3- and *E*4-isomers of **68i**.

With the relative populations in hand, and by assuming an axial attack of the hydride, summing up the percentages of *Z1* and *E4* conformers, both leading to the *S*-configuration of the product after an axial attack, and *Z2* and *E3* conformers, affording the *R*-configuration of the products, the calculated ratio could be obtained.

At this stage it became inevitable to know the absolute stereochemistry of the formed products, for enabling comparison of calculated and experimental derived ratios and such process was undertaken (see Appendix 1 for determination of the absolute configuration). The results from the determination showed that the diastereomer formed in excess had the *R*-configuration at the newly formed stereogenic centre for both proline derivatives **68** and **63**. Compound **62** showed no stereoselectivity.

Now the comparison could be made, the conformational search based calculated ratios of the imine intermediates are close to the experimentally derived ratios of the product (TABLE 4). In Entry 1, for **68** the calculated ratio 25:75 is close to the experimental ratio 21:79. When equatorial attack is assumed in the calculation, the ratio is the same but inverted.

Table 4. Experimental and calculated dr based on Boltzmann distribution analysis of the *Z*- and *E*-isomers of 68, 63 and 62 assuming axial attack by the reducing agent (NaBH(O-2-ethylhexanoyl)$_3$).[a]

Entry	*product*[b]	*experimental* *NaBH(OEh)$_3$*	*calculated* *only ax attack*	*calculated* *ax at Z1 and Z2*	*calculated* *ax at E3 and E4*
1	*SS*-**68**/*RS*-**68**	21:79	25:75	20:80	32:68
2	*RS*-**63**/*SS*-**63**	62:38	66:34	65:35	68:32
3	*SS*-**62**/*RS*-**62**	52:48	60:40	73:27	32:68

[a]*Calculations assuming equatorial attack by the reducing agent result in reversed ratios. For example, SS-**68**/RS-**68** show a calculated dr = 75:25 when all Z- and E-isomers of **68i** are attacked from the equatorial direction.*

However, by a closer inspection of the conformers in FIGURE 26, the reaction site in the *E3*-conformer is sterically hindered from the axial direction by both the trityl and ester groups. It seems impossible for a large reducing reagent to reach the trigonal carbon of the imine. Therefore, the *E3*-conformer was removed from the calculations and the calculated ratio became 36:64, still favoring the *RS*-diastereomer. However, if both *E*-conformers are removed, and the calculation was performed with only the *Z*-conformers a ratio of 20:80 was obtained, with the *RS*-diastereomer in excess. This is exactly the ratio as seen experimentally for **68**. In fact, all the calculations are close to the experimental ratio and all show that the *RS*-diastereomer prevails with the assumption of an axial attack by the reducing reagent.

For **68i**, the calculated ratios are similar in all cases and also similar to the experimental ratio, the *RS*-diastereomer prevails and an axial attack by the reducing reagent seems likely. For **62**, the calculated ratio implies that a stereoselective outcome would be likely, but different isomers prevail. However, the experimentally derived ratio did not indicate any stereoselectivity.

In the literature, correlation between conformation and reactivity is discussed.[89] The Curtin-Hammett principle says that the product distribution is solely correlated to the energy barrier of the two transition states, and an isomeric equilibrium process is said to be fast. However, Winstein/Holness and Eliel/Ro correlate the product distribution to relative reaction constants irrespective of the equilibrium rate. In the schematic reaction in FIGURE 27, A2 and A3 represent the conformers interconverting in an equilibrium fashion, and A1 and A4 are the products.[90]

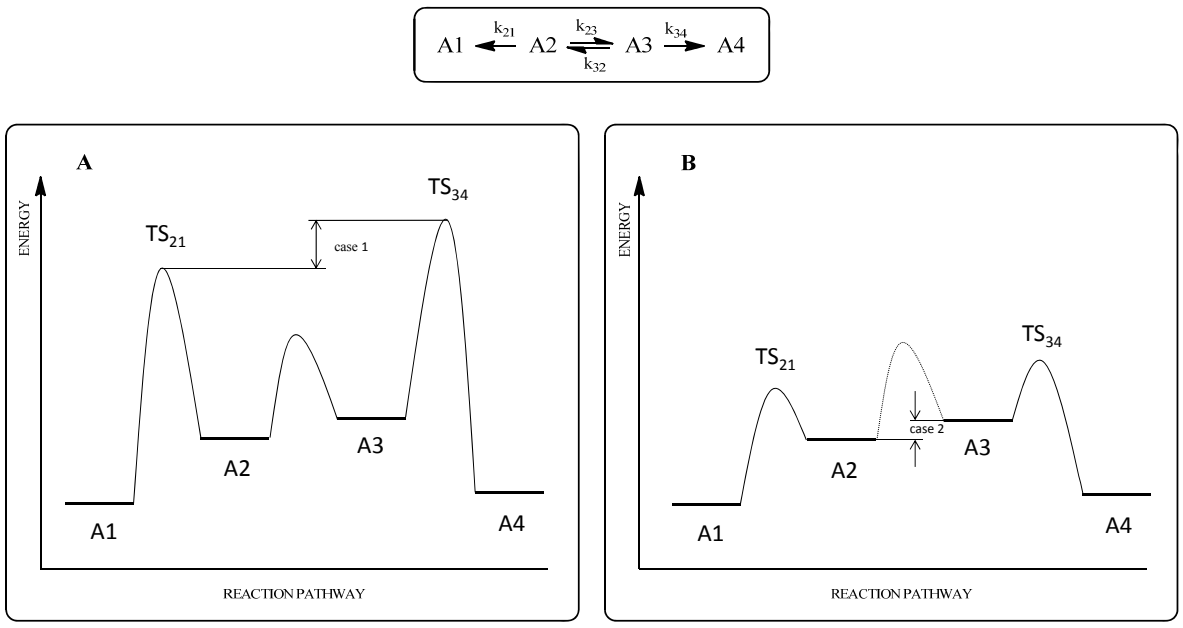

FIGURE 27. Energy diagram of the schematic reactions of two conformers (A2, A3) related by an equilibrium process, which form different products (A1, A4) according to the **A)** Curtin-Hammett Principle and **B)** the Winstein/Holness hypothesis. The energy levels are arbitrary.

In the first case, the reactions to A1 and A4 are slower than the equilibrium process, i.e. k_{21}, k_{34} << k_{23}, k_{32}, the reactions follow the line in FIGURE 27A and the so-called Curtin-Hammett principle is said to hold. The ratio of the products (A1:A4) will be determined by the formation rates, that is the difference in their two transition states TS_{21} and TS_{34}. In the second case (FIGURE 27B) the equilibrium process is slower than the reactions to A1 and A4, i.e. k_{23}, k_{32} << k_{21}, k_{34}. This means that the product ratio (A1:A4) is determined by the ratio of the conformers of the starting material which is the relative populations of A2 and A3.

As seen above, the relative populations can be derived from conformational analysis of the starting materials followed by calculation of the Boltzmann distribution.

By transferring the schematic picture in FIGURE 27 to the reductive step of *Z* and *E*-imines presented in FIGURE 25, the starting materials A2 and A3 can be represented by either the *Z*- or *E*-chair conformations. A1 and A4 represent the products, the *R*- and *S*-isomers.

Since the calculated ratios are in accordance with the experimental data, diastereomeric ratios may be predicted as described above with the assumptions made and the reaction follows the non-Curtin Hammett principle. However, no TS-calculations have been made in this thesis. The energy gap between the two starting materials could be exactly the same as the energy-gap between the two TS shown in FIGURE 27B. Two conclusions may be drawn: Since the calculated data predict the correct major diastereomer of the products, the assumption that the attack occurs from the axial direction is correct. Since the highest calculated ratio is 25:75, this seems to be the top limit for the stereoselectivity in the *N*-protected 3-piperidone L-proline system.

In the literature, discussions on the issue of stereoselectivity provide examples of borohydride reduction of either the keto function of piperidone or the imine function of cyclohexane derivatives but not on systems similar to those used in this thesis. Commonly, ketones are attacked from the equatorial side when using large reducing agents but imines are attacked from the axial direction.[83] In nucleophilic addition to a trigonal carbon steric hindrance and electronic effects are usually responsible for the stereochemical outcome. When the trigonal carbon is part of an imine the steric hindrance is increased by one or two substituents on the nitrogen.

According to Cieplak the direction of the nucleophilic attack is favoured by an antiperiplanar geometry in relation to a neighboring C-H bond over C-C or C-N bonds, which in a sixmembered heterocyclic system means from the axial direction.[91]

4.2.4 Synthesis of piperidine-based analogues (PAPER III)

The synthetic route to the peptide analogues continued. As discussed in the previous sections, the enantiomers of **37** and the diastereomers of **41** could not be synthesized in a stereochemical pure fashion. Instead, the isomers were separated by preparative HPLC using an enantioselective stationary phase (Chiralpak AD). For example, two grams of (*rac*)-**37** was separated into (*R*)- and (*S*)-**37** in 11 injections to afford sufficient amount for the synthetic route to follow. With enantiopure starting materials the synthesis towards the peptide analogues could be started, the stereochemical integrity was kept under control throughout the whole reaction sequence. No racemization or epimerization were observed after any of the amino acid coupling reactions.

The synthetic routes to the di-, tri- and tetrapeptide analogues are outlined in SCHEME 16. Aminolysis of the isolated (*R*)- and (*S*)-**37** with ammonia in methanol afforded the amides (*R*)- and (*S*)-**69**. Acidic cleavage of the Boc protecting group mediated by TFA/DCM gave (*R*)- and (*S*)-**74** ($pip_{236}G$) in quantitative yields.

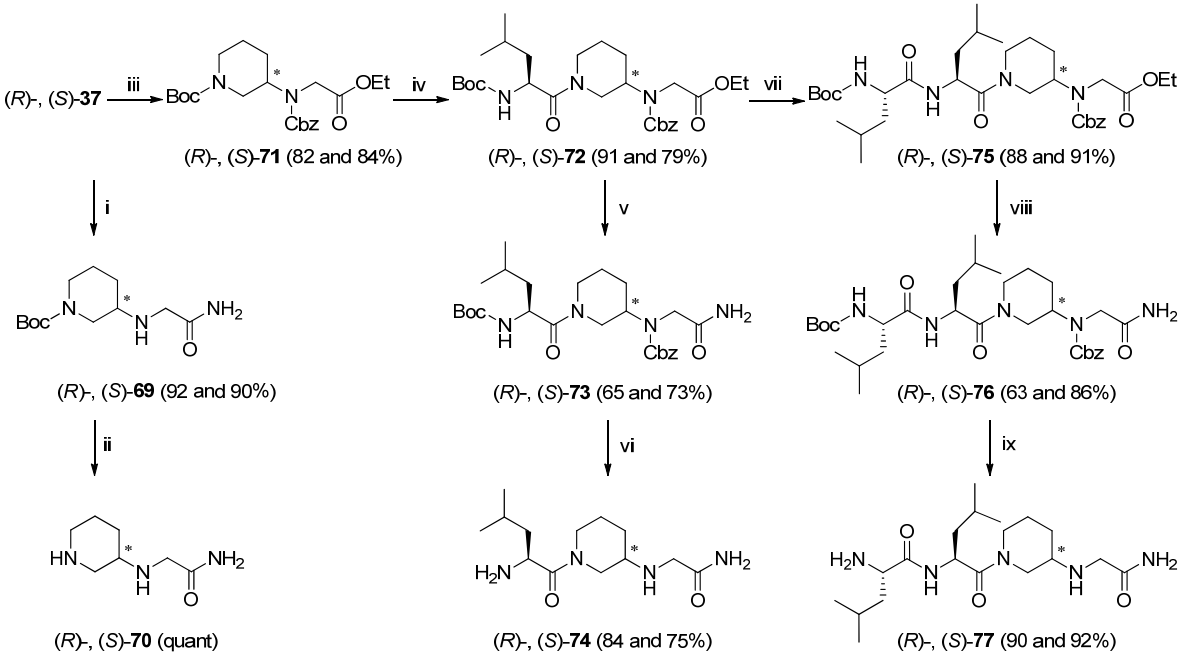

SCHEME 16. Route to the piperidine analogues (*R*)-, (*S*)-pipG (**70**), the tripeptide analogues (*R*)-, (*S*)-LpipG (**74**) and the tetrapeptide analogues (*R*)-, (*S*)-LLpipG (**77**). *Reagents and conditions*: (i) NH_3/MeOH, rt, 72 h; (ii) TFA, rt, 12 h; (iii) Cbz-OSu, Et_3N, DCM, 0 °C => rt, 17 h; (iv) 1) TFA, rt, 16 h, 2) Boc-L-Leu x H_2O, EDC, HOBt, DCM, molecular sieves, Et_3N, rt, 15 h; (v) NH_3/MeOH, rt, 72 h; (vi) 1) H_2, Pd/C, ethanol, rt, 72 h, 2) TFA/DCM, rt, 4 h; (vii) 1) TFA/DCM, rt, 16 h, 2) Boc-L-Leu x H_2O, EDC, HOBt, DCM, molecular sieves, Et_3N, rt, 15 h; (viii) NH_3/MeOH, rt, 168 h; (ix) 1) H_2, Pd/C, EtOH, 3 h, 2) TFA/DCM, rt, 14 h.

Furthermore, the isolated enantiomers (*R*)- and (*S*)-**37** were protected using Cbz-succinimide to afford (*R*)- and (*S*)-**71**. The Cbz-group was used, for its complementary stability during Boc-deprotections performed in later synthetic steps. The enantiomers (*R*)- and (*S*)-**71** were Boc-deprotected followed by coupling with Boc-L-leucine to afford (*R*)- and (*S*)-**72**. All couplings were mediated by EDC and HOBt, to pre-activate the carboxylic acid in order to react with the

nucleophilic amines.[92-93] Aminolysis afforded amides (*R*)- and (*S*)-**73**, which were deprotected to give (*R*)- and (*S*)-**74** (Lpip$_{236}$G), respectively. Boc-deprotection of (*R*)- and (*S*)-**72** and subsequent coupling to Boc-L-leucine gave (*R*)- and (*S*)-**75**, respectively. Aminolysis afforded (*R*)- and (*S*)-**76**. Finally, the Cbz- and Boc-protecting groups were removed by catalytic hydrogenation (Pd/C) and TFA cleavage, respectively, to afford (*R*)- and (*S*)-**77** (LLpip$_{236}$G). The total yield for the synthesis of (*R*)- and (*S*)-**76** over eight steps from (*R*)- and (*S*)-**37**, respectively, was 37 and 48%.

Attempts to synthesize dipeptide analogues such as pipA, pipV and pipF starting from the compounds obtained in the reductive amination study were made. Aminolysis of (*rac*)-**61** gave (*rac*)-**78** in 55% (SCHEME 17). Neither (*rac*)-**59** nor (*rac*)-**77** reacted with ammonia in methanol. Efforts to prolong the reaction times or using microwave-assisted heating were made but without detection of products, only unreacted starting material remained. Compound (*rac*)-**78** was deprotected to afford (*rac*)-**81** (quant. yield).

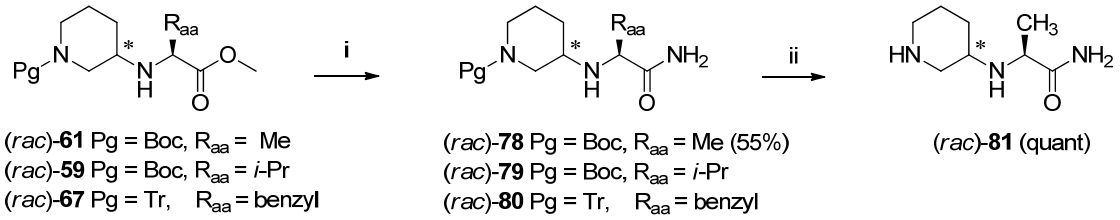

SCHEME 17. Attempts to synthesize dipeptide analogues such as pipA, pipV and pipF. *Reagents and conditions for synthesis of **81**:* (i) NH_3 in methanol, rt, 72 h; ii) TFA/DCM, rt, on.

The synthetic sequence to the tri- and tetrapeptide analogues pip$_{236}$GP (**84**) and Lpip$_{236}$GP (**86**) is shown in SCHEME 18. Ester hydrolysis of the Cbz-protected (*R*)-and (*S*)-**71** (from SCHEME 16) afforded the carboxylic acid derivatives (*R*)- and (*S*)-**82** (95 and 99%) and subsequent coupling to L-proline amide gave (*R*)- and (*S*)-**83**, respectively. Compounds (*R*)- and (*S*)-**83** was Boc-deprotected (TFA/DCM) to provide a small portion of (*R*)- and (*S*)-**84** (pip$_{236}$GP) and the rest was coupled with Boc-L-leucine mediated by HOBt and EDC to give the epimers (*R*)- and (*S*)-**85**.

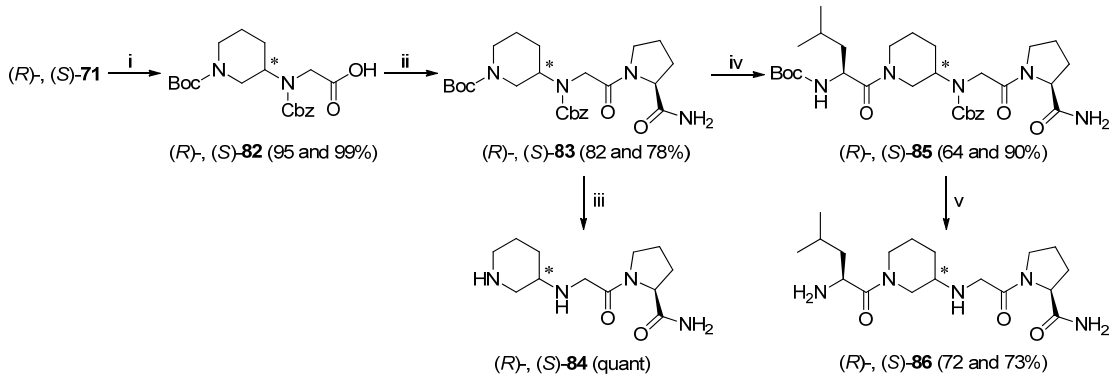

SCHEME 18. Route to the tripeptide analogues pipGP (**84**) and the tetrapeptide analogues LpipGP (**86**). *Reagents and conditions*: (i) LiOH 1M aq, THF/MeOH/H_2O 3:1:1, 0 °C 30 min, rt, 3 h; (ii) L-ProNH_2, EDC, HOBt, Et_3N, DCM, rt, 16 h; (iii) 1) H_2, Pd/C, EtOH, rt, 24 h, 2) TFA/DCM, rt, 4 h; (iv) 1) TFA, rt, 16 h, 2) Boc-L-Leu x H_2O, EDC, HOBt, DCM, molecular sieves, Et_3N, rt, 15 h; (v) 1) H_2, Pd/C, EtOH, rt, 48 and 24 h, 2) TFA/DCM, rt, 4 h.

Finally, the Cbz- and Boc-groups were removed as described above to give (*R*)- and (*S*)-**86** (Lpip$_{236}$GP). The total yield for the synthesis of (*R*)- and (*S*)-**86** over seven steps was 29 and 43%, respectively. The ^{1}H NMR spectrum of (*R*)-**85** showed five doublets assigned to the two methyl groups in the leucine side chain which implies that the molecule adopts several different conformations at room temperature. After the deprotection, the ^{1}H NMR spectrum of both (*R*)- and (*S*)-**86** showed two doublets assigned to the two non-equivalent methyl groups, as expected.

The synthesis route of the tri- and tetrapeptide analogues **89** and **90** ($Gpip_{237}P$, $LGpip_{237}P$) in which the piperidine moiety replaces Gly_{237} in the IgG sequence started by separation of (*rac*)-**41** by preparative HPLC (Chiralpak AD) to give (*R*)- and (*S*)-**41** (SCHEME 19). (The absolute configurations were determined, see Appendix 1). Diastereomers (*R*)- and (*S*)-**41** were Boc-deprotected by TFA/DCM and the free amines were coupled to EDC/HOBt-activated Boc-protected glycine to afford (*R*)- and (*S*)-**87**. Deprotection with TFA/DCM gave (*R*)- and (*S*)-**88** ($Gpip_{237}P$) as TFA salts. Another portions of (*R*)- and (*S*)-**87** were coupled with Boc-protected L-leucine to afford (*R*)- and (*S*)-**89** and subsequent deprotection with TFA/DCM afforded (*R*)- and (*S*)-**90** ($LGpip_{237}P$).

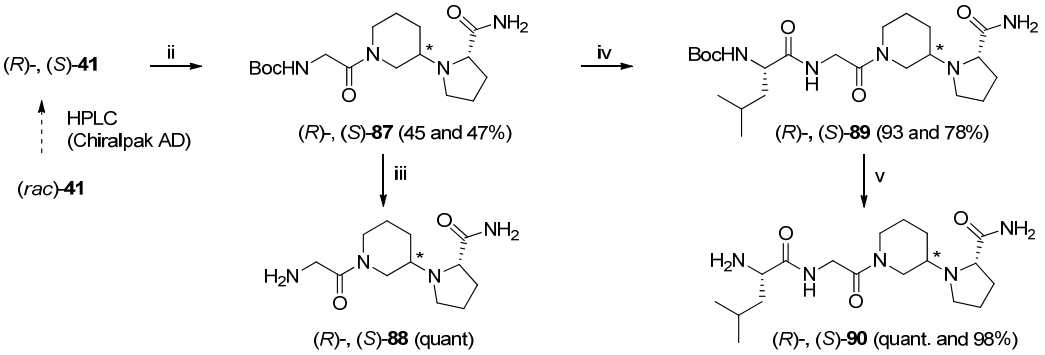

SCHEME 19. Route to the tripeptide and the tetrapeptide analogues (*R*)-, (*S*)-$Gpip_{237}P$ (**89**) and (*R*)-, (*S*)-$LGpip_{237}P$ (**90**). *Reagents and conditions*: (i) 1) L-Pro-NH_2, $NaBH(OAc)_3$, HOAc, DCM, rt, 20 h, 2) preparative HPLC (Chiralpak AD); (ii) 1) TFA/DCM, rt, 2) Boc-Gly, EDC, HOBt, DCM, 0 $^oC \rightarrow$ rt, 15 h; (iii) TFA/DCM, rt, 20 h; (iv) 1) TFA/DCM, rt, 20 h, 2) Boc-L-Leu, EDC, HOBt, Et_3N, DCM, 0 ^oC => rt, 15 h; (v) TFA/DCM, rt, 12 h.

In some instances the removal of Cbz-group resulted in *N*-ethylation. For example, *N*-ethylated by-products were formed during the Cbz-deprotection of (*R*)- and (*S*)-**73** using catalytic hydrogenation (Pd/C 10%) in ethanol. Isolation of the by-products after prolonged reaction time and subsequent TFA hydrolysis gave $LLpip_{236}EtG$ analogues (*R*)- and (*S*)-**93** (SCHEME 20). *N*-Ethylated by-products were also isolated in the deprotection of (*R*)- and (*S*)-**71** (not shown).

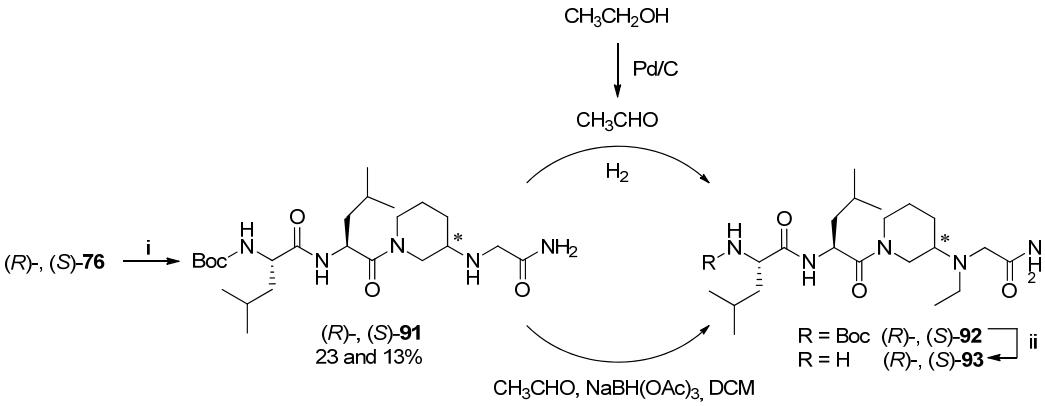

SCHEME 20. *N*-Ethylated by-products were isolated during Cbz-deprotection. *Reagents and conditions*: (i) H_2, Pd/C, EtOH, rt, 144 h (23 and 13%), ii) TFA/DCM, rt, 16 h (99 and 98%).

Already after three hours reaction time by-product formation was observed. To verify the structure, isolated Cbz-deprotected (*R*)-**91** was converted to the corresponding ethylated product (**92**) in 76% yield via reductive amination using acetaldehyde and $NaBH(OAc)_3$ (SCHEME 20). The NMR spectra of the synthesized compound and that of (*R*)-**92** were identical. It has been proposed that a Pd-catalyzed oxidation of ethanol to acetaldehyde can occur during the

hydrogenation reaction.[94-95] The acetaldehyde forms an imine with the secondary amine in **91**, and a subsequent reduction provides the ethylated by-product (SCHEME 20).

Synthesized compounds were screened for inhibition capacity, which is further discussed in the evaluation chapter.

4.3 SYNTHESIS of BICYCLIC DERIVATIVES

Initially, efforts were put into synthesizing the enaminone-based bicyclic scaffold shown in FIGURE 28A. An enaminone contains the conjugated system N-C=C-C=O.[96] Starting from *N*-protected 3,5-dioxopiperidine, three different schematic routes to such scaffolds were identified (FIGURE 28B-D). In the first route (FIGURE 28B), the nucleophilic carbon atom in the *exo*-enaminone intermediate attacks a carbonyl function with a leaving group being expelled to form the second ring. In the second route (FIGURE 28C), the nucleophilic nitrogen in a protected enaminone derivative attacks an electrophilic carbon in a ring closure process. In the third route (FIGURE 28D), the nitrogen attacks the carbonyl group present in the ring and via an intramolecular imine formation the *exo*- and *endo*-enaminone bicyclic scaffold is afforded.

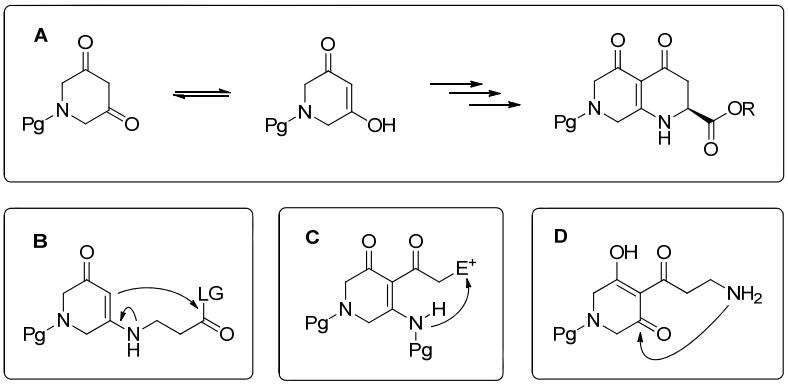

FIGURE 28. A) Initially, efforts were made to synthesize a diketo-based bicyclic scaffold starting from *N*-protected 3,5-dioxopiperidone. Three reaction routes can be rationalized, either **B**) and **C**) via *exo*-enaminones as intermediates or **D**) via a trioxo derivative.

All three routes were screened and evaluated. In SCHEME 21, alloc-protected 3,5-dioxopiperidine (**94)** was reacted with a diester of L-Asp to afford (*S*)-**95**, as described in the literature.[57] The *t*-butyl group was selectively removed by TFA/DCM to give (*S*)-**96**. Attempts to pre-activate an intramolecular reaction proved to be difficult. Pre-activation of the carboxylic acid via acid chloride, anhydride or DCC was tested but no ring closure to (*S*)-**97** was detected (NMR).

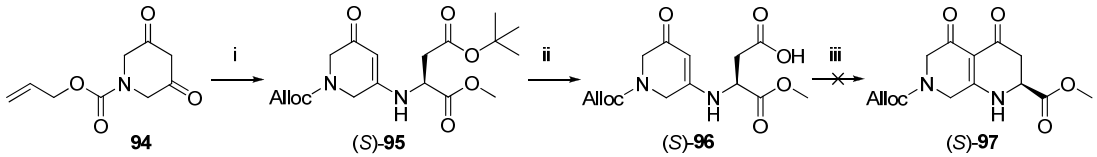

SCHEME 21. *Reagents and conditions*: i) L-Asp(*t*Bu)OMe, Et_3N, C_6H_6/NMP 9:1, MW 5 min @ 140 ºC; ii) TFA/DCM, 0 ºC => rt, 16 h (quant. yield); iii) see text (no isolated product).

Instead, the second strategy was tested (SCHEME 22). The alloc-protected **94** was reacted with benzyl amine to afford the *N*-protected exo-enaminone **98** in 29%. Attempts to react **98** with *trans*-crotonyl chloride mediated by Et_3N in xylene did however not afford any product. To test the reaction in another system, dimedone (**99**) was used as the starting material and was reacted with benzyl amine to obtain **100**.

Thereafter, **100** and *t*-crotonyl chloride were refluxed for 5 hours to give **101**, the heating was continued overnight but no ring closure was observed (NMR).

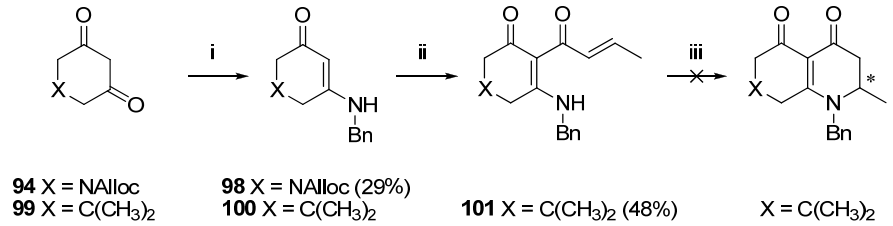

SCHEME 22. *Reagents and conditions:* i) Benzyl amine, **98:** Et_3N, C_6H_6/NMP 9:1, MW 5 min @ 140 ºC (29%), **100**: *p*-TSA, toluene, molecular sieves, rt, 16 h; ii) *t*-crotonyl chloride, Et_3N, xylene, reflux, 1 h (48%, over two steps); iii) see text (no isolated product).

In the literature, acyclic starting materials have been used for the same type of aza annulation reactions (SCHEME 23).[97] The authors claim the need of an electron withdrawing substituent in the R-position. Probably, the carbamate used as the protecting group in **98** (SCHEME 22) is not enough for the reaction to succeed. The choice of base is also important, the use of pyridine would afford an *N*-acylated product whereas when no base is used primarily 2-pyridone is formed.[98]

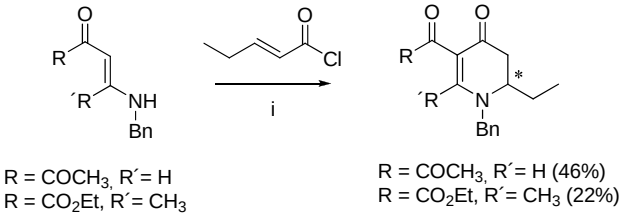

SCHEME 23. Literature example of acyclic starting material in an aza-annulation reaction.[97] *Reagents and conditions:* i) Et_3N, xylene, reflux 2 and 8 h.

Recently, a cyclization reaction was reported starting from dimedone and an α,β-unsaturated aldehyde derivative affording a dimedone-based bicyclic scaffold, although with aromatic substituents (SCHEME 24).[99]

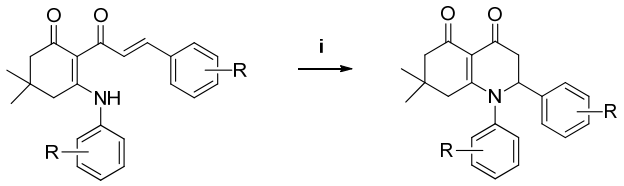

SCHEME 24. Recently reported synthesis to a dimedone-based bicyclic scaffold.[99] *Reagents and conditions:* i) toluene, reflux, 6-8 h (90%).

Eventually, the third strategy was tried (FIGURE 28D). Thus, **94** was used together with DMAP and DCC-activated Boc-L-Asp(COOH)O*t*Bu to afford the trioxo intermediate **102** but only traces of product were observed together with unreacted starting materials (LC/MS) (SCHEME 25). However, when benzyloxycarbonyl (Cbz) was used as the protecting group of 3,5-dioxopiperidine (**103**) **104** could be isolated in 7% yield (SCHEME 25). Using DIC as the coupling reagent did not improve the yield according to LC/MS analysis of the reaction mixture.

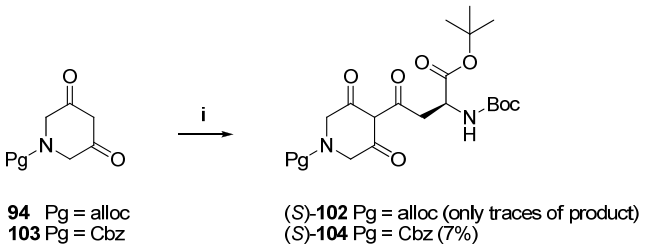

SCHEME 25. *Reagents and conditions:* i) DCC, DMAP, Boc-*N*-L-Asp(COOH)O*t*Bu, DCM, rt, on.

Instead, dimedone was reacted with DCC-activated Boc-*N*-L-Asp(COOH)O*t*Bu to afford intermediate (*S*)-**105** in a high yield (83%) (SCHEME 26).[100] Interestingly, the yields differ more than ten times depending on the choice of starting material. This means that the nitrogen atom in **94** affects the reactivity negatively. The choice of protecting groups (Cbz or alloc) did not seem to improve the yield either. However, there are more protecting groups that can be scanned in order to try to improve the yield of a piperidine-based bicyclic compound, e.g. benzyl or tosyl.[101] ^{1}H NMR spectrum of (*S*)-**105** showed a sharp peak at 17 ppm revealing a strong hydrogen bond between an enol proton and a carbonyl group. A ^{13}C NMR spectral assignment of the signals for (*S*)-**105** (in $CDCl_3$) showed that the dimedone ring is asymmetrically arranged with one enol and one keto function (SCHEME 26).

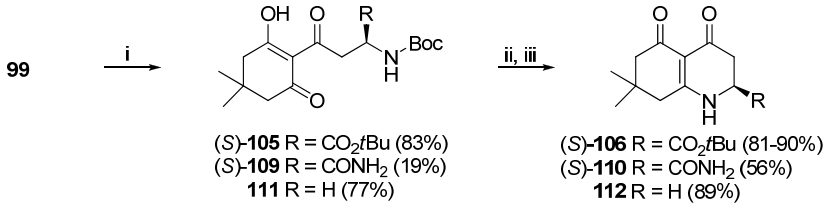

SCHEME 26. *Reagents and conditions:* i) DCC, DMAP, DCM, Boc-*N*-L-Asp(COOH)O*t*Bu, rt, 7 h; or Boc-*N*-L-Asp(COOH)NH_2, rt, 16 h; or Boc-*N*-β-Ala, rt, 16 h; ii) HCl/dioxane 4*N*, rt, 1-3 h; iii) chloroform, (*S*)-**106**: rt, 4 days (90%) or 45 ºC, 5 h (81%); (*S*)-**110**: reflux, 5 h; **112**: diluted reaction mixture (3.2 mM), 45 ºC, 18 h.

The focus was now turned to the dimedone-based bicyclic scaffold. To continue, the Boc protecting group of (*S*)-**105** was selectively removed using hydrochloric acid in dioxane (4*N*) to give the unprotected intermediate without affecting the *tert*-butyl ester (SCHEME 26). (*S*)-**106** was formed spontaneously in $CDCl_3$ when unprotected (*S*)-**105** was left in an NMR tube for 72 h, and appeared as a dark red solution. In order to decrease the reaction time, Boc-deprotected (*S*)-**105** was refluxed in toluene using either a Dean-Stark trap or microwave-assisted heating but no conversion of the starting material was observed. To investigate the reaction in more detail an NMR tube was loaded with a $CDCl_3$-solution of Boc-deprotected (*S*)-**105** and heated (45 ºC) by the NMR heating device while ^{1}H and ^{13}C NMR spectra were recorded every hour. The experiment revealed complete conversion after five hours (FIGURE 29).

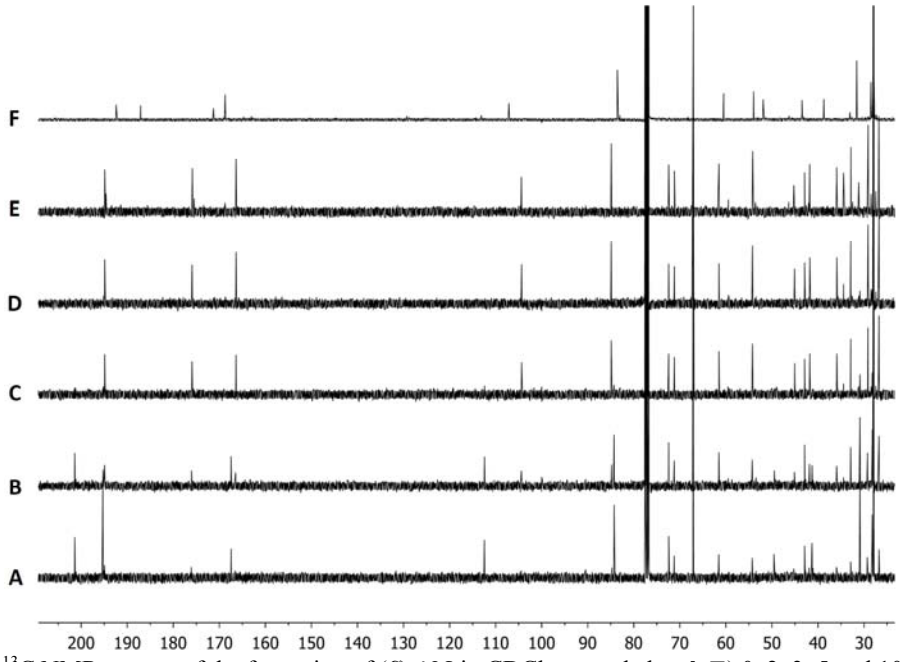

FIGURE 29. ^{13}C NMR spectra of the formation of (*S*)-**106** in $CDCl_3$, recorded at **A-E**) 0, 2, 3, 5 and 10 h while heating (45 ºC); **F**) spectrum of purified **106b**.

The reaction was later performed in large scale (4.0 g) with heating using a traditional oil bath to yield (*S*)-**106** (81%). Interestingly, depending on the work-up procedure, either simple solvent evaporation or washing steps (sat. $NaHCO_3$, followed by brine), the ^{13}C NMR spectra are significantly different indicating two isomeric forms of the product. In FIGURE 29F, the ^{13}C spectrum of basified **106b** is shown. This might indicate that two tautomers of **106** are possible to isolate (FIGURE 30). Possibly, the concentrated sample is representing the diketo/enamine structure **106**, due to the two carbonyls assign to the two peaks above 190 ppm (FIGURE 29E). To assign the basified sample to either the s-*cis* or s-*trans* enol-imine structure of **106** is more troublesome. Unfortunately, the interpretation of IR measurement gave ambiguous results. Attempts to bring the basified **106b** back to the dicarbonyl form using acidic washings were not successful. The assignment of **106b** needs further considerations.

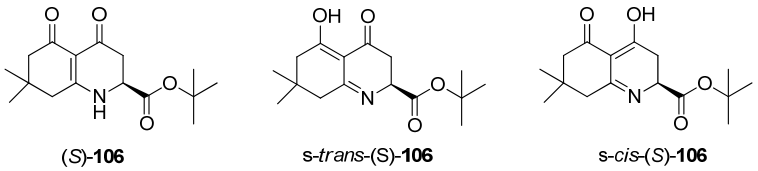

FIGURE 30. Three possible tautomers of (*S*)-**106**, the double bonds can either be arranged in a diketo/enamine system or an enol/imine system with the single bond either -*cis* or -*trans*.

To continue, the ester function of (*S*)-**106** was cleaved by TFA/DCM to give the corresponding carboxylic acid (*S*)-**107** (SCHEME 27). However, subsequent amide coupling with glycine ethyl ester did not give the expected product ((*S*)-**108**). Instead, two glycine residues react with (*S*)-**107**, one forming an amide with the carboxylic acid function via the coupling reagents used (PyBOP, HOBt) and one forming an imine with one of the carbonyl groups. The structural assignment was not performed.

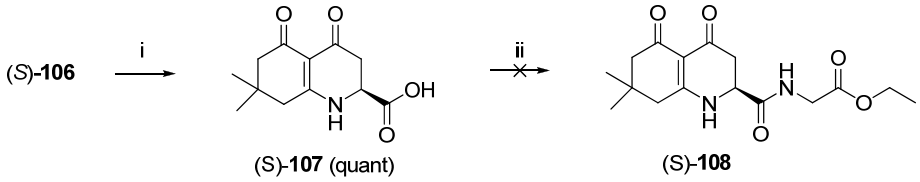

SCHEME 27. *Reagents and conditions:* i) TFA/DCM rt, 6 h (quant. yield); ii) PyBOP, HOBt, DIPEA, DCM, rt, 16 h (a diglycine derivative was isolated instead of the expected product).

Instead, attention was turned to the amide (*S*)-**110** (SCHEME 26), by starting from the carboxylic acid (*S*)-**107** and ammonium acetate. Conversion of starting materials was observed but the mono-amidated product could not be isolated due to solubility problems. Instead, dimedone and Boc-*N*-L-Asp(COOH)$CONH_2$ were coupled mediated by DCC and DMAP to afford (*S*)-**109** (19%) (SCHEME 26). Amide (*S*)-**109** was Boc-deprotected and ring closure was accomplished in refluxing chloroform to yield (*S*)-**110**. Boc-β-Ala was also coupled to dimedone mediated by DCC and DMAP providing **111** (77%) (SCHEME 26). Compound **111** was Boc-deprotected using the same protocol as earlier (HCl/dioxane 4*N*) but the ring closure was considerably slower than the previous ones. Full conversion of Boc-deprotected **111** was seen after 48 h, but only the non-dehydrated intermediate had formed. In the presence of molecular sieves full conversion of **111** was observed after 18 h but only 30% of **112** had formed, the rest was assigned to be dimers. Finally, when a diluted solution (50 times) of **111** was heated for 18 h **112** could be obtained (89%).

The naphthyridine-like scaffold was envisaged to be synthesized via aza-Diels-Alder reactions.[102-103] The first cyclization with Danishefsky´s diene and a Boc-protected imine of ethyl glyoxylate in toluene (45 ºC) afforded a racemic mixture of the Boc-protected endo-enaminone ((*rac*)-**113**) (61%) (SCHEME 28).[104-105] Iodination to **114** and subsequent vinylation mediated by a Stille-coupling formed **115**.[106] A second Boc-protected imine was used with **115** for the second aza-Diels Alder cyclization to yield **116** (40%). NMR and HPLC analysis (Chiralpak AD) of the product revealed that **116** was formed in a highly regio- and stereoselective fashion. Although the structure has three stereogenic centra only two peaks could be seen in the HPLC chromatogram. Formation of 1,7-naphthyridine could not be detected. The two Boc-groups were successfully removed by TFA/DCM to afford **117**. Mono-cyclic **115** was also used with acrylamide to afford **118** in a regioselective Diels-Alder cyclization (63%). The Boc-group was removed by TFA/DCM to give **119**.

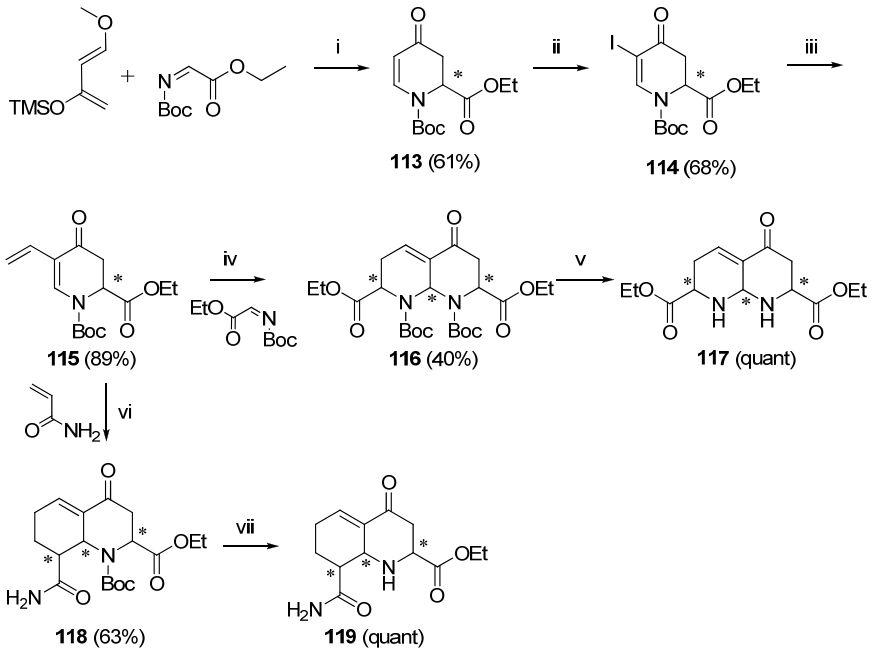

SCHEME 28. *Reagents and conditions:* i) toluene, 45 ºC 18 h; ii) NIS, HTIB, DCM, rt; iii) tributylvinylstannane, $Pd_2(dba)_3$, $AsPPh_3$, THF, 50 ºC, 2h; iv) toluene, 45-48 ºC, 44 h; v) TFA/DCM, rt, 3h; vi) toluene, 100 ºC, 48h; vii) TFA/DCM, rt, 3h.

The bicyclic compounds (**106**, **110**, **112**, **117** and **119**) were tested in IdeS and papain inhibition assays

5. EVALUATION OF POTENTIAL INHIBITORS

Synthesized compounds have been tested for their capability to inhibit IdeS, SpeB and papain. The inhibition screening was done at the universities in Lund and Umeå. Measurements of pK_a values have been performed on a small selection of compounds at AstraZeneca R&D, Sweden. In silico *docking experiments have been performed to try to explain the outcome of the test results of the peptides and piperidine-based analogues.*

5.1 INHIBITION SCREENING (PAPER I, III, IV)

To perform the inhibition screening, the compounds to be tested were pre-mixed with the enzyme and incubated at room temperature. The substrate was added followed by another incubation period at 37 ºC. Finally, the enzyme activity was quenched prior to samples being analyzed. The results are reported as remaining enzyme activity. For SpeB and papain, the assays are based on substrate cleavage yielding *p*-nitroaniline which was used for titrating. For IdeS the only substrate known is IgG and the analysis was carried out accordingly. Analysis of IgG cleavage products was performed with either surface plasmon resonance spectroscopy and/or gel electrophoresis techniques.

Since there are two scissile bonds in one IgG molecule and either one or two bonds are hydrolyzed, different cleavage products can be formed (FIGURE 26). After IdeS hydrolysis the heavy chains are held together by disulfide bridges, sugar moieties and also hydrophobic interactions. Consequently, the mono-cleaved IgG is difficult to distinguish from the intact IgG. Conditions during the analysis also affect the cleavage products further. When sugar molecules have been removed the cleavage products are held together by disulfide bridges and one or two fragments (25 kDa) are released from the mono-cleaved or double-cleaved IgG, respectively (FIGURE 26B). When the disulfide bridges also have been removed, all four chains are separated (FIGURE 26C). The heavy chain weighs 56 kDa, both the light chain and the cleaved-off fragment weigh 25 kDa, the rest (= 56-25) is a 31-kDa fragment.

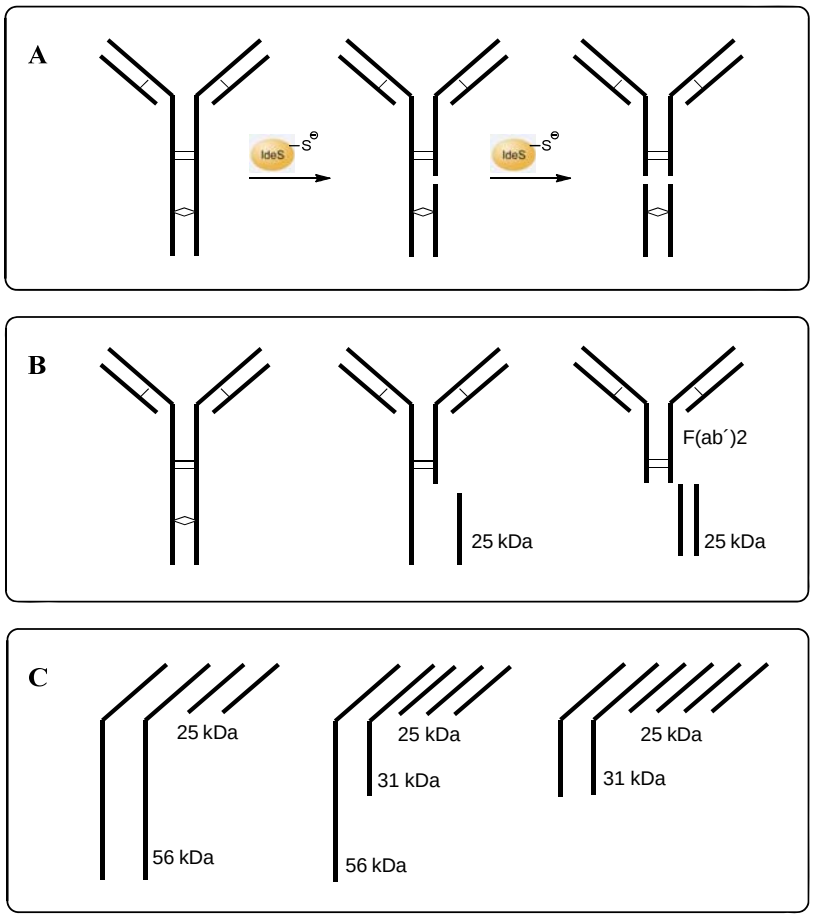

FIGURE 31. Schematic picture of intact IgG and cleavage products. **A**) Sugar moieties and disulfide bridges present; **B**) Sugar moieties absent but disulfide bridges present; **C**) Both the sugar moieties and disulfide bridges are absent.

Surface Plasmon Resonance (SPR) spectroscopy is based on an optical phenomenon used to measure interactions between two molecular species, one in solution and one stationary, attached at a specific surface. The method is implemented in a Biacore instrument (FIGURE 32A) and is applicable for binding affinity site analysis, kinetic studies and as in this thesis, concentration measurements of IgG.[107-108] The optical phenomenon is based on electron scintillation at a metal surface on a chip and is triggered by the energy from a light beam (FIGURE 32B). One side of the chip is covered with a thin gold film and on the other side the stationary species is covalently attached, in our case protein A. The protein A-side is part of the flow cell wall. Next to the gold film is a glass prism. When a light beam is passed through the prism, it becomes reflected by the gold surface and is received by a photo detector. The reflection is highly sensitive to the microenvironment in the flow cell. The microenvironment is changed as a solution with IgG is passing through the flow cell and intact IgG binds to protein A. When IgG binds, the angle is shifted. The magnitude of the angular shift is defined as response units (RU) and is an indirect measurement of the IgG concentration in the solution. The detection is in real time and a sensorgram is obtained (FIGURE 32C).

In the inhibition assay, two samples are withdrawn at t_0 (= substrate addition) and at $t_{20\ min}$, sequentially injected and then compared. If the gap between the graphs is large, less IgG is intact after 20 min and more IgG has been cleaved, which means that IdeS is active and the inhibition is low. If the gap is small, most IgG molecules are still intact, which means that IdeS is inactivated and the inhibition is strong. The conditions used during SPR analysis leave both the disulfide

bridges and the sugar moieties unaffected (cf. FIGURE 31A). SPR cannot distinguish intact from mono-cleaved IgG as both interact with protein A. Consequently, SPR analysis will only reflect inhibition of the second cleavage.

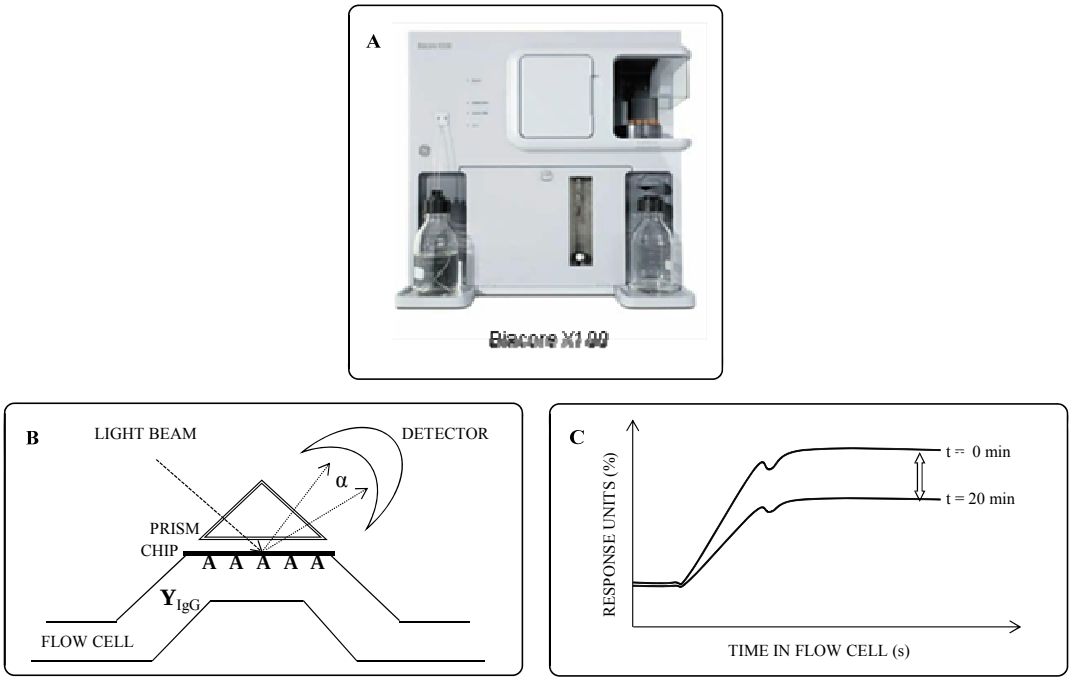

FIGURE 32. A) Biacore instrument used for SPR spectroscopy; **B)** the detection unit; **C)** sensorgram with two graphs from samples withdrawn at t_0 and t_{20min}. Comparison is done when steady state is reached.

The SDS-PAGE (sodium dodecyl sulfate polyacrylamide gel electrophoresis) technique uses electric current to separate negatively charged proteins. A correlation between charge and molecular weight means that proteins migrate differently according to their weight.[109] When the gel is stained (Coomassie blue), bands with proteins become visible and evaluation of the migrated distances is possible. The shorter migrated distance the higher molecular weight (starting from the top, FIGURE 33). Different gels separate IgG and its cleavage products according to the discussion above. Gels with reducing conditions will show the IgG chains separately (FIGURE 33).

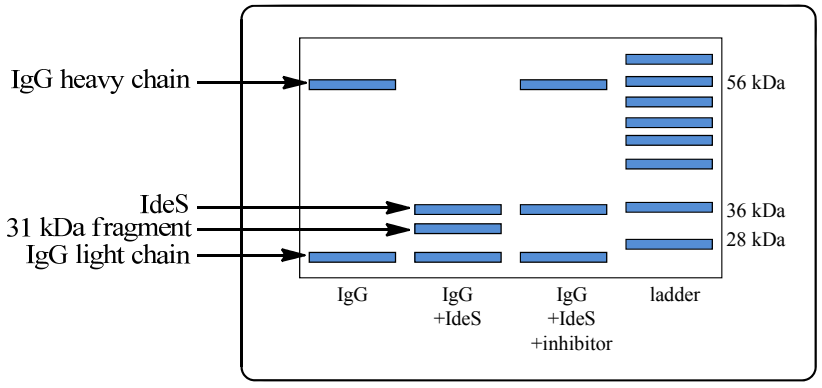

FIGURE 33. A schematic stained gel used in SDS-PAGE separation technique under reducing conditions, showing proteins as bands separated due to migration according to their weight. Fragments of intact but reduced IgG show two bands at 25 and 56 kDa. IdeS itself appears as a band of 36 kDa and the totally cleaved IgG shows bands at 31 and 25 kDa.

For IgG, both the light chain and the cleaved-off fragments weigh 25 kDa, the amount of the remaining 31 kDa-fragment is a measurement of IdeS activity. When IdeS is totally inhibited IgG is intact.

Gradient gels with non-reducing conditions can differentiate the fragments shown in FIGURE 31B, as intact IgG, mono-cleaved IgG and F(ab´)$_2$ have different molecular weights. Hence, the first cleavage of IgG can be detected by SDS-PAGE under non-reducing conditions.

5.2 TPCK/TLCK ANALOGUES AS IdeS INHIBITORS (PAPER I)

TPCK/TLCK analogues (**2-3**, **5-7**, **26-33**) were evaluated as inhibitors of IdeS (FIGURE 34). Also two aziridines (**4b-c**) were tested.

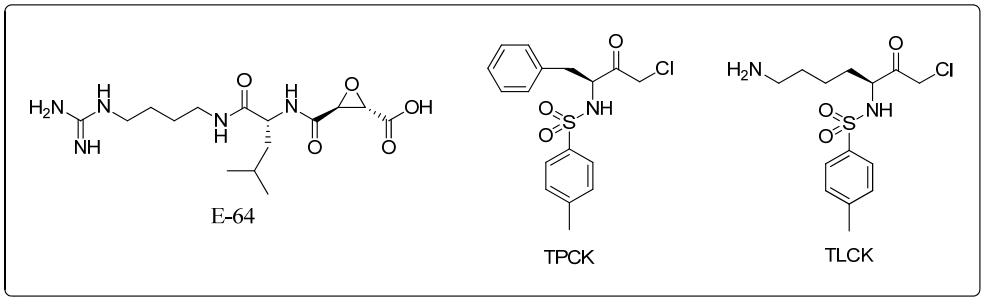

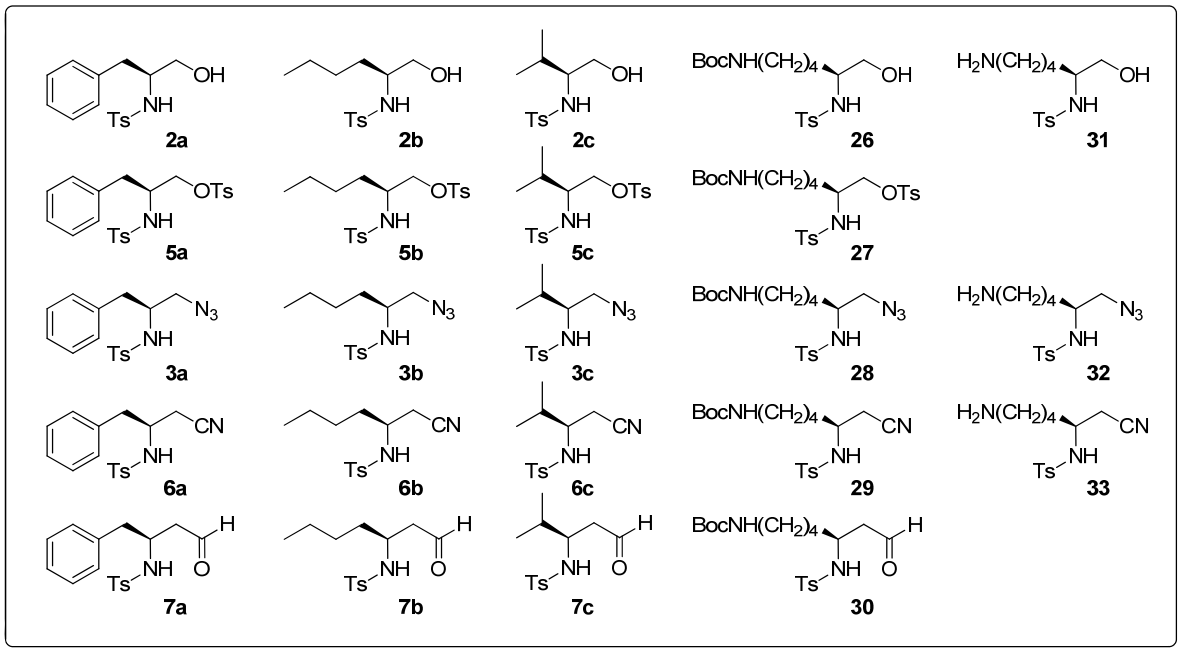

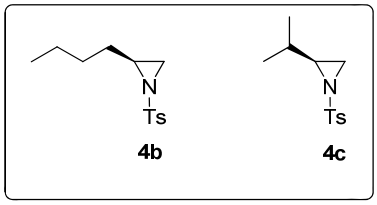

FIGURE 34. TPCK/TLCK, **2-3**, **5-7**, **26-33** and aziridines **4b-4c** tested for IdeS inhibition capacity. Different R-substituents are seen horizontally and the varied warhead functionalities vertically.

The samples were analyzed by SDS-PAGE under reducing conditions and TPCK and TLCK were included as positive controls and E-64 as a negative control (FIGURE 35A-C). Visual inspection of the stained gels showed that eight of the 25 compounds tested were able to inhibit IdeS. Compounds **7a-c** and **30** with aldehyde function as the warhead were identified as inhibitors of IdeS. In comparison, the known irreversible inhibitors TPCK/TLCK show the same degree of inhibition as **7a-c** and **30**. As no 31 kDa-fragment is observed, IdeS is totally inhibited. No differentiation of inhibition potency can therefore be made for the different R-groups in **7a-c** and **30**. Five nitrile derivatives were tested but only **6b** was identified to inhibit IdeS. Out of all the R-substituents used together with the nitrile warhead only the combination of *n*-butyl and nitrile could affect IdeS. This implies that the *n*-butyl derivative is able to interact strongest with IdeS, and that a straight aliphatic side-chain is preferred.

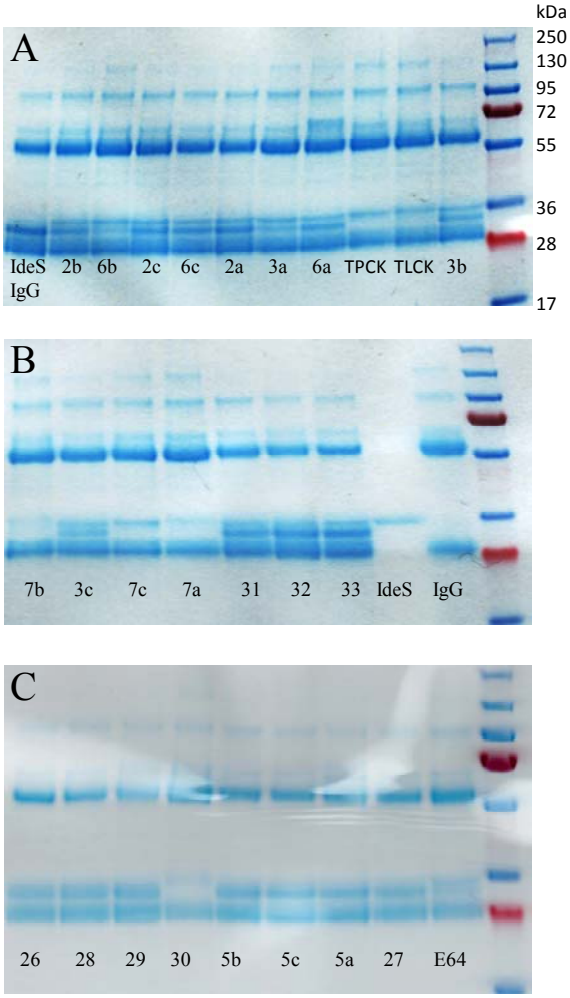

FIGURE 35A-C. Evaluation of TPCK/TLCK analogues (**2-3**, **5-7**, **26-33** and **4b-c**) as inhibitors of IdeS by SDS-PAGE under reducing conditions. Also shown, IdeS and IgG mixed and separated, as well as TPCK/TLCK and E-64.

In addition, the TPCK analogues with an azide warhead, **3a-c,** were identified as moderate inhibitors of IdeS. However, no ranking among them can be done. In contrast, the TLCK analogues **29** and **33** did not inhibit IdeS. This means that apolar R-groups are more favorable

than polar ones, as also was suggested for the nitrile warheads. Photolytic decomposition of reported azide derivatives used for inhibiting cysteine proteases prompted a stability test.[56] Azide derivative **3c** was, however, shown to be stable in the solid state and in buffer solutions at the experimental conditions for 48 h according to both ^{1}H NMR and HPLC analysis.

None of the other compounds tested was able to inhibit IdeS. That is, the compounds with functions such as alcohol (**1a-c**, **26**, **31**), tosyloxy (**5a-c**, **27**) or the aziridines (**4b**, **4c**) (data not shown) were not useful for inhibition of IdeS. Apparently, tosylesters and the aziridines did not react with Cys94 in the IdeS active site. Also, compounds containing hydrogen-bond donors (or acceptors) that do not find complementary binding partners are strongly disfavored in overall binding. Steric hindrance and unfavorable spatial orientation might also be explanations for their inability to inhibit IdeS.

In summary, all four aldehydes, one nitrile and three azide derivatives were identified as inhibitors of IdeS. As seen, hydrophobic interactions between the inhibitor´s R-group and the enzyme contribute to the binding. For substructures resembling TPCK/TLCK the warhead functionality is still important but irreversible covalent binding is not needed. All the aldehyde derivatives showed inhibitory potency as strong as the irreversible covalently bound TPCK/TLCK. Thus, reversible binding of **7a-c** and **30** is strong enough to compete with IgG for the active site and to inhibit IdeS.

5.3 PEPTIDES and PIPERIDINE ANALOGUES AS INHIBITORS (PAPER III)

5.3.1 IdeS

The purchased peptides were based on the amino acid sequence of IgG and were extended either *N*- or *C*-terminally from the cleavage site in IgG, or symmetrically to both sides (FIGURE 31). All peptides were found to be inactive as inhibitors of IdeS (data not shown). Although the sequences of the tested peptides are identical to the IgG sequence around the IdeS cleavage site these short peptides are not recognized by IdeS or are at least not interacting strongly enough to inhibit the enzyme. Perhaps the catalytic site is not accessible for the peptides, due to Arg259 residue hinderence.

FIGURE 36. Sequences of tested peptides, GG represent the cleavage site of IdeS and SpeB.

The di-, tri- and tetrapeptide analogues and also **X** and (*rac*)-**81** were screened for their inhibition capacity against IdeS and analysed by SDS-PAGE with non-reducing gels.

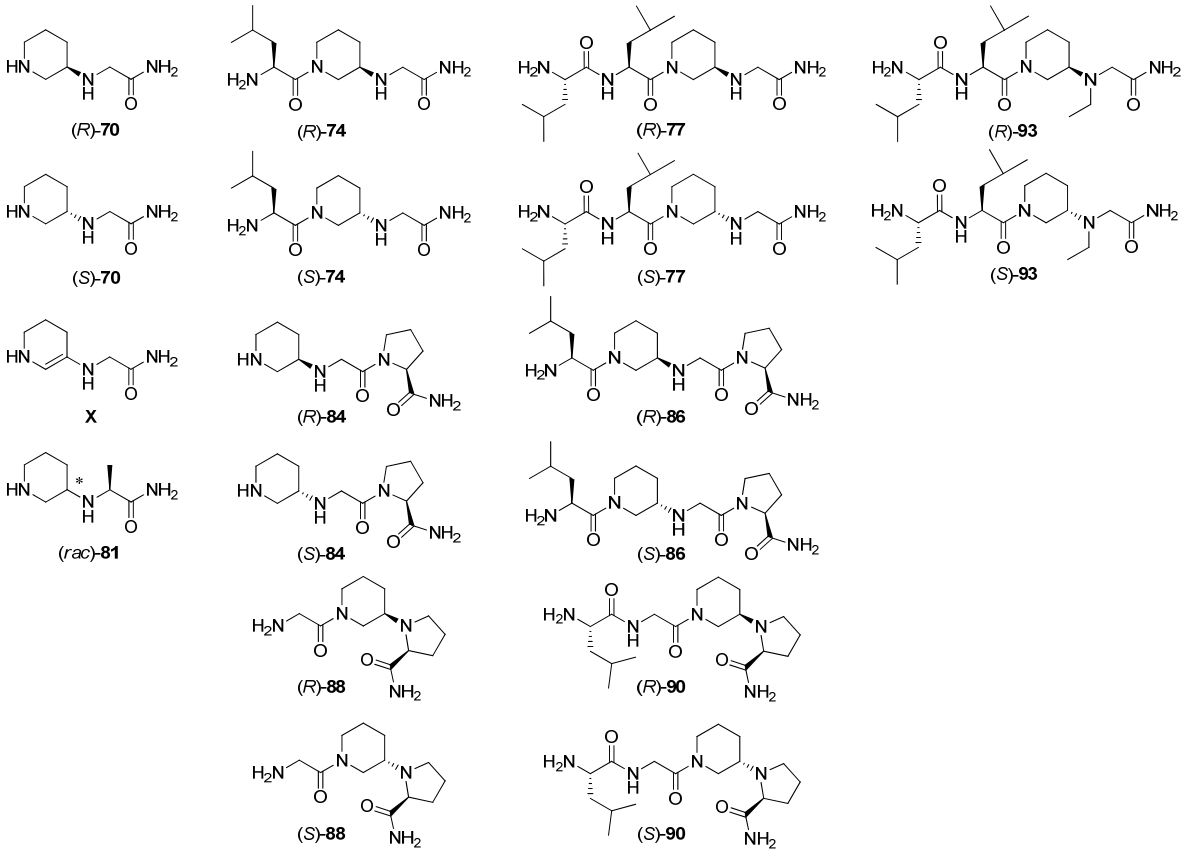

FIGURE 37. Di-, tri- and tetrapeptide analogues of GG, LLGG and LGGP peptide sequences tested for inhibition capacity. (*R*)- and (*S*)- refer to the configuration of the formed stereogenic center. All amino acids used have the *S*-configuration, if chiral.

It was found that the analogues with inhibition capability all inhibited the second IgG cleavage step of IdeS. In FIGURE 38, for both *(S)*-**70** and the reference lane, no intact IgG is present due to the first cleavage. Comparison of *(S)*-**70** and the reference shows that the band corresponding to single cleaved fragments are thicker in the *(S)*-**70** lane, due to inhibition of IdeS second cleavage.

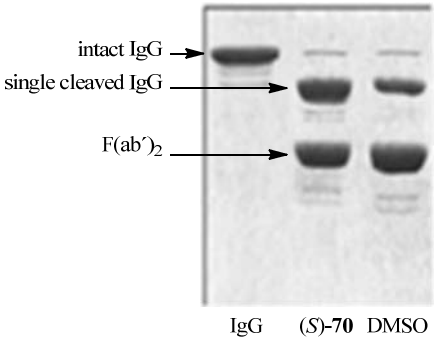

FIGURE 38. Representative SDS-PAGE analysis using non-reducing gel showing non-hydrolyzed intact, single and double cleaved IgG in the presence of inhibitor (*S*)-**70** and without (DMSO).

When analysing the inhibition data further, using SPR technique, three groups could be distinguished (FIGURE 39). A cut-off value of 80% IdeS remaining activity was set, analogues with higher remaining activity were considered unable to inhibit IdeS.

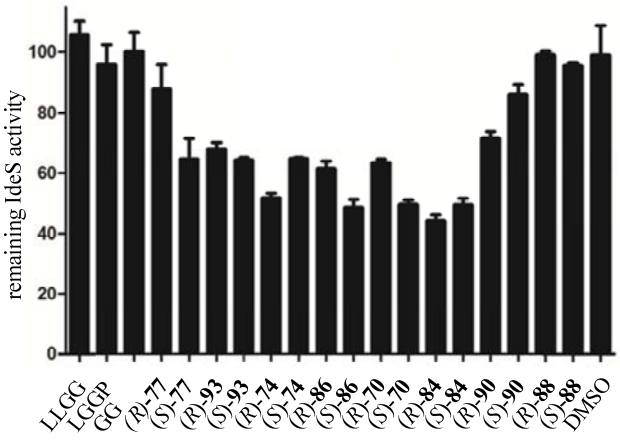

FIGURE 39. IdeS remaining activity in the presence of peptide or peptide analogue. Remaining activity is expressed relative to a standard curve obtained in absence of inhibitors.

Another limit was set at 60%. Analogues with 60-80% remaining activity were considered moderate inhibitors and analogues showing 60% or less remaining IdeS activity were considered as strong inhibitors of IdeS. The most potent inhibitors of IdeS are (*S*)- and (*R*)-**84** (pipGP), (*S*)-**70** (pipG), (*S*)-**86** (LpipGP) and (*R*)-**74 (**LpipG). This implies that extension of the $pip_{236}G$ fragment towards the *C*-terminal is favoured.

The unsaturated $pip_{236}G$ analogue **X** was also screened but showed no inhibition capacity, even though the structural resemblance with (*R*)- and (*S*)-**70** is high (data not shown). However, the unsaturated ring is less flexible than the piperidine ring and the double bond provides an altered electron density of the enamine, which possibly results in less efficient hydrogen bonding. Also (*rac*)-**81** (pipA) is structurally similar to (*R*)- and (*S*)-**70** but the racemic mixture was not able to inhibit IdeS (data not shown). The additional methyl group in (*rac*)-**81** seems to hinder the efficient binding compared to (*R*)-**70**.

There are two sets of LGGP analogues, with the piperidine moiety substituting either of the two glycine residues. Comparison of the LGGP analogues showed that the $Lpip_{236}GP$ analogues (*S*)- and (*R*)-**86** are stronger inhibitors than the $LGpip_{237}P$ analogues, (*S*)- and (*R*)-**90**. There is even larger difference for the tripeptidic GGP analogues, the $pip_{236}GP$ analogues (*S*)- and (*R*)-**84** are much stronger inhibitors than the corresponding $Gpip_{237}P$ derivatives, (*S*)- and (*R*)-**88**. The difference in distribution of the hydrogen bonding possibilities of the structures of the pip_{236} and pip_{237}-analogues may be an explanation to the potency difference. Also, sterical interactions and the flexibility of the two sets differ.

The (*R*)- and (*S*)-isomers of each analogue pair show different inhibition, although the difference in potency is small. For di- and tetrapeptide analogues the (*R*)-isomers show stronger inhibition than the corresponding (*S*)-isomers. The relationship is reversed for the tripeptide analogues. Actually, the only exception is $pip_{236}GP$ where (*R*)-**84** is equipotent with (*S*)-**84**. The largest difference is seen for the $LLpip_{236}G$ analogues, favouring (*S*)-**77**. This result is not easy to explain but could indicate that analogues of different lengths find different binding poses.

The ethylated analogues (*R*)- and (*S*)-**93** are equipotent with (*S*)-**77**. This implies that the *NH*-group of the secondary amine in (*S*)-**77** is not involved in hydrogen bonding and that the

replacement of the hydrogen with an ethyl group favours the overall binding. This also means that there must be space enough for the ethyl group.

Interestingly, the structural difference between the (*S*)-analogues of Lpip$_{236}$GP and pip$_{236}$G is two amino acids but still the two compounds (*S*)-**86** and (*S*)-**70** are equipotent. The extra amino acids are not providing any additional interactions to gain stronger binding, or are too flexible to gain favorable binding energies. With ligand efficiency in mind, where binding energy per atom is evaluated, this means that (*S*)-**70** (pip$_{236}$G) is the most efficient peptide analogue inhibitor in the whole series.[110]

5.3.1 papain/SpeB

To gain insight into whether the peptide analogues are capable of inhibiting IdeS selectively, all peptides and peptide analogues were also screened in enzyme activity assays using SpeB and papain.

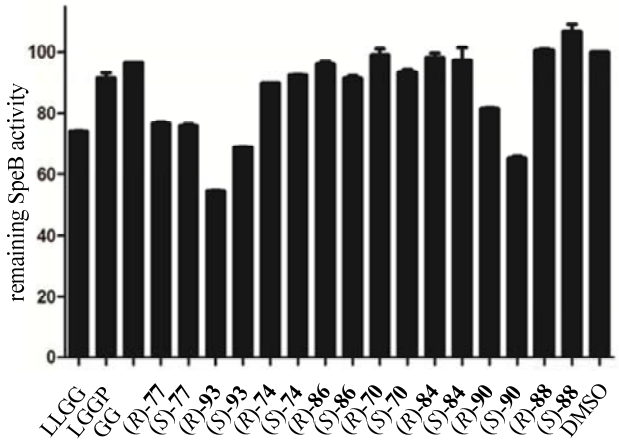

FIGURE 40. Inhibition capacity of peptides and peptide analogues of SpeB (0.28 μM inhibitor). SpeB activity is expressed relative to enzyme activity in absence of inhibitors.

Using a cut-off value of 80% remaining SpeB activity, six compounds were shown to be able to inhibit SpeB (FIGURE 40). Actually, also the LLGG peptide inhibits SpeB to some extent. With a cut-off value of 60% only the ethylated LLpip$_{236}$EtG analogue (*R*)-**93** inhibited SpeB. In addition, and in contrast to the effect observed for IdeS, also the LGpip$_{237}$P analogues (*R*)- and (*S*)-**90** inhibited SpeB activity. These analogues contain a similar tertiary amine fragment as the ethylated analogues. Thus, the absence of a hydrogen bond donating group and the rigid structure of the neighboring piperidine and proline rings appear to increase the interaction between (*R*)- and (*S*)-**90** and SpeB. Not surprisingly, the more flexible Lpip$_{236}$GP analogues (*R*)- and (*S*)-**86** do not affect SpeB activity.

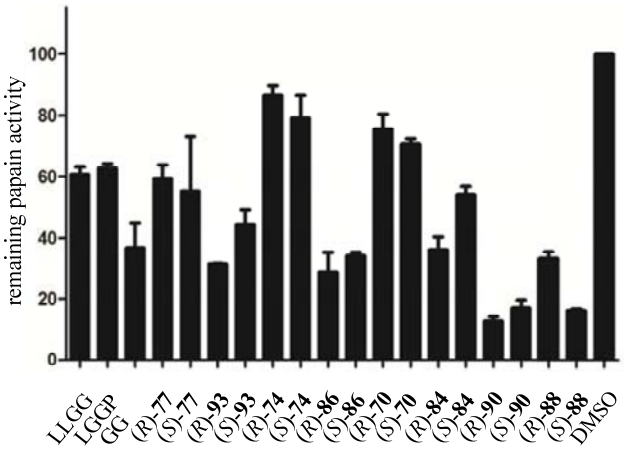

FIGURE 41. Inhibition capacity of peptides and peptide analogues of papain (0.9 μM inhibitor). Remaining activity is expressed relative to enzyme activity in absence of putative inhibitors.

As the result from the papain inhibition assay performed with the peptide analogues shows, papain was clearly very sensitive towards most compounds tested (FIGURE 41). With a cut-off value of 80% remaining activity, all but one compound ((*R*)-**74**) were able to inhibit papain. Also the peptides LLGG and LGGP acted as inhibitors, although the enzyme preferentially binds other residues in the active site. A cut-off value of 20% shows that $Gpip_{237}P$ analogues (*(R)*-**90**, *(S)*-**90**, *(R)*-**88** and *(S)*-**88**) are the strongest papain inhibitors. Interestingly, comparison of the GG peptide and the $pip_{236}G$ analogues (*R*)- and (*S*)-**70** show a large difference in potency, with the dipeptide GG being the most potent.

In summary, the most active inhibitors of IdeS, (*R*)-**84** and (*S*)-**86** are even more active towards papain, but show no inhibitory activity towards SpeB. Finally, both (*R*)- and (*S*)-**70** as well as (*R*)- and (*S*)-**74** show promising selectivity profiles as they are both potent inhibitors of IdeS but are hardly affecting papain and do not inhibit SpeB.

5.3.3 pK_a measurements

The pK_a-value for the primary amine in the amino acid leucine is 9.7. For a dipeptide Leu-X_{aa}, with X_{aa} being either Gly, Phe or Leu, the corresponding value is decreased by 1.5 units, to ~8.4.[111] The primary amine in **86** shows a value as low as ~ 5. Also, the pK_a value of piperidine is 11.22 meanwhile piperazine (5.56 and 9.83) shows reduced basicity for both amine functions. The predicted and determined pK_a-values for the epimers of **70** and **86** are shown in TABLE 5.[112] Interestingly, the two pK_a values for each compound differ considerably. The acyclic secondary amine is not protonated at physiological pH and thus able to act both as a hydrogen bond donor and acceptor.

TABLE 5. pK_a values for the $pip_{236}G$ (70) and $Lpip_{236}GP$ analogues (86).[a]

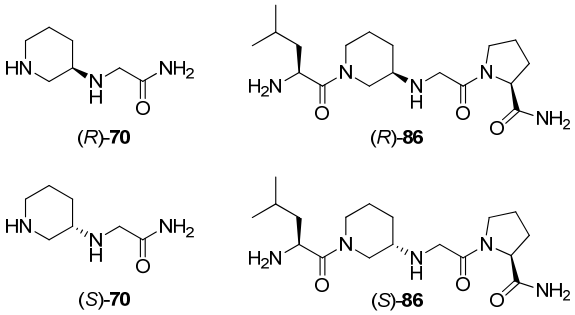

	measured		*predicted*	
cmpd	pK_a1	pK_a2	pK_a1	pK_a2
(*R*)-**70**	4.41	10.11	5.40	9.84
(*S*)-**70**	4.35	10.06		
(*R*)-**86**	5.13	8.46	7.35	9.13
(*S*)-**86**	5.21	8.53		

[a]Determination of pK_a-values performed by a screening method based on pressure-assisted capillary electrophoresis and mass spectroscopy.

5.3.4 In Silico *dockings of peptides and peptide analogues in IdeS*

The active site of the crystal structures of IdeS available for in silico *docking studies is occupied by either a sulphate ion or mercaptoethanol. Obviously, a substrate would directly be hydrolyzed when used together with the active enzyme. Without a ligand in the active site, a clear judgment of the agreement with an active and operative enzyme is highly difficult to make. The fact that two independent research groups prepared the available structures of IdeS, which to a high extent resemble each other, is an argument for the correctness of the structures. That said, the structure present in solution and in a solid crystal may not be the same. A structure derived by X-ray spectroscopy of a protein crystal is one single snap-shot of a long series of movements that eventually lead to a cleaved substrate. The fact that the side-chain of Arg259 intrudes into or covers the active site in the available X-ray structures and thus physically hinders a substrate to bind in a productive way conceals the picture and increases the challenge of structure-based design and also evaluation.*[113]

The two structures of IdeS with PDB ID 1Y08 and 2AU1 have been compared and an overlay of the two enzyme structures reveals some important differences (FIGURE 42).

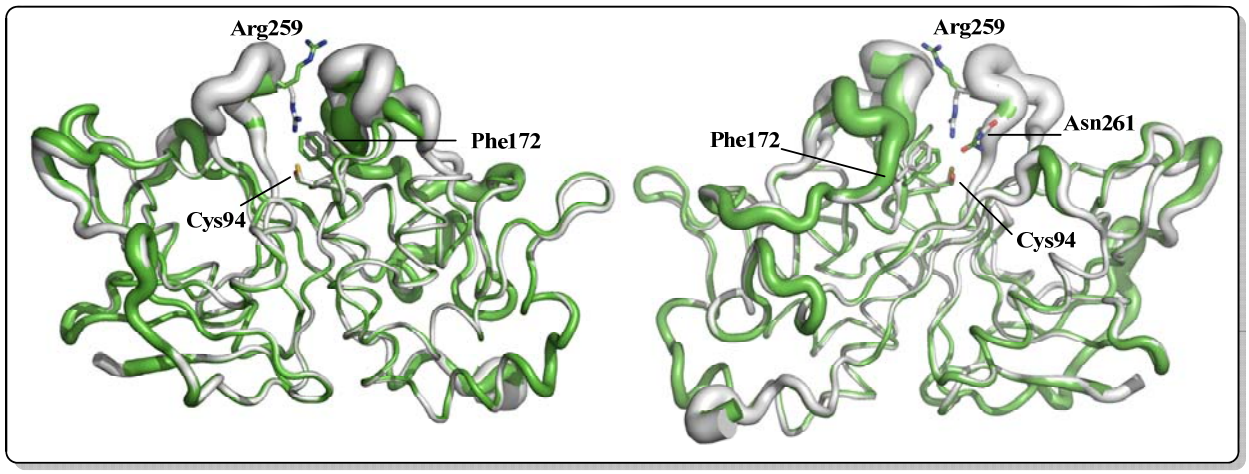

FIGURE 42. Comparison of structures; 1Y0A (green) and 2AU1 (grey). View from "front" (left) and "back" (right). The thicker back-bone the more movement of the residues.

The side chain of Arg_{259} is positioned differently, but both hinder binding through the active site. The aromatic ring of Phe_{172} adopts different positions due to rotation. However, preliminary docking results showed that the docked poses of peptide analogues were not affected by the rotation of Phe_{172}. Further, three residues close to the active site did not provide enough diffraction data during X-ray spectroscopy measurement due to high flexibility and are thus not present in the 1Y0A-structure, however they are present in the 2AU1-structure. The thickness of the back bone of the structures shown in FIGURE 42 is correlated to the R-value, a measurement of relative movements in proteins. Although the R-values for 1Y08 and 2AU1 are considered to be low, the movement close to the active site is most pronounced.

Dockings were performed using three different versions of the active site of the 2AU1 structure. In two versions the catalytic cysteine residue was either anionic or neutral. The third version also included a neutral cysteine residue but here the Asn_{261} side chain was flipped. The Arg_{259} side chain was removed in all three versions.

Different lengths of peptides were docked. As the peptides resemble a part of the IgG hinge sequence, they should show a "productive binding pose" where the nucleophilic sulphur in Cys_{94} should be able to reach the carbonyl group of the scissile amide bond in a Bürger-Dunitz fashion. Some of the docked peptides do find such a pose through the active site, but not all. In fact, even though LGGP is only a tetrapeptide, the docked poses with the scissile bond in the vicinity of Cys94 may indicate how IgG is placed when being cleaved.

The $Lpip_{236}GP$ analogues (*R*)- and (*S*)-**86** were also docked. Surprisingly, none of the poses were docked through the catalytic site. It seems that the piperidine moiety is too large to fit in the catalytic site, close to Cys94. The docked poses for both the peptide LGGP and the analogue (*R*)-**86** ($Lpip_{236}GP$) in the 2AU1-structure are shown in FIGURE 43. Other binding sites found by the analogues are either placing a part of the compound into the shallow pocket to the right or to the left. The analogues of $pip_{236}G$ (*R*)- and (*S*)-**70** were also docked. Even though the glycine moiety reached into the active site the piperidine moiety did not, implying that the walls above the active site are too narrow for such a binding pose.

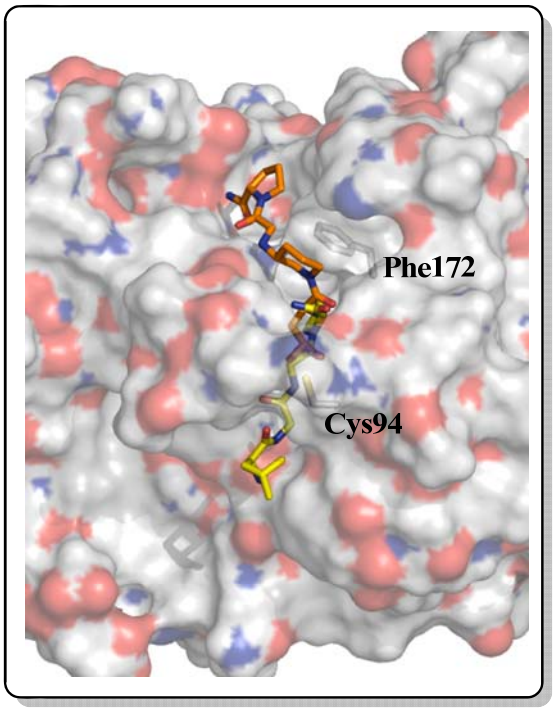

FIGURE 43. *In silico* docking poses of peptide LGGP (yellow) and (*R*)-**86** ($Lpip_{236}GP$, orange) in IdeS (2AU1).

Taken together, these findings indicate that the analogues interact differently with the enzyme compared to the peptides and thus also different to the IgG peptide sequence. IgG is cleaved by IdeS and must therefore bind through the active site. The peptides can find poses through the active site but are not able to inhibit IdeS. To explain the inability of the peptides to inhibit IdeS it can be speculated that peptides bind to the enzyme but too weakly, or that the peptides do bind but are easily replaced by IgG or even by the side-chain of Arg259. Several of the analogues are inhibiting IdeS, possibly not by binding through the active site but by other poses.

5.4 BICYCLIC COMPOUNDS as INHIBITORS (PAPER IV)

Bicyclic compounds (**106**, **110**, **112**, **117** and **119)** was evaluated as IdeS and papain inhibitors (FIGURE 44).

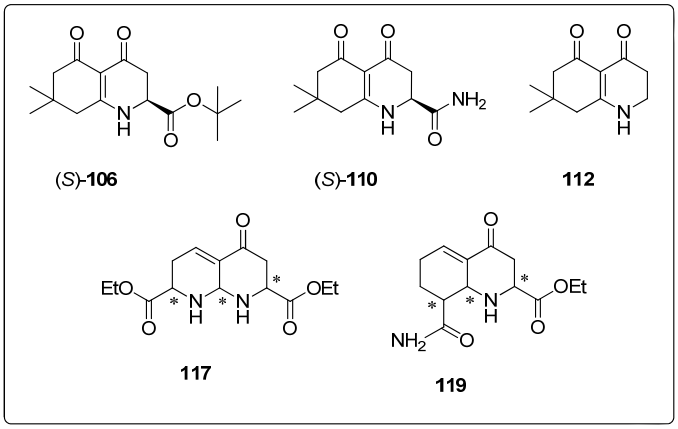

FIGURE 44. Dimedone-based and 1,8-naphthyridine and quinolone-like scaffolds tested as inhibitors in IdeS and papain assays.

For IdeS about 70% of the activity remained during the inihibition assay with **117** and **119**, compared to that of the DMSO control (FIGURE 45A). In contrast, papain was nearly totally inhibited by **117** during the condition used and **119** decreased the papain activity to ~15% (FIGURE 45B). Both compounds showed greater inhibition towards papain than IdeS.

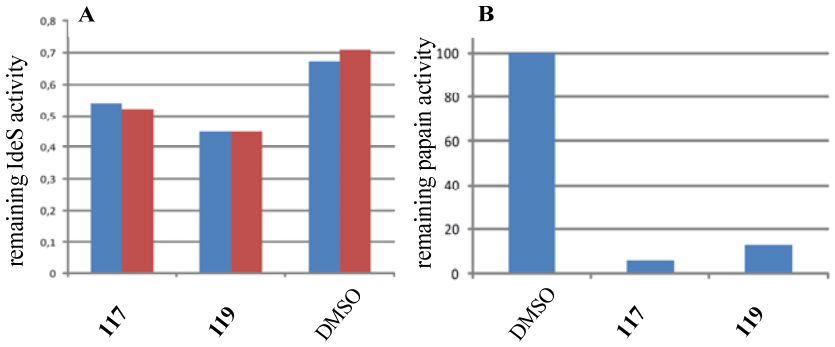

FIGURE 45. Remaining **A**) IdeS and **B**) papain activity in the presence of **117** and **118** and substrate.

A cut-off value of 80% remaining papain activity shows that **110** and **112** have none or moderate inhibition capacity (FIGURE 46). The base-treated **106c** is not affecting papain (FIGURE 46) whereas **106a** induces a strong inhibition. Result from the IdeS inhibition assay (data not shown) gave the same activity profile as shown for papain for both **106a** and **106c**. Thus, **106a** inhibits IdeS but no selectivity towards papain was obtained.

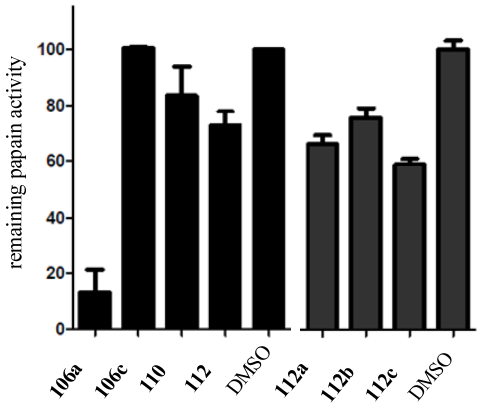

FIGURE 46. Inhibition capacity of **106**, **110** and **112** of papain (0.28 μM inhibitor). Remaining activity is expressed relative to enzyme activity in absence of putative inhibitors. **a**, **b**, and **c** represent different work-up procedures.

In contrast, the three samples of **112** showed moderate capacity of papain inhibition, but gave surprising result in the IdeS assay. Therefore, a SDS–PAGE assay with non-reducing gels was employed to be able to distinguish the single cleaved and double cleaved IgG (FIGURE 47).[114] Rapid cleavage of IgG is observed already after 20 s and only a small amount of intact IgG is still present at this time point. Single-cleaved IgG is accumulated, while only little $F(ab')_2$-fragment can be observed, meaning the second cleavage have not yet occurred. In contrast, at time point 20 min, nearly no intact IgG is left and the ratio of single and double cleaved IgG is approximately 1:1. This means that the second cleavage is much slower under the conditions used. Importantly, the two IdeS mediated hydrolysis steps occur sequentially.

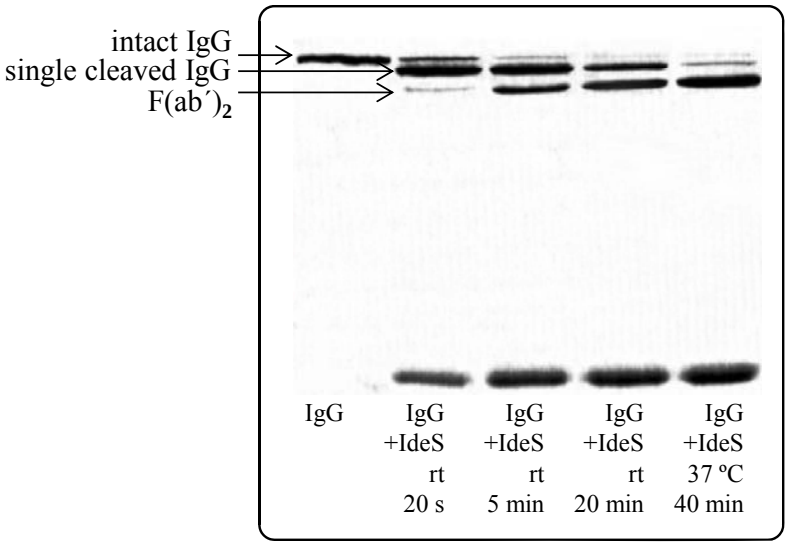

FIGURE 47. SDS-PAGE analysis (non-reducing gel) of a time-study of IdeS mediated cleavage of IgG.

In FIGURE 48, the SDS-PAGE analysis with non-reduced gel shows that **112** is a very strong inhibitor of IdeS. The concentrated **112a** prevents the second hydrolysis of IgG to occur. The basified **112c** inhibits also the first hydrolysis step, a IdeS mediated hydrolysis usually performed in 20 seconds! In fact, **112c** inhibition results in intact and mono-cleaved IgG but no $F(ab´)_2$-fragment at all. The second hydrolysis does not occur.

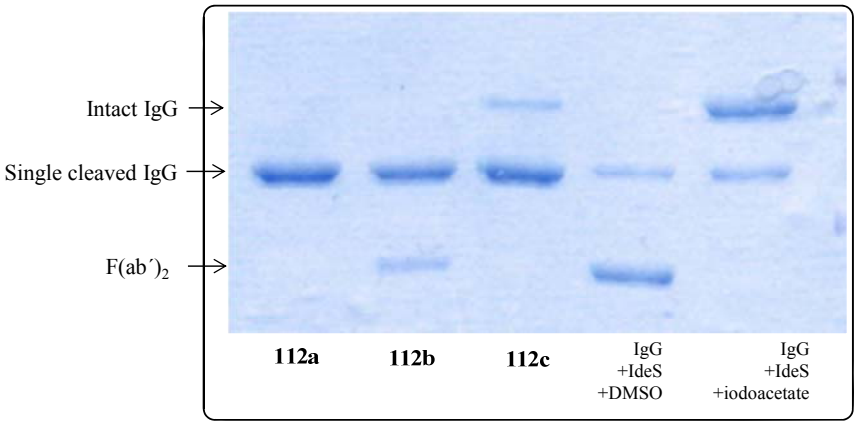

FIGURE 48. SDS-PAGE (non-reducing gel) analysis of **112,** prepared by different worked-up conditions **a**) concentrated, **b**) brine-wash and **c**) basic aqueous-wash.

In summary, five bicyclic compounds with three different scaffolds have been screened for their capacity of inhibition of IdeS and papain. **117** and **119** are strong inhibitors of papain and are shown to be selective towards IdeS. The dimedone-based compounds **106** and **112** show different activity profiles. Whereas **106** show either strong or no inhibition of both IdeS and papain depending on the work-up procedure, **112** show a very strong inhibition capacity of IdeS with moderate selectivity towards papain. Further evaluation of these highly interesting results must await the assignment of the structures. That said, the different structures of **112** assigned during NMR spectroscopy conditions or elsewhere do not necessarily correlate to conditions used in the inhibition assays.

6. SUMMARY and OUTLOOK

The bacterial cysteine protease IdeS was discovered ten years ago. It is considered highly interesting to use for therapeutic applications in autoimmune diseases due to its IgG-proteolytic ability, but it might also be of interest as a target for novel treatments of acute and severe bacterial infections. In this thesis several compounds have been synthesized that show IdeS inhibitory capacity, which can serve as a starting point for further development.

In the TPCK/TLCK project, synthetic routes were developed that allowed the synthesis of several TPCK/TLCK analogues. Eight compounds were identified to be IdeS inhibitors and some SAR conclusions could be drawn. In contrast to papain, IdeS is affected by *p*-toluylsulfonamide derivatives with lipophilic R-substituents. The questions asked at the outset of this project could be answered; the irreversible warhead is not needed for inhibition since the reversible aldehyde derivatives inhibit IdeS as efficiently as TPCK and TLCK. The R group substituent does contribute to the inhibitory effect, *n*-butyl is considerably better than the more polar 4-aminobutyl moiety.

A synthetic route to the peptide analogues was developed based on reductive amination to introduce the stereogenic center in the first step. Determination of the absolute configuration of the initially formed products allowed the assignment of the absolute configurations of all final test compounds. No racemization was detected in any of the synthetic steps. In a substrate based approach several di-, tri- and tetrapeptide analogues of GG, LGG, GGP, LLGG, and LGGP, which cover the IdeS cleavage site in IgG, were synthesized. Either of the two glycine residues was replaced by a 3-aminopiperidine moiety, a new peptidomimetic fragment. All compounds were screened for their capability to inhibit IdeS, SpeB and papain. Several compounds were identified as inhibitors, five compounds showed 50% remaining IdeS activity at 0.8 μM. The small difference in potency makes a full SAR analysis difficult for the peptide analogues, but an extension *C*-terminally in $pip_{236}G$ seems to favor activity. However, for increased selectivity against related cysteine proteases an extension *N*-terminally is suggested, as shown by the di- and tripeptide analogues $pip_{236}G$ ((*S*)-**70)** and $Lpip_{236}G$ ((*R*)-**74)**. Eight peptides covering the IdeS cleavage site of IgG were found to affect IdeS activity. *In silico* dockings were performed to elucidate the origin of the different activity profiles. The result indicates that the two sets of compounds find different binding sites. The X-ray structure used in the docking studies cannot accommodate the piperidine moiety in the catalytic site. Whether this is true also in solution needs more thorough investigations. NMR spectroscopic studies of IdeS are on-going, by understanding how IdeS interacts with an inhibitor, development of inhibitors with stronger potency will be possible.

The interesting inhibition profiles of $pip_{236}G$ ((*S*)-**70**) and $Lpip_{236}G$ ((*R*)-**74**) motivated the synthesis of novel bicyclic compounds. The strategy was to rigidify the structures and thereby increase the potency. Initially, piperidine-3,5-dione was considered as the starting material, but low product formation prompted new routes. Interestingly, when using dimedone as starting material, i.e. an analogue of piperidine-3,5-dione in which the nitrogen is replaced by a carbon atom, the yield increased more than ten times. It might be possible to optimize the yields starting also from piperidine-3,5-dione by altering the protecting group, but this was not further pursued in this thesis work. The structures of the synthesized bicyclic derivatives all comprise an enaminone function which seems to isomerize into different tautomeric forms. The detailed composition of such isomeric mixtures is not yet fully assigned, for that further actions are needed. Five bicyclic compounds based on quinolinone and naphthyridinone scaffolds were tested for their inhibitory potency on IdeS and papain. The naphthyridine derivatives were able to inhibit papain selectively over IdeS. One quinolin-4,6-dione derivative (**112**) showed very strong IdeS potency, it inhibited IdeS already in the first step of the IgG hydrolysis – a catalytic process

usually finished in 20 seconds! This compound should serve as a good starting point for further development of more potent and more selective IdeS inhibitors. Its selectivity against human cysteine proteases also needs to be investigated.

7. ACKNOWLEDGEMENTS

Prof. **Kristina L**, Tack för att du antog mig som doktorand, och för att din dörr alltid har stått öppen.

Tack Prof. **Jan K** för dina kloka råd.

Tack **Tomas F**, för idéer som omvandlas till projekt.

Ann-Therese Karlberg, examinator.

IdeS-gänget: **Lasse,** för att du lånade ut IdeS till en kemist och förmedlade kontakten till UvPR, **Björn, Ingbritt,** för er tid med de tidiga testerna**. Ulrich**, för allt samarbete, **Reine** -den sanne pipetteringsguden. -för samarbete och din screeningstid. **Christian** o **Helena**. Lycka till med era projekt. **Claes,** Tack alla labdagar ihop, och all kemi du gjort. **Devaraj,** third pair of hands into the fume hood for IdeS. Thanks for the DA chemistry.

Lars Kristian X-ray hjälp. **Madeleine, Olle** för pKa-körningar. **Susanne O** kristallgurun.

Alla som passerat dragskåpen i 8014. **Thanos**, for sharing the Jazzy time; **Peter D**, och **Henrik S** för alla pratstunder. **Bisse,** allt sedan fikastunden på NMR-centrets trapp, **Itedale**, rumskompis att lita på i torrt o vått. **Maria**, **Tina, Mariell, David -** lycka till med resten! **Tomas L,** excelkungen!

Marcus M och **Tobias A.** för alla fester.

Alla seniora forskare på våning 8 o 9 för doktorandkurser och diskussioner.

Övriga forskare, doktorander på våning 8 o 9.

Sekreterare och annan personal, tack för att hjulen snurrar. **Alpo**, datorsupport när den behövs.

AZ-kollegor och -vänner: Tack för ALL hjälp under de här åren (ingen nämnd ingen glömd)

och glada hejapå-rop. Jag har saknat er.

Tack alla som läst hela, eller valda delar av avhandlingen.

Mamma, Pappa, A-C, släkt och vänner.

Blom o **Ida, Klara, Rasmus** och **Samuel,** vad skulle jag göra utan er? Tack för att ni finns.

Henrik, min älskade du! Jag är så oändligt tacksam för att vi träffades! Tack för din fenomenala support, och alla matlådor. Och för att du hann stoppa mig i tid, efter 24h jobb, det kunde gått riktigt illa annars. Nu tillsammans mot nya äventyr!

Thanks Vetenskapsrådet and AstraZeneca R&D Mölndal, Sweden, for financial support of my graduate student fellowship.

8. APPENDICES

APPENDIX 1

Determination of the absolute configuration of **68, 63** and **41.**

In order to determine the absolute configuration of the two diastereomers of **68**, formed with the highest ratio (21:79), the mixture of (1)- and (2)-**68** was separated using preparative HPLC (Chiralpak AD) (SCHEME A1). The excess isomer (2)-**68** was crystallized from *n*-hexane. However, the flake-shaped crystals could not be used to produce satisfactory X-ray diffraction reflections for all three dimensions. Instead, (2)-**68** was deprotected using catalytic hydrogenation, subsequent Boc-protection afforded diastereomerically pure (1)-**63** (SCHEME A1). The methyl ester of (1)-**63** was aminolyzed into (1)-**41** which formed crystals from both *n*-hexane and acetonitrile but enough X-ray data could still not be collected. Instead, reference compounds had to be synthesized (SCHEME A1). Starting from enantiopure Boc-protected (*S*)-piperidinol ((*S*)-120) the tosylated intermediate (*S*)-**121** was formed. It was reacted with L-proline amide in an S_N2 reaction in the presence of pyridine affording only one diastereomer with inverted stereochemistry, (*RS*)-**41**. For comparison (*SS*)-**41** was also synthesized (not shown). Similar S_N2 reactions with a tosylated secondary alcohol derivative and either L-proline amide or *S*-piperidine carboxamide as the secondary amine have been reported to proceed with inversion.[115-116] Knowing that the absolute configuration of (1)-**41** is *RS* and comparing the retention times from HPLC (Chiralpak AD) of both (1)-**63** and (2)-**68** the diastereomers of these pairs could also be unequivocally assigned.

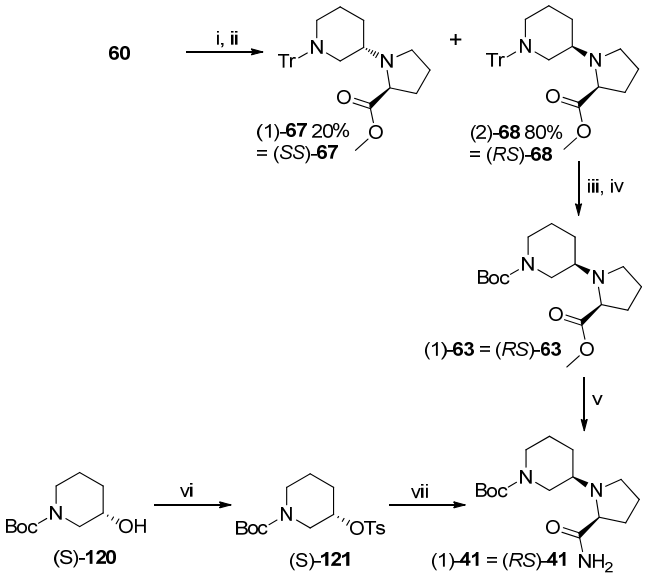

SCHEME A1. (1) and (2) reflects the elution order of the diastereomers from HPLC (Chiralpak AD). *Reagents and conditions:* i) $NaBH(O\text{-}2\text{-}ethylhexanoyl)_3$ (formed *in situ*, DCM, rt, on), L-ProlineOMe, molecular sieves, DCM, rt, 16 h (55%); ii) separation of the diastereomers on HPLC (Chiralpak AD) using hexane/2-propanol 99:1 as the mobile phase at a flow rate of 10 mL/min; iii) catalytic hydrogenation (Pd/C), 10 bar, 45 °C, 3 loops in H-cube (86%); iv) Boc_2O, ethyl acetate/EtOH 1:1, rt, 5 h (96%); v) NH_3/MeOH (7*N*), rt, 48 h (93%); vi) TsCl, DMAP, Et_3N, DCM, rt, 5 h (63%); vii) L-ProlineNH_2, pyridine, CH_3CN, reflux, 16 h (5%, the rest is unreacted starting material).

To determine the absolute stereochemistry of **62** the two diastereomers were separated by preparative HPLC (Chiralpak AD), and the first eluted diastereomer ((1)-**62**) was Boc-deprotected (SCHEME A2). The isolated TFA-salt of **62** was crystallized from THF/hexane and an X-ray crystallographic structure determination was performed, which revealed the (*SS*)-

configuration (FIGURE A1). Hence, the first eluted diastereomer of **62** also has the (*SS*)-configuration.

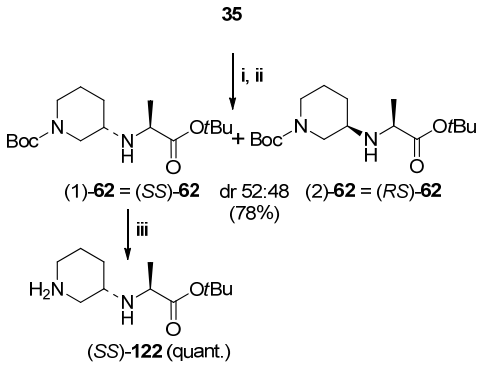

SCHEME A2. *Reagents and conditions:* (i) L-AlaO*t*Bu, NaBH(O-2-ethylhexanoyl)$_3$, DCM, rt, 16 h; (ii) preparative HPLC (Chiralpak AD); (iii) TFA/DCM, rt, 1h (quant.yield).

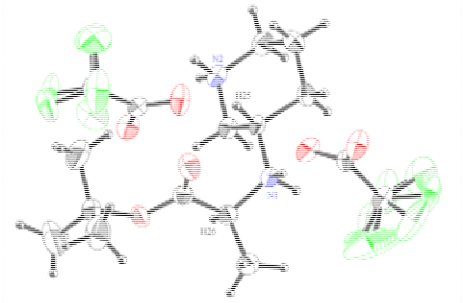

FIGURE A1: Ortep picture of the TFA salt of (*SS*)-**122**, revealing the absolute configuration of (*SS*)-**62**.

APPENDIX 2

The IdeS structure (PDB ID: 2AU1) was prepared according to the Protein Preparation Wizard implemented in Maestro, available in the Schrödinger package.[117] All water molecules and the side-chain of Arg259 were removed. The active site was modified by rotation and protonation to optimize the hydrogen bonding between Cys94 and His262. The docking grid was centred to the sulphur of the mercaptoethanol moiety located at the active site and a box of 25 $Å^3$ was chosen. Ligands were prepared according to LigPrep using OPLS2005, protonation states were used according to pK_a-measurements (*vide infra*) and the stereochemistry were kept unchanged. Docking calculations were performed in Glide with the standard precision mode (SP) without constraints.[118] The result was evaluated in a funnel-like fashion. First, all poses were visually inspected according to the number of hydrogen bonding possibilities. SiteMap was used for characterizing the binding site according to hydrophobic, hydrogen bond accepting or donating regions.[119] The poses with three or more hydrogen bonds were visually inspected for satisfying complementarity of the binding site according to the SiteMap profile. For the most promising poses so far, energy calculations were performed to evaluate the strain energy of the docked conformers. The energy of the conformer constituting the pose to be evaluated was compared with the energy of the most relaxed conformer occupying the global minimum. For Conformational Searches and Current Energy calculations in MacroModel OPLS2005, water as solvent, PRCG for minimization was used until convergence (0.05) was reached.[120] The poses of the peptides were also evaluated by distance and Bürger-Dunitz angle (107°) between the sulphur atom in Cys94 and the *CO*-group in the scissile amide bond.[121]

9. REFERENCES

(1) Rawlings, N. D.; Barrett, A. J.; Bateman, A., MEROPS: the peptidase database. *Nucleic Acids Res.* **2010**, *38*, D227-D233. http://merops.sanger.ac.uk/.

(2) Agniswamy, J.; Nagiec, M. J.; Liu, M. Y.; Schuck, P.; Musser, J. M.; Sun, P. D., Crystal structure of group A Streptococcus Mac-1: Insight into dimer-mediated specificity for recognition of human IgG. *Structure* **2006**, *14*, 225-235.

(3) Wang, C.-C.; Houng, H.-C.; Chen, C.-L.; Wang, P.-J.; Kuo, C.-F.; Lin, Y.-S.; Wu, J.-J.; Lin, M. T.; Liu, C.-C.; Huang, W.; Chuang, W.-J., Solution structure and backbone dynamics of streptopain insight into diverse substrate specificity. *J. Biol. Chem.* **2009**, *284*, 10957-10967.

(4) Kamphuis, I. G.; Kalk, K. H.; Swarte, M. B. A.; Drenth, J., Structure of papain refined at 1.65 Å resolution. *J. Mol. Biol.* **1984**, *179*, 233-256.

(5) Richardson, J. S., Schematic drawings of protein structures. *Methods Enzymol.* **1985**, *115*, 359-380.

(6) The graphics were prepared in PyMol (http://www.pymol.org/).

(7) Schechter, I.; Berger, A., On the size of the active site in proteases. *Biochem. Biophys. Res. Commun.* **1967**, *27*, 157-162.

(8) Berger, A.; Schechter, I., Mapping active site of papain with aid of peptide substrates and inhibitors. *Phil. Trans. Roy. Soc. Lond. B* **1970**, *257*, 249-264.

(9) Storer, A. C.; Ménard, R., Catalytic mechanism in papain family of cysteine peptidases. *Proteolytic Enzymes: Serine and Cysteine Peptidases* **1994**, *244*, 486-500.

(10) Barrett, A. J.; Rawlings, N. D.; Woessner, J. F. *Handbook of proteolytic enzymes*. Elsevier: London, 2004.

(11) Puente, X. S.; Sanchez, L. M.; Overall, C. M.; Lopez-Otin, C., Human and mouse proteases: A comparative genomic approach. *Nature Reviews Genetics* **2003**, *4*, 544-558.

(12) Lecaille, F.; Kaleta, J.; Bromme, D., Human and parasitic papain-like cysteine proteases: Their role in physiology and pathology and recent developments in inhibitor design. *Chem. Rev.* **2002**, *102*, 4459-4488.

(13) Leung, D.; Abbenante, G.; Fairlie, D. P., Protease inhibitors: Current status and future prospects. *J. Med. Chem.* **2000**, *43*, 305-341.

(14) Chapman, H. A.; Riese, R. J.; Shi, G. P., Emerging roles for cysteine proteases in human biology. *Ann. Rev. Physiol.* **1997**, *59*, 63-88.

(15) Otto, H. H.; Schirmeister, T., Cysteine proteases and their inhibitors. *Chem. Rev.* **1997**, *97*, 133-171.

(16) Goll, D. E.; Thompson, V. F.; Li, H. Q.; Wei, W.; Cong, J. Y., The calpain system. *Physiol. Rev.* **2003**, *83*, 731-801.

(17) Rosenthal, P. J.; Sijwali, P. S.; Singh, A.; Shenai, B. R., Cysteine proteases of malaria parasites: Targets for chemotherapy. *Curr. Pharm. Des.* **2002**, *8*, 1659-1672.

(18) Fersht, A., *Enzyme structure and mechanism*. 2nd ed.; W. H. Freeman and Company: New York, 1985.

(19) Gohlke, H.; Klebe, G., Approaches to the description and prediction of the binding affinity of small-molecule ligands to macromolecular receptors. *Angew. Chem. Int. Ed.* **2002**, *41*, 2645-2676.

(20) Schoellmann, G.; Shaw, E., Direct evidence for presence of histidine in active center of chymotrypsin. *Biochemistry* **1963**, *2*, 252-256.

(21) Petra, P. H.; Cohen, W.; Shaw, E. N., Isolation and characterization of alkylated histidine from tlck inhibited trypsin. *Biochem. Biophys. Res. Commun.* **1965**, *21*, 612-618.

(22) Powers, J. C.; Asgian, J. L.; Doğan Ekici, Ö.; Ellis James, K., Irreversible inhibitors of serine, cysteine, and threonine proteases. *Chem. Rev.* **2002**, *102*, 4639-4750.

(23) Hanada, K.; Tamai, M.; Yamagishi, M.; Ohmura, S.; Sawada, J.; Tanaka, I., Isolation and characterization of E-64, a new thiol protease inhibitor. *Agric. Biol. Chem.* **1978**, *42*, 523-528.

(24) Lowe, G.; Yuthavon.Y, Kinetic specificity in papain-catalysed hydrolyses. *Biochem. J* **1971**, *124*, 107-115.

(25) Brocklehurst, K.; Malthouse, J. P. G., Mechanism of reaction of papain with substrate-derived diazomethyl ketones - implications for difference in site specificity of halomethyl ketones for

serine proteinases and cysteine proteinases and for stereoelectronic requirements in papain catalytic mechanism. *Biochem. J* **1978**, *175*, 761-764.
(26) Magrath, J.; Abeles, R. H., Cysteine protease inhibition by azapeptide esters. *J. Med. Chem.* **1992**, *35*, 4279-4283.
(27) Bouchut, W. a., Sur le ferment digestif du Carica papaya. *Acad. Sci. Paris* **1879**, 425.
(28) Lowe, G., Cysteine proteinases. *Tetrahedron* **1976**, *32*, 291-302.
(29) Drenth, J.; Jansonius, J. N.; Koekoek, R.; Swen, H. M.; Wolthers, B. G., Structure of papain. *Nature* **1968**, *218*, 929-933.
(30) Vernet, T.; Tessier, D. C.; Chatellier, J.; Plouffe, C.; Lee, T. S.; Thomas, D. Y.; Storer, A. C.; Ménard, R., Structural and functional roles of asparagine 175 in the cysteine protease papain. *J. Biol. Chem.* **1995**, *270*, 16645-16652.
(31) Rawlings, N. D.; Tolle, D. P.; Barrett, A. J., MEROPS: the peptidase database. *Nucleic Acids Res.* **2004**, *32*, D160-D164.
(32) Wolthers, B. C., Kinetics of inhibition of papain by TLCK and TPCK in presence of BAEE as substrate. *FEBS Lett.* **1969**, *2*, 143-145.
(33) Elliott, S. D., A proteolytic enzyme produced by group A streptococci with special reference to its effect on the type-specific M antigen. *J. Exp. Med.* **1945**, *81*, 573-592.
(34) Kagawa, T. F.; Cooney, J. C.; Baker, H. M.; McSweeney, S.; Liu, M. Y.; Gubba, S.; Musser, J. M.; Baker, E. N., Crystal structure of the zymogen form of the group A Streptococcus virulence factor SpeB: An integrin-binding cysteine protease. *Proc. Nat. Acad. Sci. U. S. A.* **2000**, *97*, 2235-2240.
(35) Doran, J. D.; Nomizu, M.; Takebe, S.; Menard, R.; Griffith, D.; Ziomek, E., Autocatalytic processing of the streptococcal cysteine protease zymogen - processing mechanism and characterization of the autoproteolytic cleavage sites. *Eur. J. Biochem.* **1999**, *263*, 145-151.
(36) Kapur, V.; Topouzis, S.; Majesky, M. W.; Li, L. L.; Hamrick, M. R.; Hamill, R. J.; Patti, J. M.; Musser, J. M., A conserved streptococcus-pyogenes extracellular cysteine protease cleaves human fibronectin and degrades vitronectin. *Microb. Pathog.* **1993**, *15*, 327-346.
(37) von Pawel-Rammingen, U.; Björck, L., IdeS and SpeB: immunoglobulin-degrading cysteine proteinases of *Streptococcus pyogenes*. *Curr. Opin. Microbiol.* **2003**, *6*, 50-55.
(38) Berman, H. M.; Westbrook, J.; Feng, Z.; Gilliland, G.; Bhat, T. N.; Weissig, H.; Shindyalov, I. N.; Bourne, P. E., The protein data bank. *Nucleic Acids Res.* **2000**, *28*, 235-242.
(39) Olsen, J. G.; Dagil, R.; Niclasen, L. M.; Sørensen, O. E.; Kragelund, B. B., Structure of the mature streptococcal cysteine protease exotoxin mSpeB in its active dimeric form. *J. Mol. Biol.* **2009**, *393*, 693-703.
(40) von Pawel-Rammingen, U.; Johansson, B. P.; Björck, L., IdeS, a novel streptococcal cysteine proteinase with unique specificity for immunoglobulin G. *EMBO J.* **2002**, *21*, 1607-1615.
(41) Lei, B. F.; DeLeo, F. R.; Hoe, N. P.; Graham, M. R.; Mackie, S. M.; Cole, R. L.; Liu, M. Y.; Hill, H. R.; Low, D. E.; Federle, M. J.; Scott, J. R.; Musser, J. M., Evasion of human innate and acquired immunity by a bacterial homolog of cd11b that inhibits opsonophagocytosis. *Nature Medicine* **2001**, *7*, 1298-1305.
(42) von Pawel-Rammingen, U.; Johansson, B. P.; Tapper, H.; Björck, L., Streptococcus pyogenes and phagocytic killing. *Nature Medicine* **2002**, *8*, 1043-1044.
(43) Vincents, B.; von Pawel-Rammingen, U.; Björck, L.; Abrahamson, M., Enzymatic characterization of the streptococcal endopeptidase, IdeS, reveals that it is a cysteine protease with strict specificity for IgG cleavage due to exosite binding. *Biochemistry* **2004**, *43*, 15540-15549.
(44) Wenig, K.; Chatwell, L.; von Pawel-Rammingen, U.; Björck, L.; Huber, R.; Sondermann, P., Structure of the streptococcal endopeptidase IdeS, a cysteine proteinase with strict specificity for IgG. *Proc. Nat. Acad. Sci. U. S. A.* **2004**, *101*, 17371-17376.
(45) Nandakumar, K. S.; Johansson, B. P.; Björck, L.; Holmdahl, R., Blocking of experimental arthritis by cleavage of igg antibodies in vivo. *Arthritis and Rheumatism* **2007**, *56*, 3253-3260.
(46) Johansson, B. P.; Shannon, O.; Björck, L., Ides: A bacterial proteolytic enzyme with therapeutic potential. *PLoS ONE* **2008**, *3*, e1692.
(47) Lei, B. F.; Liu, M. Y.; Meyers, E. G.; Manning, H. M.; Nagiec, M. J.; Musser, J. M., Histidine and aspartic acid residues important for immunoglobulin G endopeptidase activity of the group A

Streptococcus opsonophagocytosis-inhibiting Mac protein. *Infection and Immunity* **2003**, *71*, 2881-2884.
(48) Cunningham, M. W., Pathogenesis of group a streptococcal infections. *Clin. Microbiol. Rev.* **2000**, *13*, 470-511.
(49) Arnholm, B.; Lundquist, A.; Strömberg, A., Immunoglobulin i hög dos - livräddande vid invasiv grupp A-streptokockinfektion. *Läkartidningen*, **2004**, 35, 2642-2644.
(50) Carapetis, J. R.; Steer, A. C.; Mulholland, E. K.; Weber, M., The global burden of group a streptococcal diseases. *Lancet Infectious Diseases* **2005**, *5*, 685-694.
(51) Burton, D. R., Immunoglobulin-G - functional sites. *Molecular Immunology* **1985**, *22*, 161-206.
(52) Olsen, R. J.; Shelburne, S. A.; Musser, J. M., Molecular mechanisms underlying group A streptococcal pathogenesis. *Cellular Microbiology* **2009**, *11*, 1-12.
(53) Harris, L. J.; Larson, S. B.; Hasel, K. W.; McPherson, A., Refined structure of an intact IgG2a monoclonal antibody. *Biochemistry* **1997**, *36*, 1581-1597.
(54) Janin, J.; Bahadur, R. P.; Chakrabarti, P., Protein-protein interaction and quaternary structure. *Quart. Rev. Biophys.* **2008**, *41*, 133-180.
(55) Agniswamy, J.; Lei, B. F.; Musser, J. M.; Sun, P. D., Insight of host immune evasion mediated by two variants of group A Streptococcus Mac protein. *J. Biol. Chem.* **2004**, *279*, 52789-52796.
(56) Le, G. T.; Abbenante, G.; Madala, P. K.; Hoang, H. N.; Fairlie, D. P., Organic azide inhibitors of cysteine proteases. *J. Am. Chem. Soc.* **2006**, *128*, 12396-12397.
(57) Larsson, A.; Spjut, S.; Kihlberg, J.; Almqvist, F., An improved procedure for the synthesis of enaminones - dimer building blocks in beta-strand mimetics. *Synthesis-Stuttgart* **2005**, 2590-2596.
(58) Phillips, S. T.; Rezac, M.; Abel, U.; Kossenjans, M.; Bartlett, P. A., "@-tides": The 1,2-dihydro-3(6H)-pyridinone unit as a beta-strand mimic. *J. Am. Chem. Soc.* **2002**, *124*, 58-66.
(59) Fairlie, D. P.; Tyndall, J. D. A.; Reid, R. C.; Wong, A. K.; Abbenante, G.; Scanlon, M. J.; March, D. R.; Bergman, D. A.; Chai, C. L. L.; Burkett, B. A., Conformational selection of inhibitors and substrates by proteolytic enzymes: Implications for drug design and polypeptide processing. *J. Med. Chem.* **2000**, *43*, 1271-1281.
(60) Gandon, L. A.; Russell, A. G.; Guveli, T.; Brodwolf, A. E.; Kariuki, B. M.; Spencer, N.; Snaith, J. S., Synthesis of 2,4-disubstituted piperidines via radical cyclization: Unexpected enhancement in diastereoselectivity with tris(trimethylsilyl) silane. *J. Org. Chem.* **2006**, *71*, 5198-5207.
(61) Lacoste, J. E.; Soucy, C.; Rochon, F. D.; Breau, L., 2-vinyl-trans-octahydro-1,3-benzoxazine: Cyclization and 1,3-dipolar cycloadditiion of nitrile oxides. *Tetrahedron Lett.* **1998**, *39*, 9121-9124.
(62) Lanman, B. A.; Myers, A. G., Efficient, stereoselective synthesis of trans-2,5-disubstituted morpholines. *Org. Lett.* **2004**, *6*, 1045-1047.
(63) Boeijen, A.; van Ameijde, J.; Liskamp, R. M. J., Solid-phase synthesis of oligourea peptidomimetics employing the Fmoc protection strategy. *J. Org. Chem.* **2001**, *66*, 8454-8462.
(64) Ho, M. F.; Chung, J. K. K.; Tang, N., A convenient synthesis of chiral *N*-Boc-amino ethers as potential peptide-bond surrogate units. *Tetrahedron Lett.* **1993**, *34*, 6513-6516.
(65) Osborn, H. M. I.; Sweeney, J., The asymmetric synthesis of aziridines. *Tetrahedron-Asymmetry* **1997**, *8*, 1693-1715.
(66) Nakajima, K.; Takai, F.; Tanaka, T.; Okawa, K., Studies on aziridine-2-carboxylic acid .1. Synthesis of optically-active l-aziridine-2-carboxylic acid and its derivatives. *Bull. Chem. Soc. Jpn.* **1978**, *51*, 1577-1578.
(67) Paulsen, H.; Patt, H., Syntheses of 2,3-diamino-2,3-dideoxypentoses. *Liebigs Ann. Chem.* **1981**, 1633-1642.
(68) Wipf, P.; Miller, C. P., An investigation of the mitsunobu reaction in the preparation of peptide oxazolines, thiazolines, and aziridines. *Tetrahedron Lett.* **1992**, *33*, 6267-6270.
(69) Hu, X. E., Nucleophilic ring opening of aziridines. *Tetrahedron* **2004**, *60*, 2701-2743.
(70) Wu, J.; Hou, X. L.; Dai, L. X., Effective ring-opening reaction of aziridines with trimethylsilyl compounds: A facile access to beta-amino acids and 1,2-diamine derivatives. *J. Org. Chem.* **2000**, *65*, 1344-1348.

(71) Farras, J.; Ginesta, X.; Sutton, P. W.; Taltavull, J.; Egeler, F.; Romea, P.; Urpi, F.; Vilarrasa, J., beta-(3)-Amino acids by nucleophilic ring-opening of *N*-nosyl aziridines. *Tetrahedron* **2001**, *57*, 7665-7674.
(72) Cariou, C. A. M.; Snaith, J. S., Stereoselective synthesis of 2,4,5-trisubstituted piperidines by carbonyl ene and prins cyclisations. *Organic and Biomolecular Chemistry* **2006**, *4*, 51-53.
(73) Damon, D. B.; Dugger, R. W.; Hubbs, S. E.; Scott, J. M.; Scott, R. W., Asymmetric synthesis of the cholesteryl ester transfer protein inhibitor torcetrapib. *Org. Process Res. Dev.* **2006**, *10*, 472-480.
(74) Sobolewski, D.; Kowalczyk, W.; Prahl, A.; Derdowska, I.; Slaninova, J.; Zabrocki, J.; Lammek, B., Analogues of arginine vasopressin and its agonist and antagonist modified in the N-terminal part of the molecule with L-beta-homophenylalanine. *J. Pept. Res.* **2005**, *65*, 465-471.
(75) Echavarren, A.; Galan, A.; Demendoza, J.; Salmeron, A.; Lehn, J. M., Anion-receptor molecules - synthesis of a chiral and functionalized binding subunit, a bicyclic guanidium group derived from L-aspargine or D-aspargine. *Helv. Chim. Acta* **1988**, *71*, 685-693.
(76) Enders, D.; Backes, M., First asymmetric synthesis of both enantiomers of Tropional (R) and their olfactory evaluation. *Tetrahedron-Asymmetry* **2004**, *15*, 1813-1817.
(77) Ghorai, M. K.; Das, K.; Kumar, A., A convenient synthetic route to enantiopure *N*-tosylazetidines from alpha-amino acids. *Tetrahedron Lett.* **2007**, *48*, 2471-2475.
(78) Brown, M. S.; Rapoport, H., Reduction of esters with sodium borohydride. *J. Org. Chem.* **1963**, *28*, 3261-3263.
(79) Seki, H.; Koga, K.; Matsuo, H.; Ohki, S.; Matsuo, I.; Yamada, S. I., Studies on optically active amino acids .5. Synthesis of optically active alpha-aminoalcohols by reduction of alpha-amino acid esters with sodium borohydride. *Chem. Pharm. Bull.* **1965**, *13*, 995-1000.
(80) Mukai, T.; Suganuma, N.; Soejima, K.; Sasaki, J.; Yamamoto, F.; Maeda, M., Synthesis of a beta-tetrapeptide analog as a mother compound for the development of matrix metalloproteinase-2-imaging agents. *Chem. Pharm. Bull.* **2008**, *56*, 260-265.
(81) Restorp, P.; Dressel, M.; Somfai, P., Synthesis of functionalized pyrrolidines by a highly stereoselective 3+2 -annulation reaction of *N*-tosyl-alpha-amino aldehydes and 1,3-bis(silyl)propenes. *Synthesis-Stuttgart* **2007**, 1576-1583.
(82) Abdel-Magid, A. F.; Carson, K. G.; Harris, B. D.; Maryanoff, C. A.; Shah, R. D., Reductive amination of aldehydes and ketones with sodium triacetoxyborohydride. Studies on direct and indirect reductive amination procedures. *J. Org. Chem.* **1996**, *61*, 3849-3862.
(83) Hutchins, R. O.; Su, W. Y.; Sivakumar, R.; Cistone, F.; Stercho, Y. P., Stereoselective reductions of substituted cyclohexyl and cyclopentyl carbon-nitrogen pi-systems with hydride reagents. *J. Org. Chem.* **1983**, *48*, 3412-3422.
(84) Yelin, E. A.; Onoprienko, V. V.; Kudelina, I. A.; Miroshnikov, A. I., The synthesis of isomeric 4-prolinylamines and 4,4 '-diprolinylamines. *Bioorg. Khim* **2000**, *26*, 862-872.
(85) Kobayashi, S.; Ishitani, H., Catalytic enantioselective addition to imines. *Chem. Rev.* **1999**, *99*, 1069-1094.
(86) Anet, F. A. L.; Yavari, I., Nitrogen inversion in piperidine. *J. Am. Chem. Soc.* **1977**, *99*, 2794-2796.
(87) Louaisil, N.; Rabasso, N.; Fadel, A., Asymmetric synthesis of (*R*)- and (*S*)-alpha-amino-3-piperidinylphosphonic acids via phosphite addition to iminium ions. *Synthesis-Stuttgart* **2007**, 289-293.
(88) Boström, J.; Norrby, P. O.; Liljefors, T., Conformational energy penalties of protein-bound ligands. *J. Comput. Aided Mol. Des.* **1998**, *12*, 383-396.
(89) Stereochemistry of Organic Compounds, Principles and Applications Nasipuri, D., 2nd ed.; New Age International Limited: New Dehli, 1991.
(90) Seeman, J. I., Effect of conformational change on reactivity in organic chemistry - evaluations, applications, and extensions of Curtin-Hammett Winstein-Holness kinetics. *Chem. Rev.* **1983**, *83*, 83-134.
(91) Cieplak, A. S., Stereochemistry of nucleophilic-addition to cyclohexanone - the importance of 2-electron stabilizing interactions. *J. Am. Chem. Soc.* **1981**, *103*, 4540-4552.

(92) Montalbetti, C.; Falque, V., Amide bond formation and peptide coupling. *Tetrahedron* **2005**, *61*, 10827-10852.
(93) Valeur, E.; Bradley, M., Amide bond formation: Beyond the myth of coupling reagents. *Chem. Soc. Rev.* **2009**, *38*, 606-631.
(94) Filira, F.; Biondi, L.; Gobbo, M.; Rocchi, R., *N*-alkylation of amino-acids during hydrogenolytic deprotection. *Tetrahedron Lett.* **1991**, *32*, 7463-7464.
(95) Hamid, M.; Slatford, P. A.; Williams, J. M. J., Borrowing hydrogen in the activation of alcohols. *Adv. Synth. Catal.* **2007**, *349*, 1555-1575.
(96) Greenhill, J. V., Enaminones. *Chem. Soc. Rev.* **1977**, *6*, 277-294.
(97) Murphy, J. P.; Hadden, M.; Stevenson, P. J., Aza-annulation of enaminones with crotonyl chloride - formal reversal of regioselectivity. *Tetrahedron* **1997**, *53*, 11827-11834.
(98) Tamura, Y.; Fujita, M.; Chen, L. C.; Inoue, M.; Kita, Y., Regioselective metalation of the 4-position of pyridine - new and convenient alkylation and acylation of 3-amino-5-methoxypyridine. *J. Org. Chem.* **1981**, *46*, 3564-3567.
(99) Rubinov, D. B.; Rubinova, I. L.; Lakhvich, F. A., Synthesis and keto-enol tautomerism of 6-alkyl-1-alkoxypyridine-2,4-diones. *Russ. J. Org. Chem.* **2011**, *47*, 277-283.
(100) Middleton, R. J.; Mellor, S. L.; Chhabra, S. R.; Bycroft, B. W.; Chan, W. C., Expedient synthesis of a novel class of pseudoaromatic amino acids: Tetrahydroindazol-3-yl- and tetrahydrobenzisoxazol-3-ylalanine derivatives. *Tetrahedron Lett.* **2004**, *45*, 1237-1242.
(101) Suzuki, H.; Tsukakoshi, Y.; Tachikawa, T.; Miura, Y.; Adachi, M.; Murakami, Y., A new synthesis of 4-oxygenated beta-carboline derivatives by Fischer indolization. *Tetrahedron Lett.* **2005**, *46*, 3831-3834.
(102) Diels, O. A., K., Synthesen in der hydroaromatischen reihe. *Justus Liebigs Ann. Chem.* **1928**, 98-122.
(103) Jörgensen, K. A., Catalytic asymmetric hetero-Diels-Alder reactions of carbonyl compounds and imines. *Angew. Chem. Int. Ed.* **2000**, *39*, 3558-3588.
(104) Kerwin, J. F.; Danishefsky, S., On the lewis acid-catalyzed cyclocondensation of imines with a siloxydiene. *Tetrahedron Lett.* **1982**, *23*, 3739-3742.
(105) Hakimelahi, G. H.; Just, G., 2 simple methods for the synthesis of trialkyl alpha-aminophosphonoacetates (3) - trifluoromethanesulfonyl azide as an azide-transfer agent. *Synth. Commun.* **1980**, *10*, 429-435.
(106) Stille, J. K.; Groh, B. L., Stereospecific cross-coupling of vinyl halides with vinyl tin reagents catalyzed by palladium. *J. Am. Chem. Soc.* **1987**, *109*, 813-817.
(107) Stenberg, E.; Persson, B.; Roos, H.; Urbaniczky, C., Quantitative-determination of surface concentration of protein with surface-plasmon resonance using radiolabeled proteins. *J. Colloid Interface Sci.* **1991**, *143*, 513-526.
(108) Fägerstam, L. G.; Frostell-Karlsson, A.; Karlsson, R.; Persson, B.; Rönnberg, I., Biospecific interaction analysis using surface-plasmon resonance detection applied to kinetic, binding-site and concentration analysis. *J. Chromatogr.* **1992**, *597*, 397-410.
(109) Swank, R. T.; Munkres, K. D., Molecular weight analysis of oligopeptides by electrophoresis in polyacrylamide gel with sodium dodecyl sulfate. *Anal. Biochem.* **1971**, *39*, 462-467.
(110) Hopkins, A. L.; Groom, C. R.; Alex, A., Ligand efficiency: A useful metric for lead selection. *Drug Discovery Today* **2004**, *9*, 430-431.
(111) Hirokawa, T.; Gojo, T.; Kiso, Y., Isotachophoretic determination of mobility and pKa by means of computer-simulation .5. evaluation of mo and pKa of 28 dipeptides and assessment of separability. *J. Chromatogr.* **1987**, *390*, 201-223.
(112) Wan, H.; Holmén, A. G.; Wang, Y. D.; Lindberg, W.; Englund, M.; Någård, M. B.; Thompson, R. A., High-throughput screening of pK_a values of pharmaceuticals by pressure-assisted capillary electrophoresis and mass spectrometry. *Rapid Commun. Mass Spectrom.* **2003**, *17*, 2639-2648.
(113) Davis, A. M.; Teague, S. J.; Kleywegt, G. J., Application and limitations of X-ray crystallographic data in structure-based ligand and drug design. *Angewandte Chemie-International Edition* **2003**, *42*, 2718-2736.
(114) Ryan, M. H.; Petrone, D.; Nemeth, J. F.; Barnathan, E.; Björck, L.; Jordan, R. E., Proteolysis of purified IgGs by human and bacterial enzymes in vitro and the detection of specific proteolytic

fragments of endogenous IgG in rheumatoid synovial fluid. *Molecular Immunology* **2008**, *45*, 1837-1846.
(115) Herold, F.; Dawidowski, M.; Wolska, I.; Chodkowski, A.; Kleps, J.; Turlo, J.; Zimniak, A., The synthesis of new diastereomers of (4S,8aS)- and (4R,8aS)-4-phenyl-perhydropyrrole 1,2-a pyrazine-1,3-dione. *Tetrahedron-Asymmetry* **2007**, *18*, 2091-2098.
(116) Dawidowski, M.; Herold, F.; Wilczek, M.; Kleps, J.; Wolska, I.; Turlo, J.; Chodkowski, A.; Widomski, P.; Bielejewska, A., The synthesis and conformational analysis of optical isomers of 4-phenyl-perhydropyrido 1,2-a pyrazine-1,3-dione: An example of 'solid state-frozen' dynamics in nitrogen-bridged bicyclic 2,6-diketopiperazines. *Tetrahedron-Asymmetry* **2009**, *20*, 1759-1766.
(117) Protein Preparation Wizard, Schrödinger Suite 2009; Epik version 2.0, Impact version 5.5; Prime version 2.1, Schrödinger, LLC, New York, NY, 2009.
(118) Glide, version 5.5, Schrödinger, LLC, New York, NY, 2009.
(119) SiteMap, version 2.3, Schrödinger, LLC, New York, NY, 2009.
(120)
(121) Bürgi, H. B.; Dunitz, J. D.; Lehn, J. M.; Wipff, G., Stereochemistry of reaction paths at carbonyl centers. *Tetrahedron* **1974**, *30*, 1563-1572.